Role of the Protein Kinase TBK1 in Insulin-Stimulated Glucose Transport

by

Maeran Uhm

A dissertation submitted in partial fulfillment
of the requirements for the degree of
Doctor of Philosophy
(Molecular and Integrative Physiology)
in the University of Michigan
2015

Doctoral Committee:

Professor Alan R. Saltiel, Chair
Associate Professor Ken Inoki
Associate Professor Jiandie Lin
Professor Jessica Schwartz
Professor John A. Williams

ACKNOWLEDGEMENTS

I would like to gratefully thank my advisor, Dr. Alan Saltiel, for his support, guidance, understanding, patience and encouragement in science and life. I feel extremely fortunate to have an advisor who affords his graduate students the freedom to explore their own ideas and pursue various projects without objection. He has taught me how to question thoughts, express my ideas, and communicate with people. This allowed me to grow as a better scientist. He is one of the smartest people I know and a great scientific leader. I hope that I could be as enthusiastic and energetic as Alan and become a good scientist like him in the future.

I would also like to thank my committee members, Dr. John Williams, Jessica Schwartz, Jiandie Lin, and Ken Inoki for serving as my committee members and their helpful discussions and guidance over the course of my graduate career. Everyone has given me always brilliant comments and suggestions.

I would like to thank all of my past and current colleagues in the Saltiel lab, including Louise Chang, Shian-Huey Chiang, Stuart Decker, Dave Bridges, Nicole Maher, Christina Sherry, Binbin Lu, Sheela Karunanithi, Alan Cheng, David Buchner, Irit Hochberg, Xiao-Wei Chen, Jon Mowers, Dara Leto, Tingting Xiong, Carey Lumeng, Melissa McGill, Shannon Reilly, Yuliya Skorobogatko, Prasanth Puthanveetil, Peng Zhao, Tae Hyeon Koo, BreAnne Poirier, Brandon Pang, Jerry Yan, Joshua Castle, Kai Yuan, Silvia Novakova, and Jamie Yost Brandon. Thank

you all for your friendship, help, and advice during my graduate training. I also would like to thank my other colleagues, including Siming Li, Grace Wang, and Di Ma for their friendship and collaboration. My special thanks also go to Dr. Ken Inoki, Ormond MacDougald, Bishr Omary, and Michele Boggs for giving me an opportunity to be trained at the University of Michigan even before the matriculation. You truly allowed me to become a PhD student.

Of course, I could not overcome many of the obstacles in my life without the endless support and love of my family. Last but not the least, I would like to give my special thanks to my lovely husband, Juil Yum, for his support, patience, and understanding throughout my graduate training. Many thanks to my family, including my parents (Dongseob Uhm and Jinsoon Park), my parents-in-law (Taewoon Yum and Soonyi Jung), my brother Hyunsik Uhm, and my baby Jay Yum for their support and prayers. None of this would have been possible without the love and patience and you made me who I am.

TABLE OF CONTENTS

LIST OF FIGURES

LIST OF ABBREVIATIONS

AcGFP1	*Aequorea coerulescens* green fluorescent protein
APS	Adaptor protein containing PH and SH2 domain
APPL1	Adaptor protein, phosphotyrosine interaction, PH domain And leucine zipper containing 1
Arf	ADP-ribosylation factor
AS160	Akt substrate of 160 kDa
AS250	Akt substrate of 250 kDa
CAP	c-Cbl associated protein
CIP4	Cdc42 interacting protein 4
Del	Deletion
EGFP	Enhanced green fluorescent protein
EM	Electron microscopy
GAP	GTPase activating protein
GDI	Guanine nucleotide dissociation inhibitor
GEF	Guanine nucleotide exchange factor
GST	Glutathione s-transferase
GSV	GLUT4-storage vesicles
GST	Glutathione s-transferase
HLH	Helix-loop-helix
IKK	IκB kinase
IR	Insulin receptor
IRAP	Insulin-responsive aminopeptidase
IRF	Interferon regulatory factor
IRS	Insulin receptor substrate
IRV	Insulin responsive GLUT4 vesicle
LZ	leucine zipper
MBP	Maltose binding protein
MBP	Myelin basic protein
PDK1	phosphoinositide-dependent kinase 1
PKC	Protein kinase C
PI3K	Phosphoinositide 3-kinase
PIP3	phosphatidylinositol-3,4,5-trisphosphate
PH	Pleckstrin homology
PTB	Phosphotyrosine binding
PTEN	phosphatase and tensin homolog deleted on chromosome ten
RGC	Ral-GAP complex
SH2	Src homology 2
SiRNA	Small interfering RNA

SNARE	Soluble N- ethylmaleimide-sensitive factor attachment protein receptor
TBK1	Tank binding kinase 1
TfR	Transferrin receptor
TGN	*trans*-Golgi network
TIRF	Total internal reflection fluorescence
TLR	Toll-like receptor
ULD	Ubiquitin-like domain
WT	Wild type

ABSTRACT

Role of the Protein Kinase TBK1 in Insulin-Stimulated Glucose Transport

by

Maeran Uhm

Chair: Alan R. Saltiel

Insulin stimulates glucose uptake in muscle and fat by promoting translocation of the facilitative transporter GLUT4 from intracellular compartments to the plasma membrane. While the pathways involved in GLUT4 vesicle trafficking are not completely understood, numerous studies have shown that small G proteins critically integrate signaling with the trafficking machineries in this process. Among the targets of these G proteins is the exocyst complex, which facilitates the tethering of GLUT4 vesicles to the plasma membrane. GLUT4 translocation requires both the assembly and recognition of the exocyst for targeted exocytosis, and G proteins mediate both of these processes. Exocyst assembly is controlled by activation of the Rho subfamily G protein TC10, while exocyst recognition is mediated by the G protein RalA. However, how GLUT4 vesicles dissociate from the G protein after binding is unclear, and the sequence of events that disengage GLUT4 vesicles from the individual subunits of the exocyst remain uncertain.

Here I report that the protein kinase TBK1 is required for insulin-stimulated glucose transport and GLUT4 translocation in parallel with the Akt signaling pathway. Upon activation of RalA, TBK1 directly phosphorylates the exocyst subunit Exo84, a crucial step in insulin-stimulated glucose uptake. Knockdown of TBK1 blocks insulin-stimulated glucose uptake and GLUT4 translocation, and ectopic overexpression of a kinase-inactive mutant of TBK1 reduces insulin-stimulated glucose uptake in 3T3-L1 adipocytes. The phosphorylation of Exo84 on multiple sites by TBK1 reduces its affinity for RalA, and allows its release from the exocyst. Therefore, the interaction of TBK1/RalA/exocyst complex is dissociated upon Exo84 phosphorylation by TBK1 but overexpression of a kinase-inactive mutant of TBK1 blocks the dissociation of the complex, and treatment of 3T3-L1 adipocytes with specific inhibitors of TBK1 reduces the rate of complex dissociation. Introduction of mutant forms of Exo84 that prevent or mimic phosphorylation blocks insulin-stimulated GLUT4 translocation. Thus, these data indicate that TBK1 controls GLUT4 vesicle engagement and disengagement from the exocyst, suggesting that the exocyst is more than just a tethering complex for the GLUT4 vesicle, but also a ‘gatekeeper’ controlling vesicle fusion at the plasma membrane.

Chapter 1

Introduction

Plasma glucose levels are tightly regulated in a narrow range in mammals (*1*). In the fasting state, serum glucose levels are maintained by hepatic glucose output, which results mainly from the breakdown of glycogen or *de novo* synthesis of glucose (gluconeogenesis). After food is ingested, glucose levels are elevated, which in turn leads to the secretion of insulin from glucose and amino acid-sensing beta cells in pancreatic islets. Insulin reduces hepatic glucose output and facilitates glucose uptake into muscle and adipose tissue, thus restoring glucose levels to baseline (*2*).

Insulin is the most potent physiological anabolic hormone known, promoting the storage and synthesis of lipids, protein, and carbohydrates and inhibiting their breakdown and release into the circulation (*3*). Diabetes mellitus is a metabolic disorder typified by chronic hyperglycemia with dysregulation of carbohydrate, fat, and protein metabolism resulting from defects in insulin secretion, insulin action, or both (*4*). Diabetes mellitus is classified into two major types. Type 1 diabetes results from the autoimmune destruction of the insulin-producing beta cells of the islets of Langerhans in the pancreas. Type 2 diabetes is more common, and results from a combination of defects in insulin secretion and action, and is often associated with obesity (*5, 6*).

The prevalence of obesity and Type 2 diabetes is described as a global epidemic (*7*). In the United States, Type 2 diabetes is the leading cause of blindness, end-stage renal disease, and nontraumatic loss of limb, with associated health care costs estimated to exceed $130 billion per year (*8*). The hallmark of Type 2 diabetes is resistance to the action of insulin, mainly resulting in a defect in insulin-stimulated glucose transport in peripheral metabolic tissues such as adipose tissue and skeletal muscle, and a failure to inhibit hepatic glucose output (*9*). While the molecular basis of insulin resistance remains unclear, the development of effective therapies will rely largely upon a better understanding of the underlying pathophysiology of insulin resistance and the molecular mechanisms of insulin action.

I. Insulin-stimulated glucose uptake

In muscle and adipose tissues, glucose uptake is the rate-limiting step by which insulin increases glucose storage. Insulin-stimulated glucose uptake is mainly mediated through the insulin responsive facilitative glucose transporter GLUT4. Insulin increases glucose uptake, not by changing the activity of the transporter, but rather by changing its location. In the basal state, GLUT4 mainly resides in intracellular compartments, and then traffics to the plasma membrane in response to insulin, a process that is critical for lowering blood glucose levels after feeding (*3, 10*).

Glucose transporter family

In mammals, glucose uptake from the bloodstream is mediated by a family of highly related hexose transporters (GLUTs or SLC2As), containing 12 transmembrane domains with both the

amino and carboxyl termini exposed on the cytoplasmic side of the plasma membrane (*11*). As facilitative transporters, these proteins catalyze hexose transport across cell membranes via an ATP-independent, facilitative diffusion mechanism (*12*). The different expression patterns and hexose binding affinities reflect the physiological role of GLUT transporters in glucose sensing and utilization in different tissues. Some GLUT proteins are constitutively localized to the plasma membrane, while others are retained intracellularly and facilitate hexose transport by trafficking to the plasma membrane in response to cellular stimuli, adding an additional mechanism by which GLUT proteins can regulate sugar uptake and metabolism. The GLUT family consists of 13 members and is divided into three classes based on conserved structural characteristics and sequence similarities. Class I consists of GLUTs 1 – 4, which are, by far, the most well characterized transporters of the family. Class II is comprised of GLUT5 (a fructose-specific transporter), and GLUTs 7, 9, and 11. Class III includes GLUTs 8, 10, 12, and the proton-myoinositol symporter H^+-*myo*-inositol cotransporter (HMIT1), all of which are largely uncharacterized (*13, 14*).

GLUT1 was the first glucose transporter to be cloned, and consequently is the best studied. GLUT1 is a widely expressed protein required for the low constitutive level of glucose transport that supports basal cellular processes (*13, 15*). GLUT2 is a low affinity transporter for glucose, but high affinity for glucosamine, and is expressed in the liver, kidney, intestine, pancreatic beta cells, and regions of the brain. The GLUT2 transporter functions as a part of the glucose sensor system in beta cells, and is also required for absorption of glucose by intestinal epithelial cells. GLUT3 is enriched in neurons, testis, and muscle. This transporter is required for glucose to cross the blood-brain barrier. GLUT4 is highly expressed in muscle and white/brown adipose

tissues and changes its localization in response to insulin (*16*). As the major insulin-responsive GLUT isoform, the study of the structure, function, and localization of GLUT4 has been a major focus in understanding the development of Type 2 diabetes (*17-21*). The crucial role of GLUT4 in maintaining glucose homeostasis has been demonstrated in various genetically engineered mouse models. A global reduction in GLUT4 (as shown in mice heterozygous for GLUT4) results in diabetes (*22*). Muscle-specific GLUT4 knockout (MG4KO) mice show both decreased insulin- and exercise-induced glucose uptake in muscle, hyperglycemia, glucose intolerance and insulin resistance in the liver and adipose tissue (*23*). Adipose-specific GLUT4 knockout (AG4KO) mice show insulin resistance in liver and muscle and hyperinsulinemia (*24*). On the other hand, transgenic mice expressing high levels of GLUT4 in adipose tissue (*25*) or in skeletal muscle (*26*) show increased insulin sensitivity and glucose tolerance.

GLUT4 compartmentalization

The first evidence in support of the hypothesis that insulin causes the redistribution of what was then described as “glucose transport activity” from intracellular membrane compartments to the plasma membrane was presented from two independent groups in 1980 (*27, 28*). By measuring glucose binding and transport activity in membrane fractions isolated from rat adipocytes, they found that insulin decreased the number and function of glucose transporters in intracellular fractions, while increasing transporter function at the plasma membrane. Afterward, five independent groups identified and cloned the cDNA encoding GLUT4 (*17-21*). These early studies enabled the generation of isoform-specific antibodies and confirmed that the glucose transport activity identified in the 1980 experiments corresponded to the translocation of GLUT4

to the cell surface in response to insulin (*13*). However, in addition to the translocation hypothesis, several studies have also suggested that insulin may also regulate the intrinsic transport activity of a glucose transporter already present at the plasma membrane (*29, 30*) or insulin could stimulate gene expression of a transporter (*31*) inhibit its degradation, or both (*32*).

Although the redistribution of GLUT4 to the plasma membrane in response to insulin remains the dominant paradigm, controversy still exists regarding the compartmentalization and cycling of this specialized transporter. In the basal state and after insulin stimulation, GLUT4 is constantly recycling between the intracellular compartments and the plasma membrane. Insulin increases the rates of exocytosis and endocytosis to augment the surface levels of GLUT4 (**Figure 1.1**).

In the basal state, 4 – 10 % of GLUT4 is located at the cell surface and > 90% at intracellular compartments. This steady-state distribution of GLUT4 is the balance of its fast endocytosis and slow recycling (*33*). It is widely accepted that GLUT4 is internalized from the plasma membrane through clathrin-mediated endocytosis and clathrin-independent endocytosis (*34*). Diverse microscopy approaches have shown that GLUT4 is localized in small vesicular structures, early sorting recycling endosomal compartments, and trans-golgi network (TGN) (*35*). Studies involving the chemical ablation of transferrin receptor (TfR)-containing compartments using peroxidase-loaded TfR consistently identified two populations of GLUT4 pools: one overlapping with TfR, which is an endosomal recycling compartment marker, and another separate pool that sorted into a specialized GLUT4 storage compartment that lacks endocytotic markers, but

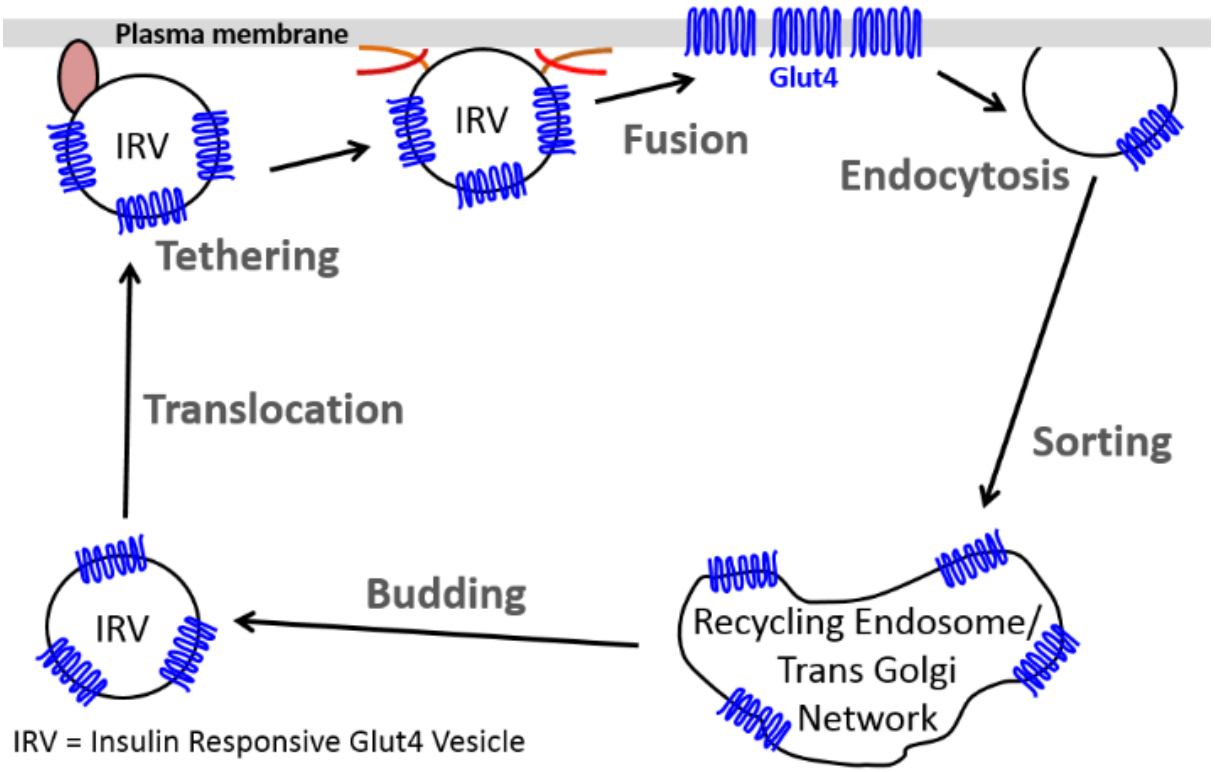

Figure 1.1 Schematic diagram of GLUT4 trafficking itinerary.
In the basal states, GLUT4 is sequestered in the intracellular compartments, GLUT4-storage vesicles (GSVs), which undergo dynamic sorting steps between early/recycling endosomes and the trans-golgi-network (TGN). GSVs finally sort into the insulin-responsive GLUT4 vesicles (IRVs). Following insulin stimulation, these IRVs translocate to the plasma membrane through targeted exocytosis, which process involves tethering, docking, and fusion. Insulin-stimulated GLUT4 translocation allows glucose uptake into cells. GLUT4 then undergoes endocytosis and resorting to recycle the IRVs.

contains markers of the TGN, such as the t-SNAREs (an acronym derived from soluble N-ethylmaleimide-sensitive factor attachment protein receptor") syntaxins 6, 16 and the clathrin adaptor AP-1 (*36-38*). This pool is also known as the insulin-responsive vesicles (IRVs) or GLUT4-storage vesicles (GSVs).

Most of the IRVs rapidly undergo exocytosis to the plasma membrane in response to insulin (*39*). While how GLUT4 is retained intracellularly remains uncertain, several studies suggested that GLUT4 is sequestered via a futile intracellular cycle of continual budding and fusion between recycling endosomes, the TGN, or both (*40*). The tethering protein called TUG may also play a role in basal retention by physically interacting with components of the IRVs and preventing them from translocating to the plasma membrane (*41*). Insulin, on the other hand, permits escape from the futile cycle, thereby stimulating exocytosis of GLUT4 vesicles to the plasma membrane. Therefore, IRVs sequester GLUT4 from the generalized recycling pathway to maintain low surface levels of GLUT4 in the basal state, but allow for GLUT4 trafficking to the plasma membrane in response to insulin. Biochemical characterization of the IRV has been difficult because of the presence of GLUT4 in many different membrane compartments within the cell, in addition to a lack of IRV-specific markers that can be used to purify this vesicle population. However, several studies have identified GLUT4, IRAP, sortillin, VAMP2, and most recently LRP1 as major components of the IRVs (*36*, *42-49*). The mechanisms that selectively recruit GLUT4 and other proteins into IRVs, as well as the means by which insulin stimulates the tethering, docking, and fusion of IRVs at the plasma membrane, remain to be further elucidated.

GLUT4 exocytosis

Exocytosis of the IRVs involves multiple steps including translocation to the plasma membrane (approach to the plasma membrane), tethering at sites that contain the necessary machinery for vesicle fusion, and finally fusion of the vesicles with the plasma membrane (*50*).

GLUT4 traffics to the plasma membrane along microtubule and actin cytoskeletal tracks. Evidence supporting the role of the cytoskeleton in GLUT4 translocation came from cytoskeleton-perturbing reagents such as nocodazole (for microtubules) and latrunculin (for actin filaments), resulting in the disruption of the integrity of the GLUT4 storage compartments (*51, 52*) and impaired insulin-stimulated glucose uptake and GLUT4 translocation (*52-60*).

Once at the plasma membrane, IRVs are targeted to specific tethering sites. The application of total internal reflection fluorescence (TIRF) microscopy to GLUT4 trafficking has provided significant advances in our understanding of insulin action in exocytosis of the IRVs. Although TIRF microscopy only analyzes trafficking events occurring within 150 nm of the cell surface (referred to as the TIRF zone) (*50*), these studies suggests that major sites of insulin regulation are at a tethering step and a step after tethering and before fusion called priming, which may represent SNARE complex formation (*61-63*). This tethering process is mediated by the exocyst, a large, evolutionarily conserved octameric protein complex (*64*). The exocyst consists of eight different subunits, Sec3, Sec5, Sec6, Sec8, Sec10, Sec15, Exo70, and Exo84. The exocyst functions in tethering events in localized membrane expansion, including basolateral protein sorting in epithelial cells, neuronal synaptogenesis, cytokinesis, and GLUT4 exocytosis (*65-69*).

The exocyst was originally identified in budding yeast three decades ago (*70*). Isolation of the complete complex from rat neurons established a role for the exocyst in mammalian vesicle exocytosis (*71*). Deletion of exocyst components in yeast, drosophila, and mice results in lethality, demonstrating that this complex is essential in yeast and higher organisms (*72-75*). Early studies in budding yeast implicated Sec3 and Exo70 as landmarks for the site of exocytosis (*76, 77*). Although it is not clear whether the rest of the subunits of the exocyst arrive individually or already assembled together, it was proposed that exocyst subunits arriving on vesicles assembled with Exo70 and Sec3 at the plasma membrane (*64, 77*). A low-resolution electron microscopy (EM) structure revealed that the exocyst forms a 'Y'-shaped structure (*78*). Structural studies further provided a model for exocyst architecture and assembly. Partial fragments of Exo70, Exo84, Sec15, and Sec6 were crystallized and these crystal structures of exocyst subunits display a common motif of tandem helical bundles that form extended rod-like structures, despite little sequence homology (*79-83*). EM studies of the mammalian brain exocyst and biochemical studies predict that the subunits pack together in a side-by-side manner in the assembled holocomplex (*78*). Purified exocyst fixed with glutaraldehyde takes on a 'Y'-shaped structure, proposing that each tip of the 'Y' bridging the approaching secretory vesicle in close enough proximity to the plasma membrane for SNARE complexes to form (*78, 79*). Consistent with this idea, electron tomography studies of cell plate formation in *Arabidopsis thaliana* showed 'Y-shaped' structures linking vesicles (*84*).

In addition to the conserved helical bundles, several exocyst subunits contain additional functional domains that interact with a number of small GTPases (*85-88*). It has been suggested that vesicle recognition by the exocyst and the exocyst assembly are regulated by small GTPases

(*64, 88-91*). Active Cdc42 and Rho1 bind competitively to the N-terminus of Sec3 in budding cells and target Sec3 to regions of the plasma membrane (*92, 93*). The yeast exocyst subunit Exo70 interacts with active Rho3 at the plasma membrane, and mutation of Rho3 disrupts secretory vesicle targeting and fusion (*94, 95*). However, the regulation of Exo70 by Rho3 is unclear, since yeast expressing a mutant form of the G protein that cannot bind to Exo70 failed to disrupt membrane recruitment of Exo70 (*96*). Targeting of exocytic vesicles to the plasma membrane not only depends on Exo70 and Sec3 binding to Rho GTPases but also binding to the phospholipid PI(4,5)P2 at the plasma membrane (*96, 97*). Genetic studies in yeast provided further insights on the regulation of the exocyst by small GTPases. Active Rab GTPase Sec4p on the secretory vesicle directly binds to Sec15, presumably for specific secretory vesicle recognition (*89*). Sec4p also bridges secretory vesicles to actin cables by interacting with the actin motor Myo2p (*98-101*). Therefore, it is likely that the coordination of the exocyst with small G proteins and motor proteins confers spatial and temporal specificity to secretory vesicle delivery.

Exocyst interactions with small GTPases are conserved in higher eukaryotes as well. In both mammals and *Drosophila*, Sec15 interacts with the Rab GTPase Rab11 to regulate endocytic recycling (*102-104*). ARF6 also controls endocytic recycling through its interaction with Sec10 (*105*). The interaction of RalA with two different exocyst subunits Exo84 and Sec5 recognizes the exocytic vesicles (*106, 107*). At the plasma membrane, the Rho GTPase TC10 interacts with Exo70 to mark the site of exocytosis (*67, 108*). These studies suggest that targeted exocytosis is regulated by various signaling inputs through interactions with this tethering complex.

The exocyst was first implicated in GLUT4 trafficking when Exo70 was identified as an effector protein for TC10 in a yeast two-hybrid screen (*67*). TC10 is activated downstream of the insulin receptor in lipid rafts (*109*) and Exo70 interacts with active TC10 on the plasma membrane, providing a site for the assembly of other exocyst proteins including Sec6 and Sec8 (*67, 110*). Disruption of the interaction between Exo70 and TC10 inhibits GLUT4 insertion into the plasma membrane, indicating that the exocyst functions at a step just prior to fusion (*67*). Studies have demonstrated that RalA resides on vesicles containing GLUT4 and is activated by insulin, resulting in its binding to the exocyst subunits, Exo84 and Sec5. RalA also interacts with the Calmodulin light chain of Myo1c and acts as a cargo recognition protein on the surface of GLUT4 vesicles for movement along actin tracks. Therefore, RalA engages with the exocyst and facilitates GLUT4 translocation to the plasma membrane in response to insulin (*111*). These studies identified essential roles of the exocyst and small G proteins in insulin-stimulated GLUT4 translocation (**Figure 1.2**).

Fusion of vesicles with their target membranes requires SNARE proteins. These proteins are localized in the transport vesicle (v-SNARE) as well as on the target membrane (t-SNARE) (*112*). Direct interactions between t-SNARE and v-SNARE proteins, in combination with accessory proteins, determine trafficking specificity required for membrane fusion (*113*).

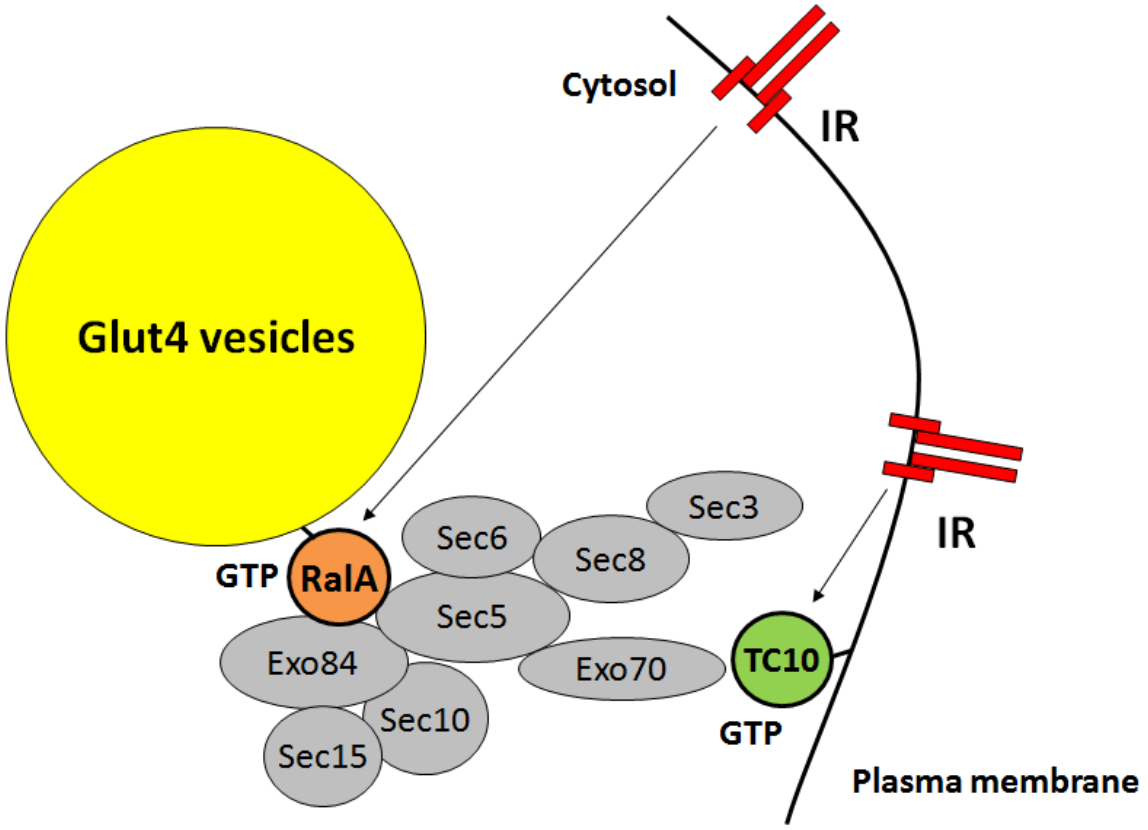

Figure 1.2 The exocyst in GLUT4 exocytosis.
Insulin stimulates exocyst assembly by activation of TC10 on the plasma membrane. The exocyst is also recognized by GLUT4 vesicles by activation of RalA in response to insulin. RalA engages with the exocyst by interacting with its effectors Sec5 and Exo84 and facilitates GLUT4 translocation to the plasma membrane.

Syntaxin 4 and SNAP23, which are t-SNAREs on the plasma membrane, have been implicated in insulin-stimulated GLUT4 vesicle trafficking in adipocytes. Synaptobrevin 2 (also known as VAMP2) and cellubrevin (also known as VAMP3) are two potential GLUT4 vesicle v-SNAREs expressed in adipocytes (*114-118*). Following translocation and docking of GLUT4 vesicles to the plasma membrane, these two v-SNAREs can form stable complexes with Syntaxin 4.

While the SNARE proteins comprise the minimal machinery necessary for membrane fusion, additional SNARE-associated proteins regulate fusion events (*13*). Synip interacts with Syntaxin 4 in the absence of insulin and prevents VAMP2 from pairing with Syntaxin 4. Insulin stimulation decreases the interaction between Synip and Syntaxin 4, thus permitting SNARE complex formation and GLUT4 fusion (*119*). Although insulin stimulation results in phosphorylation of Synip at Ser99 by the insulin-stimulated protein kinase Akt2, the importance of this phosphorylation event in regulating Synip binding to Sytaxin-4 is controversial (*120-122*). Moreover, several groups have shown that overexpression of Munc18c inhibits GLUT4 vesicle translocation, by binding to Syntaxin 4 with high affinity and blocking its ability to interact with VAMP2 (*123-125*). However, the role of Munc18c in regulating GLUT4 vesicle fusion is complicated and not completely understood. While initial experiments suggested that Munc18c dissociates from syntaxin-4 in response to insulin, follow-up reports have instead suggested that the interaction site between Munc18 and syntaxin-4 changes upon insulin stimulation, allowing SNARE complex formation and vesicle fusion (*124, 126*).

II. Insulin signaling pathways in GLUT4 translocation

Insulin regulates energy metabolism by exerting a variety of effects on cells. It controls cell growth and survival as well as synthesis and storage of proteins, carbohydrates, and lipids. Following a meal, increased nutrients in the blood lead to secretion of insulin to maintain glucose homeostasis. In muscle and adipose tissues, insulin activates signaling cascades that stimulate glucose uptake by engaging the trafficking machineries that regulate GLUT translocation to the plasma membrane (*1, 3, 10*).

Insulin receptor

Insulin signaling is initiated when insulin binds to its cell surface receptor, which belongs to a subfamily of receptor tyrosine kinases (*127, 128*). The insulin receptor (IR) is heterotetrameric protein complex, consisting of two extacellular α subunits and two transmembrane β subunits with tyrosine kinase activity (*13, 129*). Upon binding of insulin to the α subunits, the IR undergoes a conformational change that brings each β subunit in close proximity to allow for transphosphorylation on specific tyrosine residues in the kinase domain (*130-132*). This results in the increased catalytic activity of the kinase, and increased autophosphorylation at multiple tyrosine residues in the juxtamembrane regions and intracellular tail (*133*). Once activated, the IR recruits and phosphorylates a number of intracellular substrates, such as insulin receptor substrate family (IRS1 – 4), Shc, Grb1, and APS (*134-139*). The phosphorylated tyrosine residues in these substrates serve as docking sites for proteins that contain the Src homology 2 (SH2) domain that specifically recognize different phosphotyrosine motifs (*139-141*).

To examine the role of the IR in energy homeostasis, several genetic ablation studies were carried out in mice (*142*). Whole-body IR knockout mice are born with normal features, but develop early postnatal diabetes and die of ketoacidosis before reaching adulthood (*143*, *144*). Mice lacking IR in specific cell types as a result of conditional mutagenesis further provided specific roles in insulin signaling. Conditional IR knockout in skeletal muscle (MIRKO) leads to impaired insulin signaling and decreased insulin-stimulated glucose transport, without systemic insulin resistance (*145*). Mice with combined ablation of IR in muscle and adipose tissue show impaired glucose tolerance and develop a more severe metabolic phenotype than MIRKO mice, suggesting that adipose tissue provides partial metabolic compensation for muscle insulin resistance in MIRKO mice (*146*). Mice with a specific knockout of the IR in both white and brown fat (FIRKO) are protected against obesity, and have normal glucose tolerance (*147*). Liver-specific IR knockout (LIRKO) mice exhibit dramatic insulin resistance, severe glucose intolerance, and a failure of insulin to suppress hepatic glucose production and to regulate hepatic gene expression (*148*). Mice lacking IR in beta cells (βIRKO) result in a selective impairment of glucose-dependent insulin release, and thus impaired glucose tolerance (*149*). Brown adipose tissue-specific IR knockout (BATIRKO) mice result in beta cell failure, giving rise to hyperglycemia (*150*). Neuron-specific IR knockout (NIRKO) mice result in increased food intake and moderate diet-dependent obesity (*151*). These data indicate that the insulin receptor plays a variety of roles in different tissues.

Phosphoinositide 3-kinase (PI3K)-dependent signaling

Among the IR substrates, the best characterized is the IRS family (*139*). These proteins contain a pleckstrin homology (PH) domain and phosphotyrosine binding (PTB) domain at the N-terminus. The PTB domain binds to the NPXY motif on the IR, and PH domain mediates the interaction of protein with phosphatidylinositol lipids in the plasma membrane. Tyrosine-phosphorylated IRS serves as docking sites for the SH2 domain of the p85 regulatory subunit of class I PI3K, and directly activates the p110 catalytic subunits of PI3K leading to the activation of the enzyme (*152*). Active PI3K subsequently generates phosphatidylinositol-3,4,5-trisphosphate (PtdIns(3,4,5)P_3; PIP3) from PtdIns(4,5)P_2 at the plasma membrane. This conversion is reversed by the tumor suppressor protein PTEN (phosphatase and tensin homolog deleted on chromosome ten), which is a phospholipid phosphatase that antagonizes the action of PI3K by dephosphorylating PIP3 (*153, 154*). PIP3 in turn binds to several PH domain-containing Ser/Thr kinases, including phosphoinositide-dependent kinase 1 (PDK1) and AKT (also known as PKB) (*155, 156*).

Pharmacological inhibitors, small interfering RNA (siRNA)-mediated knockdown, and animal models have established the essential role of PI3K in glucose uptake and energy homeostasis. Treatment of cells with the PI3K inhibitors wortmannin or LY294002, or transfection with dominant-negative PI3K blocks insulin-stimulated glucose uptake, whereas overexpression of constitutively active PI3K stimulates GLUT4 translocation (*157-161*). In mouse models, deletion of the catalytic subunit of PI3K results in glucose intolerance, and deletion of PTEN in adipose tissue increases insulin sensitivity (*162, 163*).

Akt is a kinase belonging to the AGC (PKA/PKG/PKC) family of serine/threonine kinases and shares a common domain structure with other members of this family of kinases. Akt contains a PH domain at its N-terminus that binds to PIP3, followed by a catalytic domain, and a regulatory hydrophobic motif at its C terminus. Translocation of Akt to the plasma membrane is mediated through the interaction between its PH domain and PIP3, which is the rate-limiting step in Akt activation (*164*). PDK1 phosphorylates Akt on Thr308 in the catalytic domain, but full activation of Akt also requires phosphorylation of Ser473 in the hydrophobic motif at the C-terminus by the Rictor/mTOR/Sin1 protein complex, called mTORC2 (*165-170*). Once activated, Akt phosphorylates multiple target proteins at a consensus RXRXXS/T motif (*171, 172*).

Akt is a critical regulator of insulin-stimulated glucose transport. Mammals have three highly homologous isoforms of Akt (Akt 1 – 3). Overexpression of a constitutively active myristoylated Akt mutant increases insulin-stimulated glucose uptake and GLUT4 translocation (*173, 174*). In contrast, overexpression of a dominant-negative mutant of Akt, siRNA-mediated knockdown of Akt isoforms, or inhibitors of Akt block insulin-stimulated Glut4 translocation (*175-178*). Targeted deletion of Akt1 in mice suggests that Akt1 is required for growth but is dispensable for maintenance of glucose homeostasis (*179*). In contrast, mice lacking Akt2 develop insulin resistance and diabetes (*180, 181*). Akt3 knockout mice display normal glucose metabolism but Akt2 and Akt3 double knockout mice display a phenotype similar to Akt2, indicating that Akt3 is likely not a significant player in regulating glucose homeostasis (*182, 183*).

Akt serves as a central hub to regulate insulin-stimulated glucose uptake by connecting insulin signaling with downstream regulators of GLUT4 trafficking (*10*). Interestingly, Akt seems to

play a role in multiple steps during GLUT4 trafficking. Using antibodies that recognize phosphorylation of proteins at Akt consensus sites (RXRXXpS/pT; termed the phospho-Akt substrate antibody) has been a useful tool for the identification of novel Akt substrates, some of which play a critical role in regulating GLUT4 vesicle trafficking. The most well known targets of AKT are the Rab GTPase activating proteins (GAP) AS160 (also known as TBC1D4, which targets RAB8, RAB10 and RAB14) and the Ral-GAP complex (RGC, which is comprised of a regulatory subunit (RGC1) and a catalytic subunit (RGC2) and targets RalA). Akt directly phosphorylates AS160, containing six consensus Akt phosphorylation sites (*184-187*). AS160 undergoes phosphorylation in response to insulin and this phosphorylation inhibits its GAP activity, and thus results in increased activity of their cognate G proteins (*184, 188*). However, the identity of these Rabs and their role in GLUT4 trafficking remain unclear. Similarly, AS250 (Akt substrate of 250 kDa), now known as RGC2, is identified by virtue of its interaction with a phospho-Akt substrate antibody (*189, 190*). Insulin inhibits the RGC1/2 through Akt2-catalyzed phosphorylation of RGC2 on at least three different residues allowing RalA activation (*189*). This phosphorylation of RGC2 also mediates the interaction with 14-3-3 proteins, and this interaction inhibits RGC function in cells (*191*). Although the precise regulation of RGC1/2 and the role of RalA in GLUT4 trafficking remain unclear, RGC1/2 links PI3K/Akt signaling to RalA activation in response to insulin and RalA is required for insulin-stimulated glucose uptake. Akt is also known to regulate the fusion process of GLUT4 vesicles by directly targeting SNARE regulatory proteins, such as Synip and CDP138, a previously uncharacterized protein containing a Ca^{2+}-binding C2 domain (*119, 122, 192*). Insulin-mediated regulation of Synip occurrs through Akt-catalyzed phosphorylation at Ser99, but the importance of this phosphorylation in GLUT4 trafficking is controversial. Overexpression of a phosphorylation-

deficient S197A mutant or a Ca^{2+}- and lipid binding-deficient mutant of CDP138 blocked GLUT4 vesicle fusion but had no effect on vesicle accumulation at the plasma membrane, suggesting that CDP138 positively regulates GLUT4 insertion into the plasma membrane. Whether Akt regulates other steps in GLUT4 trafficking remains unknown, and the search for additional Akt targets will probably give further insight into the specific steps of GLUT4 trafficking that are regulated by this kinase.

PI3K-independent signaling

Several studies suggest that signals independent of the PI3K pathway also regulate insulin-stimulated glucose uptake (*193-195*). The discovery of a pool of IR in caveolae suggests that a separate insulin signaling pathway exists within this microdomain of the plasma membrane (*196, 197*). Caveolae are a subset of lipid rafts that are microdomains of the plasma membrane, enriched in cholesterol, sphingolipids, glycolipids, and lipid-modified signaling proteins (*198*). Inhibition of the PI3K pathway with pharmacological inhibitors does not affect signaling from lipid rafts. Furthermore, interruption of caveolae in mature adipocytes leads to defects in insulin receptor localization, insulin signaling, and glucose uptake, establishing that the caveolae-localized insulin receptor is active and initiates a second signaling cascade that regulates GLUT4 trafficking independently of PI3K (*197*). Mutants of the IR have been identified in which the stimulation of PI3K activity is intact, but which are defective in promoting GLUT4 translocation (*199*). Incubating cells with a cell-permeable analog of PIP3 does not stimulate glucose uptake in the absence of insulin (*194*). Consistent with this, overexpression of constitutively active PI3K mutants do not fully mimic insulin-stimulated GLUT4 translocation to the plasma membrane

(*159*). These studies indicate that the PI3K pathway is required for insulin-stimulated GLUT4 translocation but additional parallel signaling pathways exist.

The PI3K independent signaling pathway is initiated in adipocytes when activation of the IR promotes tyrosine phosphorylation of APS, an adaptor protein containing PH and SH2 domains. APS exists as a homodimer, and is recruited to the IR upon its activation and autophosphorylation (*200, 201*). Phosphorylated APS recruits a complex that comprises the proto-oncogene c-Cbl and CAP (c-Cbl-associated protein). The SH2 domain in c-Cbl binds to the pY618 residue on APS, while an SH3 domain within CAP interacts with proline-rich sequences in APS (*202-204*). CAP also interacts with an integral membrane protein that localizes to caveolae called flotillin through its N-terminal SoHo (Sorbin Homology) domain (*205, 206*). This recruitment triggers IR-catalyzed Tyr phosphorylation of c-Cbl (*204*). Phosphorylated c-Cbl then interacts with the adaptor protein CRK, which constitutively associates with the guanine nucleotide exchang factor (GEF) C3G (*135, 207-209*). Recruited C3G in turn catalyzes the activation of the small G protein TC10, a member of the Rho family of small GTPases that is localized in lipid rafts (*109, 210*). Active TC10 interacts with effector proteins that regulates GLUT4 vesicle exocytosis. For example, the exocyst subunit Exo70 is one of the effector proteins of TC10. Exo70 is required for targeting of GLUT4 vesicle to the plasma membrane, and targeting of Exo70 to lipid rafts is required for glucose uptake and GLUT4 docking at the plasma membrane in response to insulin (*67*). In skeletal muscle, the PI3K-dependent signaling pathway is absolutely required for GLUT4 exocytosis but the necessity of the PI3K-independent pathway is unknown (*10*). Disrupting individual components of the PI3K-dependent or the PI3K-independent signaling pathways in adipocytes, either with pharmacological inhibitors or by

siRNA-mediated knockdown, inhibits GLUT4 exocytosis and glucose uptake (*158, 160, 203, 211-213*). These studies suggest that these pathways coordinate each other to regulate insulin-stimulated glucose uptake (**Figure 1.3**).

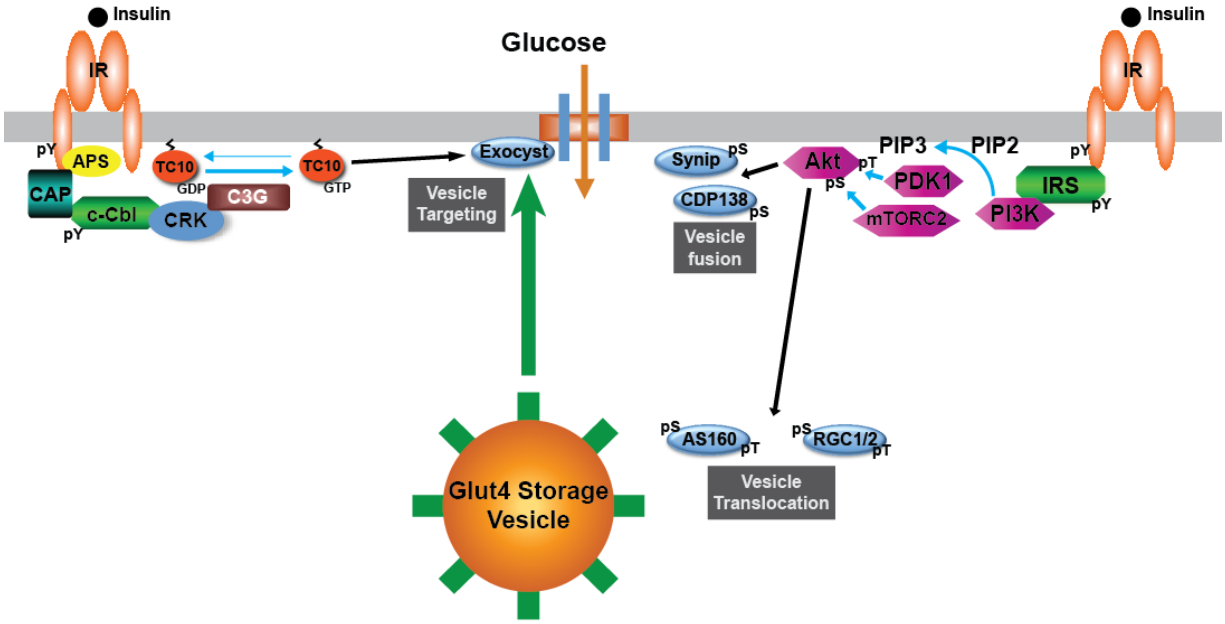

Figure 1.3 Insulin signaling regulates GLUT4 trafficking.
Insulin causes GLUT4 translocation to the plasma membrane through two distinct major pathways. In the PI3K-dependent pathway, insulin increases the tyrosine phosphorylation of IRS proteins, promoting the association and activation of PI3K. PIP3 is the major phosphoinositide generated by PI3K. It recruits and activates PDK1, which phosphorylates and activates Akt. Phosphorylation of AS160 and RGC1/2 by Akt allows GLUT4 trafficking to proceed. Phosphorylation of Synip and CDP138 allows GLUT4 vesicles to fuse with the plasma membrane. In the adipose cell-specific PI3K-independent pathway, the insulin receptor phosphorylates Cbl, a process that requires APS and CAP. Cbl then recruits a complex containing the adapter protein CrkII and the guanyl nucleotide exchange factor C3G, which in turn activates the lipid raft-associated protein TC10. Both of these signaling cascades are required for insulin-stimulated GLUT4 translocation in adipocytes.

III. Small G proteins in insulin-stimulated glucose uptake

The small G protein superfamily consists of more than 100 small molecular weight (20 - 25 kDa) proteins that bind to guanosine nucleotides. The members of this superfamily are structurally classified into at least five families: the Ras, Rho, Rab, Sar1/Arf, and Ran families. They regulate a wide variety of cell functions spatially and temporally. The Ras family regulates gene expression, the Rho family regulates cytoskeletal reorganization and gene expression, the Rab and Sar1/Arf families regulate vesicle trafficking, and the Ran family regulates nucleocytoplasmic transport and microtubule organization (*214*). Insulin tightly regulates the activity of G proteins at distinct locations (*215*). G proteins integrate signals from upstream proteins to engage GLUT4 trafficking machineries in response to insulin.

Regulation of G proteins

All small G proteins have consensus amino acid sequences responsible for specific interactions with GDP, GTP, and for GTPase activity, which hydrolyzes bound GTP to GDP and inorganic phosphate (Pi) (*216-218*). They also have a region for interacting with downstream effectors. These proteins behave as “molecular switches”, and their activity changes depending on the nucleotide binding state, allowing these proteins to turn biological processes on or off. G proteins contain two enzymatic activities: a hydrolysis activity that converts GTP to GDP, and an exchange activity that allows the protein to release GDP and bind to GTP (*216, 217*). In the GTP-bound form (active state), G proteins bind to downstream proteins, called effectors, which mediate the biological effects of upstream signaling events. Some G proteins share overlapping effectors, while other effectors have high affinity binding for only one G protein. In the GDP-

bound form (inactive state), the G protein does not interact with effector proteins, and thus halts the transmission of upstream signals. In addition, small G proteins belonging to Ras, Rho/Rac/Cdc42, and Rab family proteins have sequences at their C termini that undergo post-translational modification with lipid, such as farnesyl, geranylgeranyl, palmitoyl, and methyl moieties, and proteolysis (*217*, *219*-*222*). Therefore, the activity state and differential subcellular localization of G proteins provide spatial and temporal regulation of signaling events.

The transition between the active and inactive state is controlled by at least three families of regulatory proteins. The slow intrinsic GTPase activity of G proteins is accelerated by GTPase activating proteins (GAPs), which promote GTP hydrolysis. Guanine nucleotide exchange factors (GEFs) stimulate the exchange of GDP for GTP to generate the active form. In addition, guanine nucleotide dissociation inhibitors (GDIs) prevent dissociation of GDP, thereby maintaining G proteins in an inactive state (*223*) (**Figure 1.4**). GEFs or GAPs are tightly regulated by changing their subcellular localization or conformation. These can be mediated through signaling by upstream regulators, phosphorylation, and interaction with either proteins or lipids (*224*, *225*).

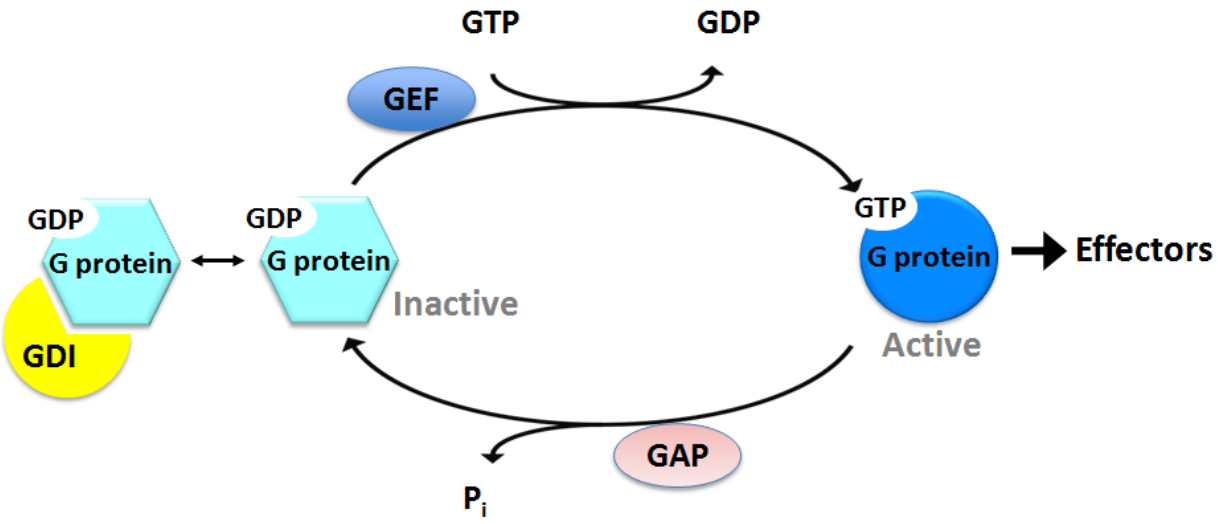

Figure 1.4 The regulation of G protein cycle by GEFs, GAPs, and GDIs.
G proteins cycle slowly between an inactive (GDP-bound) and an active (GTP-bound) conformation. To ensure signaling specificity, G proteins are controlled by their regulators. GEFs bind with highest affinity to GDP-bound G proteins and promote exchange of GDP for GTP. GAPs bind with highest affinity to GTP-bound G proteins and promote GTP hydrolysis. GAPs and GEFs are highly regulated by upstream signals. In some cases, GDIs prevent dissociation of GDP, thereby maintaining G proteins in inactive state. When G proteins are bound to GTP, effectors are recruited to mediate the downstream effects of the GTPases.

Small G proteins in insulin-stimulated glucose uptake

G proteins of the Ras, Rho, Rab, and Arf subfamilies have all been implicated in the regulation of GLUT4 translocation in multiple steps including GLUT4 compartmentalization, cytoskeletal rearrangements, tethering, and docking (**Figure 1.5**).

Ras subfamily

Ras is activated downstream of the IR and initiates a signaling pathway that leads to phosphorylation and activation of mitogen-activating protein kinase (MAPK) by the upstream MAPK kinase (MEK). The role of MAPK in insulin-stimulated glucose uptake is still controversial (*226-230*). Activation of the Ras/MAPK pathway by stimulation with PDGF or EGF, or inhibition of the pathway by treatment with the MEK inhibitor PD98059 had no effect on insulin-stimulated glucose uptake in 3T3-L1 adipocytes (*195*, *226*, *228*). However, treatment with the MEK inhibitor U-0126 or the MAPK inhibitor SB203580 blocked insulin-stimulated glucose uptake, without affecting translocation of GLUT4 in 3T3-L1 adipocytes (*231*, *232*). Transgenic mice overexpressing Ras in adipose tissue also increase basal and insulin-stimulated glucose uptake by upregulating GLUT1 expression rather than affecting GLUT4 translocation (*227*, *230*).

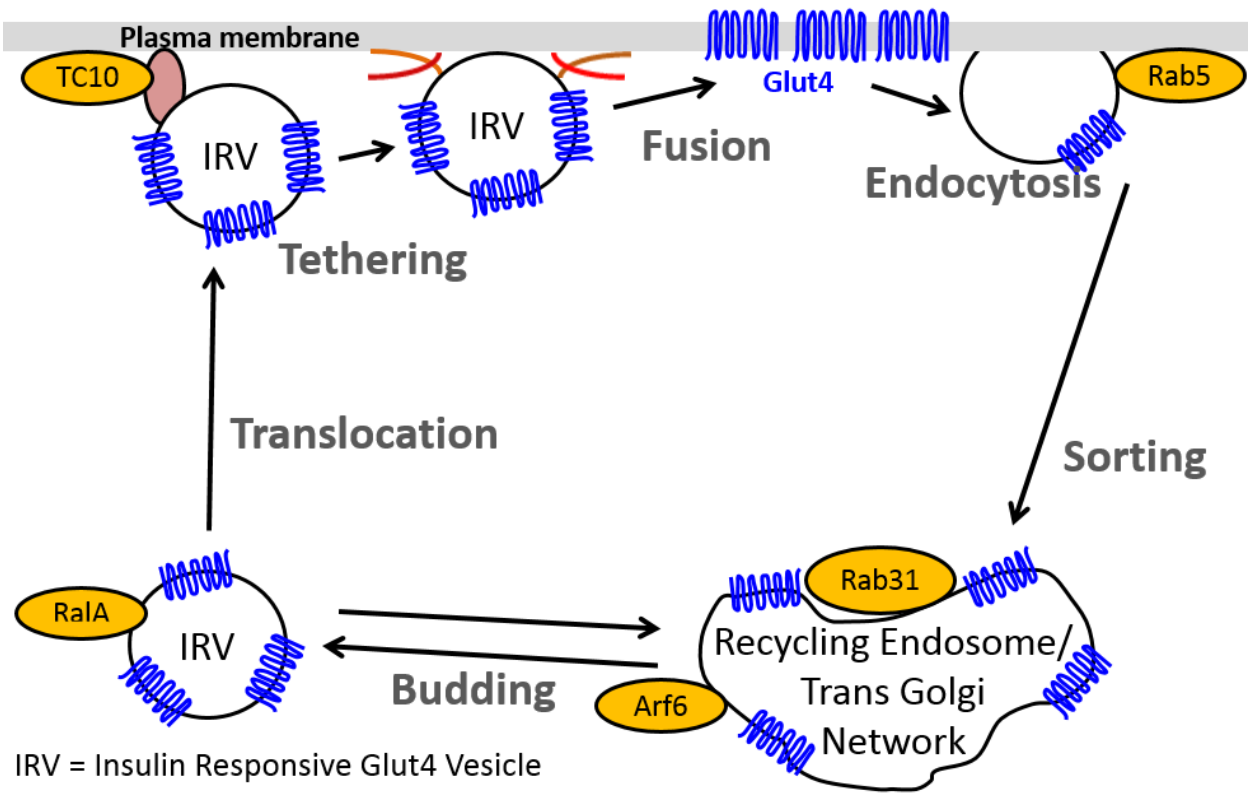

Figure 1.5 Small G proteins in GLUT4 trafficking.
GLUT4 is internalized dependent upon Rab5 activity. GLUT4 is sorted from early/sorting endosomes into recycling endosomes or TGN. Arf6 may be involved in biogenesis of IRVs. Rab31 retains GLUT4 at the intracellular compartments by promoting a futile cycle between IRVs and endosomal compartments in the basal state. RalA is co-localized in GLUT4-containing vesicles and facilitates GLUT4 translocation by tethering GLUT4 vesicles at the plasma membrane. TC10 targets GLUT4 vesicles to sites of exocytosis on the plasma membrane.

Two highly related Ral GTPases, RalA and RalB are members of the Ras superfamily (*233*). Although they are 85% identical and share similar structure and effectors, they do not completely functionally overlap in cells. While both RalA and RalB can interact with subunits of the exocyst, the affinity for RalB is lower than RalA, and RalA may play a bigger role in exocyst function in certain physiological settings, such as basolateral membrane trafficking in epithelial cells (*65*). The exocyst subunits Exo84 and Sec5 bind competitively to active RalA and RalB (*87, 106, 107*). As discussed previously, RalA associates with the GLUT4 vesicle through engaging the exocyst and the myosin motor Myo1c to transport and tether GLUT4 vesicles to the plasma membrane (*111*). Interaction between RalA and the exocyst is required for insulin-stimulated GLUT4 translocation (*234*).

Rho subfamily

Mammalian Rho GTPases comprise a family of 20 intracellular signaling molecules containing classically activated Rho GTPases and atypical proteins, which are not thought to be regulated by GEF/GAPs but regulated by gene expression, protein stability, and phosphorylation. Most Rho GTPases regulate a variety of processes, including morphogenesis, migration, neuronal development, cell division/adhesion, vesicle transport, microtubule dynamics, cell cycle progression, and gene expression (*235*). Cytoskeletal rearrangement plays an important role in GLUT4 vesicle trafficking (*13*). However, the role of Rho, Rac, and Cdc42 in insulin-stimulated glucose transport remains controversial. Overexpression of Rho and Rac had no effect on GLUT4 exocytosis, but others also showed that Rho and Rac are positive regulators in GLUT4 translocation (*109, 236-239*). Furthermore, insulin activates Rac in a PI3K dependent manner

(*240*). Similarly, Cdc42 had no effect on GLUT4 translocation and glucose uptake, but others showed that insulin activates Cdc42 and depletion of Cdc42 decreases insulin-stimulated GLUT4 translocation (*109, 241*). The reasons for these discrepancies are not clear.

TC10α and TC10β are mammalian G proteins closely related to Cdc42. However, they play distinct roles in cells probably depending on their subcellular localization (*242-245*). Several studies suggest that TC10 plays an important role in insulin-stimulated glucose transport. TC10 is highly expressed in insulin-responsive tissues such as muscle and fat, and is rapidly activated in response to insulin (*109, 210*). Knockdown of TC10α blocks insulin-stimulated GLUT4 translocation and glucose uptake (*213*). Overexpression of dominant-negative TC10α, but not TC10β, also blocks insulin-stimulated GLUT4 exocytosis, suggesting TC10α primarily functions in adipocytes to regulate glucose uptake (*210*).

The TC10 effectors CIP4, Par6 of the Par3/6 complex, and Exo70 have all been implicated in GLUT4 exocytosis (*67, 246, 247*). In an effort to identify downstream targets of TC10, the adaptor protein CIP4 (Cdc42-interacting protein 4) was identified as a TC10 effector in a yeast two-hybrid screen. Upon TC10 activation in response to insulin, CIP4 is recruited to the plasma membrane, where it binds to active TC10. Overexpression of a CIP4 mutant that cannot translocate to the plasma membrane or interact with TC10 results in inhibition of GLUT4 translocation (*246*). CIP4 forms a stable complex with Gapex-5 through an interaction between CIP4's SH3 domain and a proline-rich sequence within Gapex-5. Gapex-5 contains a RasGAP domain at its N-terminus and a VPS9 domain at its C-terminus that has exchange activity toward Rab5 family members. In the basal state, CIP4 is constitutively associated with Gapex-5, which

activates the Rab5 family G protein Rab31 (*248, 249*). Rab31 promotes the IRVs recycling back into the recycling endosome that results in GLUT4 retention in intracellular compartments (*248*). Translocation of CIP4 and Gapex-5 to the plasma membrane in response to insulin leads to the reduction of Rab31 activity, allowing exit of GLUT4 vesicles from the futile cycle, and traffic to the plasma membrane (*248*). Once recruited to the plasma membrane, Gapex-5 activates Rab5, which increases PIP3 formation at the plasma membrane, a phosphoinositide species that facilitates targeting of GLUT4 through a mechanism that may involve APPL1 (adaptor protein, phosphotyrosine interaction, PH domain and leucine zipper containing 1) (*249-251*).

Atypical PKCs (PKC ζ/λ) belong to the AGC subfamily of kinases that can be phosphorylated by PDK1 in response to insulin. Atypical PKCs have been shown to play an important role in glucose transport (*247, 252-255*). Par3 and Par6 are scaffolding proteins that link PKC ζ/λ with the Rho family GTPases Cdc42 and Rac (*256*). Upon TC10 activation in response to insulin, active TC10 interacts with Par6 leading to the localization to the plasma membrane. Owing to the close proximity to PDK1, PDK1 phosphorylates and activates PKC ζ/λ. Therefore, Par6 seems to be a convergent downstream target to regulate GLUT4 exocytosis between the PI3K-dependent and PI3K-independent pathways in response to insulin (*247*).

Another protein identified in a yeast two-hybrid screen using TC10 as bait is Exo70, a subunit of the exocyst (*67, 96*). Active TC10 recruits Exo70 to the plasma membrane by direct interaction and other exocyst subunits Sec6 and Sec8 undergo similar translocation. Knockdown of exocyst subunits or overexpression of dominant interfering mutant of Exo70, which blocks the

interaction with active TC10 inhibits GLUT4 fusion, indicating that assembly of the exocyst is a critical step in insulin-stimulated GLUT4 translocation (*67, 110*).

Rab subfamily

Rab proteins constitute the largest family of small G proteins. Numerous studies have shown that Rab GTPases are critical for tethering/docking of vesicles to their target compartments, budding of vesicles, and movement of vesicles along the cytoskeleton (*257*). A number of different Rab proteins, including Rab4, 5, 8, 10, 11, 14 and 31 have been implicated in GLUT4 trafficking. These GTPases are localized to distinct subcellular compartments and influence various steps of GLUT4 vesicle trafficking including endocytosis, exocytosis, and intracellular retention of GLUT4.

Rab4 localizes to the early and recycling endosomes and regulates sorting from this compartment (*258-260*). Rab 4 has also been detected in IRVs (*261*). Overexpression of the Rab4 dominant negative mutant blocks insulin-stimulated GLUT4 translocation (*262*). The Rab4 and Rab5 effector Rabip4 may be involved in endosome sorting of GLUT4 into IRVs and overexpression of Rabip4 increases insulin-stimulated GLUT4 translocation (*263*). However, the exact molecular mechanism by which Rabip4 regulates GLUT translocation is unclear. Rab4 is also activated downstream of PI3K/PKCλ, and upon activation interacts with the motor protein KIF3 to mediate microtubule movement of IRVs to the plasma membrane (*264*).

Rab5 has been implicated in GLUT4 endocytosis and exocytosis. Rab5 may regulate endocytosis of the vesicle due to its interaction with dynein, a motor protein that is involved in clathrin-dependent internalization of Glut4 (*265*). In contrast, binding of Rab5 to its effector APPL1 positively regulates GLUT4 exocytosis (*250, 251*).

Rab11 regulates the traffic of recycling endosomes to the TGN as well as recycling endosomes back to the plasma membrane (*266, 267*). Rab11 is associated with GLUT4 vesicles, and these pools are translocated to the plasma membrane in response to insulin (*268*). Overexpression of a dominant interfering fragment of a Rab11 effector Rab11-BP blocks GLUT4 sorting into the IRVs (*37*). Similarly, overexpression of dominant negative Rab11 in muscle cells blocks insulin-stimulated GLUT4 translocation and glucose uptake (*269*).

Rab8, 10, and 14 were identified as AS160 targets (*270*). Overexpression of wild type or constitutively active Rab10 in 3T3-L1 adipocytes increases basal GLUT4 exocytosis without effecting insulin-stimulated GLUT4 exocytosis, whereas knockdown of Rab10 decreased insulin-stimulated GLUT4 translocation without effect on basal GLUT4 translocation (*271*, *272*). However, overexpression of wild type Rab8 or Rab14 in the presence of phosphorylation-deficient AS160 (4P-AS160) partially overcomes the inhibitory effect of 4P-AS160 on basal and insulin-stimulated GLUT4 exocytosis (*273*). Rab10 is a *bona fide* target of AS160 and active Rab10 can increase the GTP binding of RalA by recruiting the Ral GEF Rlf/Rgl2 (*274*). However, insulin-stimulated activation of Rabs 8, 10, 14 has not been shown, and the trafficking machineries regulated by these Rabs are still unknown.

ADP-ribosylation factors (Arfs)

The ARF subfamily of small G proteins recruits coat proteins from the cytosol to membrane compartments to mediate protein sorting, membrane deformation, and vesicle budding. In the inactive state, ARFs are localized in the cytosol. Upon activation, these proteins recruit coat proteins to the site of vesicle bud formation in the membrane compartment (*275, 276*). In adipocytes, Arf proteins are thought to be involved in the formation of IRVs from the TGN and/or recycling endosomes. Recent studies have suggested that Arf6 forms a vesicle coat in coordination with clathrin, AP-1, GGAs (Golgi-localized, γ-ear-containing, Arf-binding proteins), and ACAP-1 to package IRV proteins into vesicles budding from the TGN/endosome. Expression of dominant negative GGA2 in 3T3-L1 adipocytes decreases insulin-stimulated glucose uptake, reduces the amount of GLUT4 in small vesicles, and increases the amount of GLUT4 in the TGN/recycling endosome, suggesting a defect in generation of IRV pools (*277, 278*). GGAs likely mediate IRV formation by interacting with the cytoplasmic domain of sortillin, which recent evidence suggests is in a complex with GLUT4 and other IRV components, and concentrates these proteins into vesicles forming on the TGN/recycling endosome (*277, 279*). There is also evidence that Arf interacts with the clathrin adaptor protein AP-1 on the TGN/recycling endosome and participates in IRV biogenesis, perhaps in coordination with GGAs (*280-282*). The ArfGAP ACAP-1 interacts with both clathrin heavy chain (CHC) and GLUT4 during vesicle formation on the TGN/recycling endosome and ACAP-1 and CHC is required for insulin-stimulated GLUT4 translocation (*283*).

IV. Roles of IKK-related kinases

The IκB kinase (IKK) family of protein is composed of four members: IKKα, IKKβ, IKKε, and TBK1 (Tank binding kinase 1) (*284*). IKKα, IKKβ and IKKγ form the classical IKK complex in response to diverse extracellular stimuli, including bacterial/viral infection, pro-inflammatory cytokines, and DNA damaging agents, such as phorbol esters and ultraviolet irradiation (*285, 286*). IKK-related kinases (IKKε and TBK1) were identified via sequence similarity to IKKα and IKKβ (*287-290*). Like IKKα and IKKβ, IKKε and TBK1 have a kinase domain in N-terminal, LZ (leucine zipper) and a potential HLH (helix-loop-helix) motif in C-terminal (**Figure 1.6**). Except IKKα, IKKβ, IKKε, and TBK1 also contain ubiquitin-like domain (ULD) whose function is not clear (*291*). IKKε and TBK1 are not components of the classical IKK complex. Instead, they bind to their scaffolding protein TANK to form the noncanonical IKK-related kinase complex. In addition, IKKε and TBK1 are activated by various stimuli such as PMA, LPS, and PDGF (platelet-derived growth factor) (*284*).

In the classical IKK complex, IKKα and IKKβ are catalytic subunits and IKKγ is a regulatory subunit of the complex (*292-294*). The formation of classical IKK complex is important to phosphorylate IκBs, which are inhibitory proteins of NFκB transcription factors (*295, 296*). Upon phosphorylation of IκBs in N terminus, IκB proteins are polyubiquitinated and then degraded by the 26S proteasome (*297*). Therefore, phosphorylation of IκBs by IKK complex liberates NFκBs to enter the nucleus, where it promotes transcription of target genes encoding cytokines, chemokines, and regulators of apoptosis (*286, 298, 299*). NFκB transcription factors form a heterodimer composed of members of the NFκB/Rel family. There are five NFκB

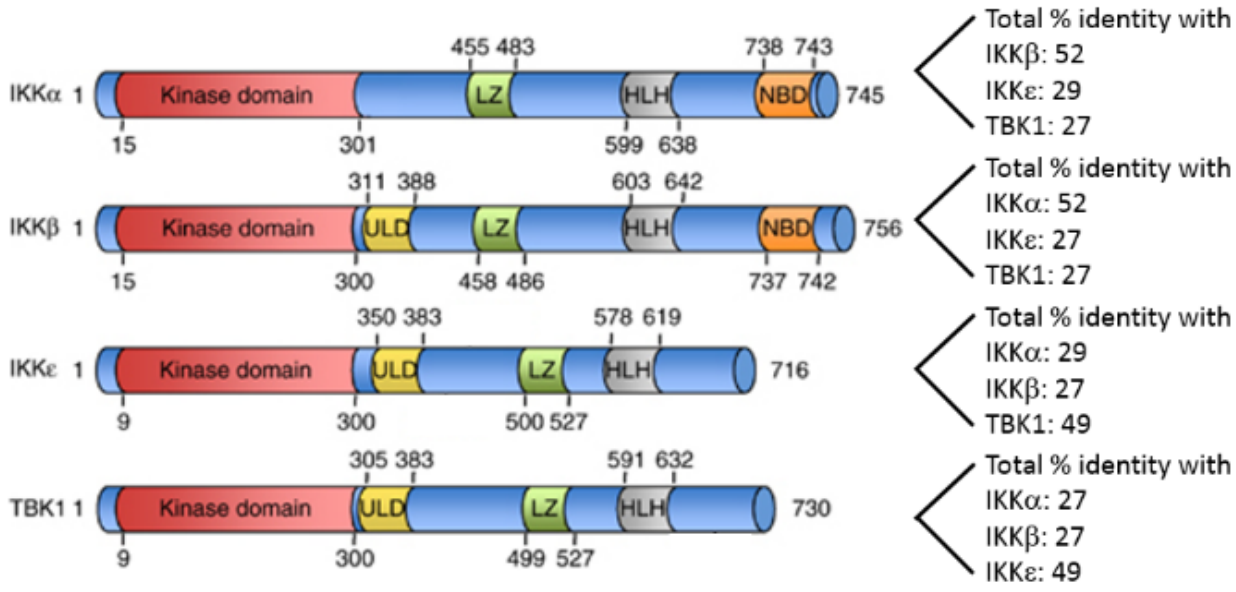

Figure 1.6 Structural comparison of the classical and noncanonical IKKs.
Each IKK kinase is composed of the major domains as shown with amino-acid numbers that correspond to the human proteins. IKK kinases contain kinase domain, leucine zipper (LZ), and helix-loop-helix (HLH). The kinase domain of IKKε exhibits 29% and 27% identity to IKKα and IKKβ respectively, and TBK1 shares 49% identity to IKKε. The classical IKKs have NEMO-binding domain to form the classical complex. IKKβ, IKKε, and TBK1 have ubiquitin-like domain (ULD), whose function remains unclear. Adapted from (*291*, *300*).

Subunits: NFκB1 (also called p50 and its precursor p105), NFκB2 (also called p52 and its precursor p100), c-Rel, RelA (p65), and RelB (*286*). The canonical pathway activates NFκB heterodimeric transcription factors composed of RelA or c-Rel, and p50. It is activated mainly through the catalytic activity of IKKβ, usually for the immediate response (*301, 302*). The non-canonical pathway, however, activates a different NFκB heterodimer (RelB and p52) through activation of IKK-related kinases or the catalytic activity of IKKα. The response of the alternative pathway is slower and encodes different gene sets mediating different functions (*285*).

Numerous studies have suggested a role for IKKε and TBK1 in the innate immune response, cell proliferation and oncogenesis (*303*). The differential expression of IKKε and TBK1 may reflect their distinct roles. IKKε expression is inducible in certain types of cells after inflammatory stimuli, and also induced by high fat feeding of mice, where it plays a key role in the development of insulin resistance, obesity, and hepatosteatosis (*287, 288, 304*). IKKε is predominantly expressed in specific tissues such as the pancreas, thymus, spleen, fat, liver and peripheral blood leukocytes (*287, 288*). In contrast, TBK1 is ubiquitously and constitutively expressed (*305*). These IKK-related kinases may enhance NFκB transcriptional activity through phosphorylation of p65 (RelA), a subunit of NFκB (*306*). Toll-like receptor (TLR) activation causes IKKε/TBK1 to activate NFκB (*307*). However, NFκB is not activated in mouse embryonic fibroblasts from IKKα and IKKβ double knockout mice, whereas it is activated in MEFS with double knock out of IKKe/TBK1, suggesting that IKKε/TBK1 are not strictly required for the activation of NFκB pathway, although it may signal through NFκB pathway in certain inflammatory stimuli by phosphorylating p65 (RelA) (*308*). Therefore, the role of IKKε/TBK1 in NFκB pathway remains incomplete. However, both IKKε and TBK1 contain

NFκB regulatory sites in their promoter regions, allowing them to be induced upon NFκB activation (*309*). Therefore, they are more likely downstream mediators of NFκB. Recent studies also have shown that there is a cross-talk between canonical IKK and IKK-related kinase signaling pathways. Both TLR3 and TLR4 activate the canonical IKK pathway, which subsequently phosphorylates Ser172 of IKK-related kinases in the activation loop. IKK-related kinases then negatively regulate the canonical IKK complex to dampen NFκB signaling as a feedback mechanism (*310*).

IKKε and TBK1 are thought to mainly regulate transcription through the phosphorylation of the transcription factors, interferon regulatory factor 3 (IRF3), IRF7, or STAT1, which are critical for the expression of interferon (IFN)-stimulated genes (*311-317*). Although both IKKε and TBK1 have been shown to be activated downstream of PI3 kinase, and activate Akt in some cases in different cell types (*318-320*), their potential roles beyond inflammatory signaling pathways remain poorly defined.

The activity of the canonical IKK kinases is regulated by the phosphorylation at Ser176/180 or Ser177/181 in the activation loop of IKKα and IKKβ, respectively (*292, 293, 321*). TAK1 phosphorylates Ser177/181 of IKKβ causing a conformational change leading to IKKβ activation (*322*). Substitution of Ser177/181 to alanine dramatically reduces IKKβ activity, while substitution to phosphomimetic glutamate generates a constitutively active kinase (*321, 323*). Therefore, phosphorylation of the activation loop is strongly indicative of IKK family member activity. In contrast, the regulation of the activity of the noncanonical IKK kinases remains poorly understood. Phosphorylation of Ser172 on TBK1 and IKKε has been associated with

increased activity, and this residue is required for activity. However, substitution of Ser172 to either alanine or glutamate results in decreased kinase activity (*324*). In addition, when TBK1 and IKKε were inhibited by their inhibitors, the phosphorylation of TBK1 and IKKε at Ser172 in response to their stimuli (LPS, poly (I:C), interleukin-1α, and tumor necrosis factor α) is enhanced rather than blocked (*323*). These evidences demonstrate that the phosphorylation of Ser172 and the activation of TBK1 and IKKε are catalyzed by an unknown distinct protein kinase(s), and that TBK1 and IKKε control a negative feedback loop that limits their activation in response to their stimuli to prevent the hyperactivation of these enzymes (*310, 323*). Furthermore, several adaptor proteins have been identified that regulate TBK1 activity. Adaptor proteins NAP1 (NF-κB activating kinase-associated protein-1), Sintbad (similar to NAP1 TBK1 adaptor), TANK (TRAF family member-associated NF-κB activator), STING (stimulator of interferon genes), DOK3 (downstream of kinase 3) may be required for TBK1 activation (*290, 325-328*). Post-translational modifications including SUMOylation and ubiquitination of TBK1 and IKKε are also important for its activation (*329-331*). Therefore, the way the activity of TBK1 and IKKε is regulated needs further attention to understand its function.

V. Summary

Although there has been significant progress in the identification of insulin signaling pathways leading to the assembly and recognition of the exocyst, the mechanism by which the small GTPases dissociate from the tethering complex remain obscure. Glut4 vesicles must engage with, and subsequently disengage from the exocyst for efficient docking and fusion with the plasma membrane. Normally, the small G proteins disengage from their effectors by activating GAPs,

but RalA-exocyst dissociation does not result from RalA inactivation because RGC1/2 proteins are reserved for activation of RalA, as it is persistently inhibited by insulin-dependent Akt phosphorylation (*189*). Recent studies suggested that phosphorylation of Sec5 by the protein kinase PKC reduces its affinity for RalA. Therefore, Sec5 phosphorylation mimics a cycling process of increasing its intrinsic GTPase activity by GAP (*234*). While little is known about the process of disengagement of Rals from the tethering complex that ensures the continuation of exocytosis in insulin-stimulated Glut4 translocation, it is likely that phosphorylation of effectors plays a crucial role. Interestingly, recent studies showed that the constitutively active form of RalB induces the interaction between Sec5 and TBK1 to support cancer cell survival (*332*). Furthermore, subcellular localization of TBK1 was found in Sec5-containing perinuclear vesicles (*327*). Given the important roles of the exocyst and Ral GTPases (described above) in insulin-stimulated glucose transport, these observations led us to examine the role of TBK1 in the regulation of glucose transport in 3T3-L1 adipocytes. In the following chapters I will describe the role of TBK1 in GLUT4 trafficking. In Chapter 2, I will discuss the role of TBK1 and its involvement in insulin signaling pathway to regulate insulin-stimulated glucose transport. In Chapter 3, I will discuss how TBK1 mediates insulin-stimulated glucose transport by directly phosphorylating the exocyst subunit Exo84. In Chapter 4 I will discuss how TBK1-mediated Exo84 phosphorylation results in disengagement of GLUT4 vesicles from the exocyst and disruption of the exocyst to contribute to efficient recycling of vesicles and fusion with the plasma membrane. Together, these studies suggest that TBK1 is a novel regulator in insulin-stimulated glucose transport in 3T3-L1 adipocytes.

References

1. A. R. Saltiel, C. R. Kahn, Insulin signalling and the regulation of glucose and lipid metabolism. *Nature* **414**, 799 (Dec 13, 2001).
2. E. D. Rosen, B. M. Spiegelman, Adipocytes as regulators of energy balance and glucose homeostasis. *Nature* **444**, 847 (Dec 14, 2006).
3. L. Chang, S. H. Chiang, A. R. Saltiel, Insulin signaling and the regulation of glucose transport. *Mol Med* **10**, 65 (Jul-Dec, 2004).
4. A. R. Saltiel, New perspectives into the molecular pathogenesis and treatment of type 2 diabetes. *Cell* **104**, 517 (Feb 23, 2001).
5. K. G. Alberti, P. Z. Zimmet, Definition, diagnosis and classification of diabetes mellitus and its complications. Part 1: diagnosis and classification of diabetes mellitus provisional report of a WHO consultation. *Diabetic medicine : a journal of the British Diabetic Association* **15**, 539 (Jul, 1998).
6. M. A. Lazar, How obesity causes diabetes: not a tall tale. *Science* **307**, 373 (Jan 21, 2005).
7. S. Wild, G. Roglic, A. Green, R. Sicree, H. King, Global prevalence of diabetes: estimates for the year 2000 and projections for 2030. *Diabetes care* **27**, 1047 (May, 2004).
8. P. Hogan, T. Dall, P. Nikolov, Economic costs of diabetes in the US in 2002. *Diabetes care* **26**, 917 (Mar, 2003).
9. P. R. Shepherd, B. B. Kahn, Glucose transporters and insulin action--implications for insulin resistance and diabetes mellitus. *The New England journal of medicine* **341**, 248 (Jul 22, 1999).
10. D. Leto, A. R. Saltiel, Regulation of glucose transport by insulin: traffic control of GLUT4. *Nature reviews. Molecular cell biology* **13**, 383 (Jun, 2012).
11. H. G. Joost *et al.*, Nomenclature of the GLUT/SLC2A family of sugar/polyol transport facilitators. *American journal of physiology. Endocrinology and metabolism* **282**, E974 (Apr, 2002).
12. P. W. Hruz, M. M. Mueckler, Structural analysis of the GLUT1 facilitative glucose transporter (review). *Molecular membrane biology* **18**, 183 (Jul-Sep, 2001).
13. R. T. Watson, M. Kanzaki, J. E. Pessin, Regulated membrane trafficking of the insulin-responsive glucose transporter 4 in adipocytes. *Endocrine reviews* **25**, 177 (Apr, 2004).
14. A. L. Olson, J. E. Pessin, Structure, function, and regulation of the mammalian facilitative glucose transporter gene family. *Annual review of nutrition* **16**, 235 (1996).
15. M. Mueckler, R. C. Hresko, M. Sato, Structure, function and biosynthesis of GLUT1. *Biochemical Society transactions* **25**, 951 (Aug, 1997).
16. B. Thorens, M. Mueckler, Glucose transporters in the 21st Century. *Am J Physiol Endocrinol Metab* **298**, E141 (Feb).
17. M. J. Birnbaum, Identification of a novel gene encoding an insulin-responsive glucose transporter protein. *Cell* **57**, 305 (Apr 21, 1989).
18. M. J. Charron, F. C. Brosius, 3rd, S. L. Alper, H. F. Lodish, A glucose transport protein expressed predominately in insulin-responsive tissues. *Proc Natl Acad Sci U S A* **86**, 2535 (Apr, 1989).

19. H. Fukumoto *et al.*, Cloning and characterization of the major insulin-responsive glucose transporter expressed in human skeletal muscle and other insulin-responsive tissues. *J Biol Chem* **264**, 7776 (May 15, 1989).
20. D. E. James, M. Strube, M. Mueckler, Molecular cloning and characterization of an insulin-regulatable glucose transporter. *Nature* **338**, 83 (Mar 2, 1989).
21. K. H. Kaestner *et al.*, Sequence, tissue distribution, and differential expression of mRNA for a putative insulin-responsive glucose transporter in mouse 3T3-L1 adipocytes. *Proc Natl Acad Sci U S A* **86**, 3150 (May, 1989).
22. A. E. Stenbit *et al.*, GLUT4 heterozygous knockout mice develop muscle insulin resistance and diabetes. *Nat Med* **3**, 1096 (Oct, 1997).
23. A. Zisman *et al.*, Targeted disruption of the glucose transporter 4 selectively in muscle causes insulin resistance and glucose intolerance. *Nat Med* **6**, 924 (Aug, 2000).
24. E. D. Abel *et al.*, Adipose-selective targeting of the GLUT4 gene impairs insulin action in muscle and liver. *Nature* **409**, 729 (Feb 8, 2001).
25. E. Tozzo, P. R. Shepherd, L. Gnudi, B. B. Kahn, Transgenic GLUT-4 overexpression in fat enhances glucose metabolism: preferential effect on fatty acid synthesis. *The American journal of physiology* **268**, E956 (May, 1995).
26. T. S. Tsao, R. Burcelin, E. B. Katz, L. Huang, M. J. Charron, Enhanced insulin action due to targeted GLUT4 overexpression exclusively in muscle. *Diabetes* **45**, 28 (Jan, 1996).
27. K. Suzuki, T. Kono, Evidence that insulin causes translocation of glucose transport activity to the plasma membrane from an intracellular storage site. *Proc Natl Acad Sci U S A* **77**, 2542 (May, 1980).
28. S. W. Cushman, L. J. Wardzala, Potential mechanism of insulin action on glucose transport in the isolated rat adipose cell. Apparent translocation of intracellular transport systems to the plasma membrane. *J Biol Chem* **255**, 4758 (May 25, 1980).
29. H. G. Joost, T. M. Weber, S. W. Cushman, I. A. Simpson, Insulin-stimulated glucose transport in rat adipose cells. Modulation of transporter intrinsic activity by isoproterenol and adenosine. *The Journal of biological chemistry* **261**, 10033 (Aug 5, 1986).
30. A. E. Clark, G. D. Holman, I. J. Kozka, Determination of the rates of appearance and loss of glucose transporters at the cell surface of rat adipose cells. *The Biochemical journal* **278 (Pt 1)**, 235 (Aug 15, 1991).
31. Z. W. Yu *et al.*, Insulin can enhance GLUT4 gene expression in 3T3-F442A cells and this effect is mimicked by vanadate but counteracted by cAMP and high glucose--potential implications for insulin resistance. *Biochimica et biophysica acta* **1535**, 174 (Feb 14, 2001).
32. L. B. Liu, W. Omata, I. Kojima, H. Shibata, The SUMO conjugating enzyme Ubc9 is a regulator of GLUT4 turnover and targeting to the insulin-responsive storage compartment in 3T3-L1 adipocytes. *Diabetes* **56**, 1977 (Aug, 2007).
33. H. Zaid, C. N. Antonescu, V. K. Randhawa, A. Klip, Insulin action on glucose transporters through molecular switches, tracks and tethers. *Biochem J* **413**, 201 (Jul 15, 2008).
34. C. N. Antonescu, M. Foti, N. Sauvonnet, A. Klip, Ready, set, internalize: mechanisms and regulation of GLUT4 endocytosis. *Biosci Rep* **29**, 1 (Feb, 2009).

35. J. W. Slot, H. J. Geuze, S. Gigengack, G. E. Lienhard, D. E. James, Immuno-localization of the insulin regulatable glucose transporter in brown adipose tissue of the rat. *J Cell Biol* **113**, 123 (Apr, 1991).
36. S. Martin *et al.*, The glucose transporter (GLUT-4) and vesicle-associated membrane protein-2 (VAMP-2) are segregated from recycling endosomes in insulin-sensitive cells. *J Cell Biol* **134**, 625 (Aug, 1996).
37. A. Zeigerer *et al.*, GLUT4 retention in adipocytes requires two intracellular insulin-regulated transport steps. *Mol Biol Cell* **13**, 2421 (Jul, 2002).
38. J. S. Hah *et al.*, Transient changes in four GLUT4 compartments in rat adipocytes during the transition, insulin-stimulated to basal: implications for the GLUT4 trafficking pathway. *Biochemistry* **41**, 14364 (Dec 3, 2002).
39. T. A. Kupriyanova, V. Kandror, K. V. Kandror, Isolation and characterization of the two major intracellular Glut4 storage compartments. *J Biol Chem* **277**, 9133 (Mar 15, 2002).
40. O. Karylowski, A. Zeigerer, A. Cohen, T. E. McGraw, GLUT4 is retained by an intracellular cycle of vesicle formation and fusion with endosomes. *Mol Biol Cell* **15**, 870 (Feb, 2004).
41. J. S. Bogan, N. Hendon, A. E. McKee, T. S. Tsao, H. F. Lodish, Functional cloning of TUG as a regulator of GLUT4 glucose transporter trafficking. *Nature* **425**, 727 (Oct 16, 2003).
42. L. B. Martin, A. Shewan, C. A. Millar, G. W. Gould, D. E. James, Vesicle-associated membrane protein 2 plays a specific role in the insulin-dependent trafficking of the facilitative glucose transporter GLUT4 in 3T3-L1 adipocytes. *J Biol Chem* **273**, 1444 (Jan 16, 1998).
43. K. V. Kandror, L. Yu, P. F. Pilch, The major protein of GLUT4-containing vesicles, gp160, has aminopeptidase activity. *J Biol Chem* **269**, 30777 (Dec 9, 1994).
44. K. V. Kandror, P. F. Pilch, gp160, a tissue-specific marker for insulin-activated glucose transport. *Proceedings of the National Academy of Sciences of the United States of America* **91**, 8017 (Aug 16, 1994).
45. S. R. Keller, H. M. Scott, C. C. Mastick, R. Aebersold, G. E. Lienhard, Cloning and characterization of a novel insulin-regulated membrane aminopeptidase from Glut4 vesicles. *The Journal of biological chemistry* **270**, 23612 (Oct 6, 1995).
46. S. A. Ross *et al.*, Characterization of the insulin-regulated membrane aminopeptidase in 3T3-L1 adipocytes. *J Biol Chem* **271**, 3328 (Feb 9, 1996).
47. B. Z. Lin, P. F. Pilch, K. V. Kandror, Sortilin is a major protein component of Glut4-containing vesicles. *J Biol Chem* **272**, 24145 (Sep 26, 1997).
48. N. J. Morris *et al.*, Sortilin is the major 110-kDa protein in GLUT4 vesicles from adipocytes. *J Biol Chem* **273**, 3582 (Feb 6, 1998).
49. M. P. Jedrychowski *et al.*, Proteomic analysis of GLUT4 storage vesicles reveals LRP1 to be an important vesicle component and target of insulin signaling. *J Biol Chem* **285**, 104 (Jan 1).
50. J. Stockli, D. J. Fazakerley, D. E. James, GLUT4 exocytosis. *Journal of cell science* **124**, 4147 (Dec 15, 2011).
51. A. Guilherme *et al.*, Perinuclear localization and insulin responsiveness of GLUT4 requires cytoskeletal integrity in 3T3-L1 adipocytes. *J Biol Chem* **275**, 38151 (Dec 8, 2000).

52. V. Patki *et al.*, Insulin action on GLUT4 traffic visualized in single 3T3-l1 adipocytes by using ultra-fast microscopy. *Mol Biol Cell* **12**, 129 (Jan, 2001).
53. M. Kanzaki, J. E. Pessin, Insulin-stimulated GLUT4 translocation in adipocytes is dependent upon cortical actin remodeling. *The Journal of biological chemistry* **276**, 42436 (Nov 9, 2001).
54. T. Tsakiridis, M. Vranic, A. Klip, Disassembly of the actin network inhibits insulin-dependent stimulation of glucose transport and prevents recruitment of glucose transporters to the plasma membrane. *J Biol Chem* **269**, 29934 (Nov 25, 1994).
55. T. Tsakiridis *et al.*, Role of the actin cytoskeleton in insulin action. *Microscopy research and technique* **47**, 79 (Oct 15, 1999).
56. Q. Wang, P. J. Bilan, T. Tsakiridis, A. Hinek, A. Klip, Actin filaments participate in the relocalization of phosphatidylinositol3-kinase to glucose transporter-containing compartments and in the stimulation of glucose uptake in 3T3-L1 adipocytes. *Biochem J* **331 (Pt 3)**, 917 (May 1, 1998).
57. W. Omata, H. Shibata, L. Li, K. Takata, I. Kojima, Actin filaments play a critical role in insulin-induced exocytotic recruitment but not in endocytosis of GLUT4 in isolated rat adipocytes. *Biochem J* **346 Pt 2**, 321 (Mar 1, 2000).
58. P. Tong *et al.*, Insulin-induced cortical actin remodeling promotes GLUT4 insertion at muscle cell membrane ruffles. *J Clin Invest* **108**, 371 (Aug, 2001).
59. A. L. Olson, A. R. Trumbly, G. V. Gibson, Insulin-mediated GLUT4 translocation is dependent on the microtubule network. *The Journal of biological chemistry* **276**, 10706 (Apr 6, 2001).
60. M. Emoto, S. E. Langille, M. P. Czech, A role for kinesin in insulin-stimulated GLUT4 glucose transporter translocation in 3T3-L1 adipocytes. *The Journal of biological chemistry* **276**, 10677 (Apr 6, 2001).
61. V. A. Lizunov, H. Matsumoto, J. Zimmerberg, S. W. Cushman, V. A. Frolov, Insulin stimulates the halting, tethering, and fusion of mobile GLUT4 vesicles in rat adipose cells. *J Cell Biol* **169**, 481 (May 9, 2005).
62. F. Koumanov, B. Jin, J. Yang, G. D. Holman, Insulin signaling meets vesicle traffic of GLUT4 at a plasma-membrane-activated fusion step. *Cell Metab* **2**, 179 (Sep, 2005).
63. L. Bai *et al.*, Dissecting multiple steps of GLUT4 trafficking and identifying the sites of insulin action. *Cell Metab* **5**, 47 (Jan, 2007).
64. M. R. Heider, M. Munson, Exorcising the exocyst complex. *Traffic* **13**, 898 (Jul, 2012).
65. M. Shipitsin, L. A. Feig, RalA but not RalB enhances polarized delivery of membrane proteins to the basolateral surface of epithelial cells. *Mol Cell Biol* **24**, 5746 (Jul, 2004).
66. M. Murthy, D. Garza, R. H. Scheller, T. L. Schwarz, Mutations in the exocyst component Sec5 disrupt neuronal membrane traffic, but neurotransmitter release persists. *Neuron* **37**, 433 (Feb 6, 2003).
67. M. Inoue, L. Chang, J. Hwang, S. H. Chiang, A. R. Saltiel, The exocyst complex is required for targeting of Glut4 to the plasma membrane by insulin. *Nature* **422**, 629 (Apr 10, 2003).
68. I. Cascone *et al.*, Distinct roles of RalA and RalB in the progression of cytokinesis are supported by distinct RalGEFs. *EMBO J* **27**, 2375 (Sep 17, 2008).
69. X. W. Chen, M. Inoue, S. C. Hsu, A. R. Saltiel, RalA-exocyst-dependent recycling endosome trafficking is required for the completion of cytokinesis. *J Biol Chem* **281**, 38609 (Dec 15, 2006).

70. P. Novick, C. Field, R. Schekman, Identification of 23 complementation groups required for post-translational events in the yeast secretory pathway. *Cell* **21**, 205 (Aug, 1980).
71. S. C. Hsu *et al.*, The mammalian brain rsec6/8 complex. *Neuron* **17**, 1209 (Dec, 1996).
72. F. P. Finger, P. Novick, Synthetic interactions of the post-Golgi sec mutations of Saccharomyces cerevisiae. *Genetics* **156**, 943 (Nov, 2000).
73. G. A. Friedrich, J. D. Hildebrand, P. Soriano, The secretory protein Sec8 is required for paraxial mesoderm formation in the mouse. *Dev Biol* **192**, 364 (Dec 15, 1997).
74. M. Murthy, R. O. Teodoro, T. P. Miller, T. L. Schwarz, Sec5, a member of the exocyst complex, mediates Drosophila embryo cellularization. *Development* **137**, 2773 (Aug).
75. M. Murthy, T. L. Schwarz, The exocyst component Sec5 is required for membrane traffic and polarity in the Drosophila ovary. *Development* **131**, 377 (Jan, 2004).
76. F. P. Finger, T. E. Hughes, P. Novick, Sec3p is a spatial landmark for polarized secretion in budding yeast. *Cell* **92**, 559 (Feb 20, 1998).
77. C. Boyd, T. Hughes, M. Pypaert, P. Novick, Vesicles carry most exocyst subunits to exocytic sites marked by the remaining two subunits, Sec3p and Exo70p. *J Cell Biol* **167**, 889 (Dec 6, 2004).
78. S. C. Hsu *et al.*, Subunit composition, protein interactions, and structures of the mammalian brain sec6/8 complex and septin filaments. *Neuron* **20**, 1111 (Jun, 1998).
79. M. Munson, P. Novick, The exocyst defrocked, a framework of rods revealed. *Nat Struct Mol Biol* **13**, 577 (Jul, 2006).
80. G. Dong, A. H. Hutagalung, C. Fu, P. Novick, K. M. Reinisch, The structures of exocyst subunit Exo70p and the Exo84p C-terminal domains reveal a common motif. *Nat Struct Mol Biol* **12**, 1094 (Dec, 2005).
81. Z. A. Hamburger, A. E. Hamburger, A. P. West, Jr., W. I. Weis, Crystal structure of the S.cerevisiae exocyst component Exo70p. *J Mol Biol* **356**, 9 (Feb 10, 2006).
82. B. A. Moore, H. H. Robinson, Z. Xu, The crystal structure of mouse Exo70 reveals unique features of the mammalian exocyst. *J Mol Biol* **371**, 410 (Aug 10, 2007).
83. M. V. Sivaram, M. L. Furgason, D. N. Brewer, M. Munson, The structure of the exocyst subunit Sec6p defines a conserved architecture with diverse roles. *Nat Struct Mol Biol* **13**, 555 (Jun, 2006).
84. J. M. Segui-Simarro, J. R. Austin, 2nd, E. A. White, L. A. Staehelin, Electron tomographic analysis of somatic cell plate formation in meristematic cells of Arabidopsis preserved by high-pressure freezing. *The Plant cell* **16**, 836 (Apr, 2004).
85. M. Yamashita *et al.*, Structural basis for the Rho- and phosphoinositide-dependent localization of the exocyst subunit Sec3. *Nature structural & molecular biology* **17**, 180 (Feb, 2010).
86. S. Fukai, H. T. Matern, J. R. Jagath, R. H. Scheller, A. T. Brunger, Structural basis of the interaction between RalA and Sec5, a subunit of the sec6/8 complex. *The EMBO journal* **22**, 3267 (Jul 1, 2003).
87. R. Jin *et al.*, Exo84 and Sec5 are competitive regulatory Sec6/8 effectors to the RalA GTPase. *The EMBO journal* **24**, 2064 (Jun 15, 2005).
88. H. Wu, G. Rossi, P. Brennwald, The ghost in the machine: small GTPases as spatial regulators of exocytosis. *Trends in cell biology* **18**, 397 (Sep, 2008).
89. W. Guo, D. Roth, C. Walch-Solimena, P. Novick, The exocyst is an effector for Sec4p, targeting secretory vesicles to sites of exocytosis. *EMBO J* **18**, 1071 (Feb 15, 1999).

90. D. R. TerBush, P. Novick, Sec6, Sec8, and Sec15 are components of a multisubunit complex which localizes to small bud tips in Saccharomyces cerevisiae. *J Cell Biol* **130**, 299 (Jul, 1995).
91. B. Goud, A. Salminen, N. C. Walworth, P. J. Novick, A GTP-binding protein required for secretion rapidly associates with secretory vesicles and the plasma membrane in yeast. *Cell* **53**, 753 (Jun 3, 1988).
92. W. Guo, F. Tamanoi, P. Novick, Spatial regulation of the exocyst complex by Rho1 GTPase. *Nat Cell Biol* **3**, 353 (Apr, 2001).
93. X. Zhang *et al.*, Cdc42 interacts with the exocyst and regulates polarized secretion. *J Biol Chem* **276**, 46745 (Dec 14, 2001).
94. J. E. Adamo, G. Rossi, P. Brennwald, The Rho GTPase Rho3 has a direct role in exocytosis that is distinct from its role in actin polarity. *Mol Biol Cell* **10**, 4121 (Dec, 1999).
95. N. G. Robinson *et al.*, Rho3 of Saccharomyces cerevisiae, which regulates the actin cytoskeleton and exocytosis, is a GTPase which interacts with Myo2 and Exo70. *Mol Cell Biol* **19**, 3580 (May, 1999).
96. B. He, F. Xi, X. Zhang, J. Zhang, W. Guo, Exo70 interacts with phospholipids and mediates the targeting of the exocyst to the plasma membrane. *EMBO J* **26**, 4053 (Sep 19, 2007).
97. X. Zhang *et al.*, Membrane association and functional regulation of Sec3 by phospholipids and Cdc42. *J Cell Biol* **180**, 145 (Jan 14, 2008).
98. D. Roth, W. Guo, P. Novick, Dominant negative alleles of SEC10 reveal distinct domains involved in secretion and morphogenesis in yeast. *Mol Biol Cell* **9**, 1725 (Jul, 1998).
99. D. W. Pruyne, D. H. Schott, A. Bretscher, Tropomyosin-containing actin cables direct the Myo2p-dependent polarized delivery of secretory vesicles in budding yeast. *J Cell Biol* **143**, 1931 (Dec 28, 1998).
100. D. Schott, J. Ho, D. Pruyne, A. Bretscher, The COOH-terminal domain of Myo2p, a yeast myosin V, has a direct role in secretory vesicle targeting. *J Cell Biol* **147**, 791 (Nov 15, 1999).
101. W. Wagner, P. Bielli, S. Wacha, A. Ragnini-Wilson, Mlc1p promotes septum closure during cytokinesis via the IQ motifs of the vesicle motor Myo2p. *EMBO J* **21**, 6397 (Dec 2, 2002).
102. X. M. Zhang, S. Ellis, A. Sriratana, C. A. Mitchell, T. Rowe, Sec15 is an effector for the Rab11 GTPase in mammalian cells. *J Biol Chem* **279**, 43027 (Oct 8, 2004).
103. S. Wu, S. Q. Mehta, F. Pichaud, H. J. Bellen, F. A. Quiocho, Sec15 interacts with Rab11 via a novel domain and affects Rab11 localization in vivo. *Nat Struct Mol Biol* **12**, 879 (Oct, 2005).
104. H. Jafar-Nejad *et al.*, Sec15, a component of the exocyst, promotes notch signaling during the asymmetric division of Drosophila sensory organ precursors. *Developmental cell* **9**, 351 (Sep, 2005).
105. M. Prigent *et al.*, ARF6 controls post-endocytic recycling through its downstream exocyst complex effector. *J Cell Biol* **163**, 1111 (Dec 8, 2003).
106. S. Moskalenko *et al.*, The exocyst is a Ral effector complex. *Nat Cell Biol* **4**, 66 (Jan, 2002).
107. S. Moskalenko *et al.*, Ral GTPases regulate exocyst assembly through dual subunit interactions. *J Biol Chem* **278**, 51743 (Dec 19, 2003).

108. J. Liu, X. Zuo, P. Yue, W. Guo, Phosphatidylinositol 4,5-bisphosphate mediates the targeting of the exocyst to the plasma membrane for exocytosis in mammalian cells. *Mol Biol Cell* **18**, 4483 (Nov, 2007).
109. S. H. Chiang *et al.*, Insulin-stimulated GLUT4 translocation requires the CAP-dependent activation of TC10. *Nature* **410**, 944 (Apr 19, 2001).
110. M. Inoue, S. H. Chiang, L. Chang, X. W. Chen, A. R. Saltiel, Compartmentalization of the exocyst complex in lipid rafts controls Glut4 vesicle tethering. *Mol Biol Cell* **17**, 2303 (May, 2006).
111. X. W. Chen, D. Leto, S. H. Chiang, Q. Wang, A. R. Saltiel, Activation of RalA is required for insulin-stimulated Glut4 trafficking to the plasma membrane via the exocyst and the motor protein Myo1c. *Dev Cell* **13**, 391 (Sep, 2007).
112. D. C. Thurmond, J. E. Pessin, Molecular machinery involved in the insulin-regulated fusion of GLUT4-containing vesicles with the plasma membrane (review). *Molecular membrane biology* **18**, 237 (Oct-Dec, 2001).
113. R. Jahn, R. H. Scheller, SNAREs--engines for membrane fusion. *Nature reviews. Molecular cell biology* **7**, 631 (Sep, 2006).
114. B. Cheatham *et al.*, Insulin-stimulated translocation of GLUT4 glucose transporters requires SNARE-complex proteins. *Proceedings of the National Academy of Sciences of the United States of America* **93**, 15169 (Dec 24, 1996).
115. A. Volchuk *et al.*, Cellubrevin is a resident protein of insulin-sensitive GLUT4 glucose transporter vesicles in 3T3-L1 adipocytes. *J Biol Chem* **270**, 8233 (Apr 7, 1995).
116. A. Volchuk *et al.*, Syntaxin 4 in 3T3-L1 adipocytes: regulation by insulin and participation in insulin-dependent glucose transport. *Molecular biology of the cell* **7**, 1075 (Jul, 1996).
117. A. L. Olson, J. B. Knight, J. E. Pessin, Syntaxin 4, VAMP2, and/or VAMP3/cellubrevin are functional target membrane and vesicle SNAP receptors for insulin-stimulated GLUT4 translocation in adipocytes. *Mol Cell Biol* **17**, 2425 (May, 1997).
118. M. Kawanishi *et al.*, Role of SNAP23 in insulin-induced translocation of GLUT4 in 3T3-L1 adipocytes. Mediation of complex formation between syntaxin4 and VAMP2. *J Biol Chem* **275**, 8240 (Mar 17, 2000).
119. J. Min *et al.*, Synip: a novel insulin-regulated syntaxin 4-binding protein mediating GLUT4 translocation in adipocytes. *Mol Cell* **3**, 751 (Jun, 1999).
120. S. Okada *et al.*, Synip phosphorylation is required for insulin-stimulated Glut4 translocation. *Biochem Biophys Res Commun* **356**, 102 (Apr 27, 2007).
121. H. Sano, S. Kane, E. Sano, G. E. Lienhard, Synip phosphorylation does not regulate insulin-stimulated GLUT4 translocation. *Biochem Biophys Res Commun* **332**, 880 (Jul 8, 2005).
122. E. Yamada *et al.*, Akt2 phosphorylates Synip to regulate docking and fusion of GLUT4-containing vesicles. *J Cell Biol* **168**, 921 (Mar 14, 2005).
123. J. T. Tellam *et al.*, Characterization of Munc-18c and syntaxin-4 in 3T3-L1 adipocytes. Putative role in insulin-dependent movement of GLUT-4. *The Journal of biological chemistry* **272**, 6179 (Mar 7, 1997).
124. D. C. Thurmond *et al.*, Regulation of insulin-stimulated GLUT4 translocation by Munc18c in 3T3L1 adipocytes. *J Biol Chem* **273**, 33876 (Dec 11, 1998).

125. D. C. Thurmond, M. Kanzaki, A. H. Khan, J. E. Pessin, Munc18c function is required for insulin-stimulated plasma membrane fusion of GLUT4 and insulin-responsive amino peptidase storage vesicles. *Mol Cell Biol* **20**, 379 (Jan, 2000).
126. N. P. Smithers, C. P. Hodgkinson, M. Cuttle, G. J. Sale, Insulin-triggered repositioning of munc18c on syntaxin-4 in GLUT4 signalling. *Biochem J* **410**, 255 (Mar 1, 2008).
127. M. E. Patti, C. R. Kahn, The insulin receptor--a critical link in glucose homeostasis and insulin action. *Journal of basic and clinical physiology and pharmacology* **9**, 89 (1998).
128. J. Lee, P. F. Pilch, The insulin receptor: structure, function, and signaling. *The American journal of physiology* **266**, C319 (Feb, 1994).
129. C. W. Ward, M. C. Lawrence, Ligand-induced activation of the insulin receptor: a multi-step process involving structural changes in both the ligand and the receptor. *Bioessays* **31**, 422 (Apr, 2009).
130. L. Ellis *et al.*, Replacement of insulin receptor tyrosine residues 1162 and 1163 compromises insulin-stimulated kinase activity and uptake of 2-deoxyglucose. *Cell* **45**, 721 (Jun 6, 1986).
131. J. Lee, T. O'Hare, P. F. Pilch, S. E. Shoelson, Insulin receptor autophosphorylation occurs asymmetrically. *J Biol Chem* **268**, 4092 (Feb 25, 1993).
132. M. F. White, S. E. Shoelson, H. Keutmann, C. R. Kahn, A cascade of tyrosine autophosphorylation in the beta-subunit activates the phosphotransferase of the insulin receptor. *J Biol Chem* **263**, 2969 (Feb 25, 1988).
133. Y. Zick, Insulin resistance: a phosphorylation-based uncoupling of insulin signaling. *Trends in cell biology* **11**, 437 (Nov, 2001).
134. A. Kharitonenkov *et al.*, A family of proteins that inhibit signalling through tyrosine kinase receptors. *Nature* **386**, 181 (Mar 13, 1997).
135. V. Ribon, A. R. Saltiel, Insulin stimulates tyrosine phosphorylation of the proto-oncogene product of c-Cbl in 3T3-L1 adipocytes. *Biochem J* **324 (Pt 3)**, 839 (Jun 15, 1997).
136. S. A. Moodie, J. Alleman-Sposeto, T. A. Gustafson, Identification of the APS protein as a novel insulin receptor substrate. *The Journal of biological chemistry* **274**, 11186 (Apr 16, 1999).
137. T. Sasaoka *et al.*, Evidence for a functional role of Shc proteins in mitogenic signaling induced by insulin, insulin-like growth factor-1, and epidermal growth factor. *The Journal of biological chemistry* **269**, 13689 (May 6, 1994).
138. M. Holgado-Madruga, D. R. Emlet, D. K. Moscatello, A. K. Godwin, A. J. Wong, A Grb2-associated docking protein in EGF- and insulin-receptor signalling. *Nature* **379**, 560 (Feb 8, 1996).
139. M. F. White, The IRS-signaling system: a network of docking proteins that mediate insulin and cytokine action. *Recent progress in hormone research* **53**, 119 (1998).
140. M. F. White, The insulin signalling system and the IRS proteins. *Diabetologia* **40 Suppl 2**, S2 (Jul, 1997).
141. F. Liu, R. A. Roth, Binding of SH2 containing proteins to the insulin receptor: a new way for modulating insulin signalling. *Molecular and cellular biochemistry* **182**, 73 (May, 1998).
142. T. Kitamura, C. R. Kahn, D. Accili, Insulin receptor knockout mice. *Annual review of physiology* **65**, 313 (2003).
143. D. Accili *et al.*, Early neonatal death in mice homozygous for a null allele of the insulin receptor gene. *Nat Genet* **12**, 106 (Jan, 1996).

144. R. L. Joshi *et al.*, Targeted disruption of the insulin receptor gene in the mouse results in neonatal lethality. *EMBO J* **15**, 1542 (Apr 1, 1996).
145. J. C. Bruning *et al.*, A muscle-specific insulin receptor knockout exhibits features of the metabolic syndrome of NIDDM without altering glucose tolerance. *Mol Cell* **2**, 559 (Nov, 1998).
146. D. Lauro *et al.*, Impaired glucose tolerance in mice with a targeted impairment of insulin action in muscle and adipose tissue. *Nature genetics* **20**, 294 (Nov, 1998).
147. M. Bluher *et al.*, Adipose tissue selective insulin receptor knockout protects against obesity and obesity-related glucose intolerance. *Developmental cell* **3**, 25 (Jul, 2002).
148. M. D. Michael *et al.*, Loss of insulin signaling in hepatocytes leads to severe insulin resistance and progressive hepatic dysfunction. *Mol Cell* **6**, 87 (Jul, 2000).
149. R. N. Kulkarni *et al.*, Tissue-specific knockout of the insulin receptor in pancreatic beta cells creates an insulin secretory defect similar to that in type 2 diabetes. *Cell* **96**, 329 (Feb 5, 1999).
150. C. Guerra *et al.*, Brown adipose tissue-specific insulin receptor knockout shows diabetic phenotype without insulin resistance. *The Journal of clinical investigation* **108**, 1205 (Oct, 2001).
151. J. C. Bruning *et al.*, Role of brain insulin receptor in control of body weight and reproduction. *Science* **289**, 2122 (Sep 22, 2000).
152. B. Vanhaesebroeck *et al.*, Synthesis and function of 3-phosphorylated inositol lipids. *Annual review of biochemistry* **70**, 535 (2001).
153. L. C. Cantley, B. G. Neel, New insights into tumor suppression: PTEN suppresses tumor formation by restraining the phosphoinositide 3-kinase/AKT pathway. *Proceedings of the National Academy of Sciences of the United States of America* **96**, 4240 (Apr 13, 1999).
154. T. Maehama, J. E. Dixon, PTEN: a tumour suppressor that functions as a phospholipid phosphatase. *Trends Cell Biol* **9**, 125 (Apr, 1999).
155. J. A. Engelman, J. Luo, L. C. Cantley, The evolution of phosphatidylinositol 3-kinases as regulators of growth and metabolism. *Nat Rev Genet* **7**, 606 (Aug, 2006).
156. A. Mora, D. Komander, D. M. van Aalten, D. R. Alessi, PDK1, the master regulator of AGC kinase signal transduction. *Seminars in cell & developmental biology* **15**, 161 (Apr, 2004).
157. B. Cheatham *et al.*, Phosphatidylinositol 3-kinase activation is required for insulin stimulation of pp70 S6 kinase, DNA synthesis, and glucose transporter translocation. *Mol Cell Biol* **14**, 4902 (Jul, 1994).
158. T. Okada, Y. Kawano, T. Sakakibara, O. Hazeki, M. Ui, Essential role of phosphatidylinositol 3-kinase in insulin-induced glucose transport and antilipolysis in rat adipocytes. Studies with a selective inhibitor wortmannin. *J Biol Chem* **269**, 3568 (Feb 4, 1994).
159. S. S. Martin *et al.*, Activated phosphatidylinositol 3-kinase is sufficient to mediate actin rearrangement and GLUT4 translocation in 3T3-L1 adipocytes. *J Biol Chem* **271**, 17605 (Jul 26, 1996).
160. P. M. Sharma *et al.*, Inhibition of phosphatidylinositol 3-kinase activity by adenovirus-mediated gene transfer and its effect on insulin action. *J Biol Chem* **273**, 18528 (Jul 17, 1998).

161. K. Ueki *et al.*, Positive and negative roles of p85 alpha and p85 beta regulatory subunits of phosphoinositide 3-kinase in insulin signaling. *J Biol Chem* **278**, 48453 (Nov 28, 2003).
162. S. M. Brachmann, K. Ueki, J. A. Engelman, R. C. Kahn, L. C. Cantley, Phosphoinositide 3-kinase catalytic subunit deletion and regulatory subunit deletion have opposite effects on insulin sensitivity in mice. *Mol Cell Biol* **25**, 1596 (Mar, 2005).
163. C. Kurlawalla-Martinez *et al.*, Insulin hypersensitivity and resistance to streptozotocin-induced diabetes in mice lacking PTEN in adipose tissue. *Mol Cell Biol* **25**, 2498 (Mar, 2005).
164. A. Bellacosa *et al.*, Akt activation by growth factors is a multiple-step process: the role of the PH domain. *Oncogene* **17**, 313 (Jul 23, 1998).
165. D. R. Alessi *et al.*, Characterization of a 3-phosphoinositide-dependent protein kinase which phosphorylates and activates protein kinase Balpha. *Curr Biol* **7**, 261 (Apr 1, 1997).
166. J. Yang *et al.*, Molecular mechanism for the regulation of protein kinase B/Akt by hydrophobic motif phosphorylation. *Mol Cell* **9**, 1227 (Jun, 2002).
167. M. P. Scheid, P. A. Marignani, J. R. Woodgett, Multiple phosphoinositide 3-kinase-dependent steps in activation of protein kinase B. *Mol Cell Biol* **22**, 6247 (Sep, 2002).
168. D. D. Sarbassov, D. A. Guertin, S. M. Ali, D. M. Sabatini, Phosphorylation and regulation of Akt/PKB by the rictor-mTOR complex. *Science* **307**, 1098 (Feb 18, 2005).
169. R. C. Hresko, M. Mueckler, mTOR.RICTOR is the Ser473 kinase for Akt/protein kinase B in 3T3-L1 adipocytes. *J Biol Chem* **280**, 40406 (Dec 9, 2005).
170. E. Jacinto *et al.*, SIN1/MIP1 maintains rictor-mTOR complex integrity and regulates Akt phosphorylation and substrate specificity. *Cell* **127**, 125 (Oct 6, 2006).
171. D. R. Alessi, F. B. Caudwell, M. Andjelkovic, B. A. Hemmings, P. Cohen, Molecular basis for the substrate specificity of protein kinase B; comparison with MAPKAP kinase-1 and p70 S6 kinase. *FEBS Lett* **399**, 333 (Dec 16, 1996).
172. T. Obata *et al.*, Peptide and protein library screening defines optimal substrate motifs for AKT/PKB. *J Biol Chem* **275**, 36108 (Nov 17, 2000).
173. A. D. Kohn *et al.*, Construction and characterization of a conditionally active version of the serine/threonine kinase Akt. *The Journal of biological chemistry* **273**, 11937 (May 8, 1998).
174. A. D. Kohn, S. A. Summers, M. J. Birnbaum, R. A. Roth, Expression of a constitutively active Akt Ser/Thr kinase in 3T3-L1 adipocytes stimulates glucose uptake and glucose transporter 4 translocation. *The Journal of biological chemistry* **271**, 31372 (Dec 6, 1996).
175. Q. Wang *et al.*, Protein kinase B/Akt participates in GLUT4 translocation by insulin in L6 myoblasts. *Molecular and cellular biology* **19**, 4008 (Jun, 1999).
176. L. N. Cong *et al.*, Physiological role of Akt in insulin-stimulated translocation of GLUT4 in transfected rat adipose cells. *Molecular endocrinology* **11**, 1881 (Dec, 1997).
177. Z. Y. Jiang *et al.*, Insulin signaling through Akt/protein kinase B analyzed by small interfering RNA-mediated gene silencing. *Proceedings of the National Academy of Sciences of the United States of America* **100**, 7569 (Jun 24, 2003).
178. C. J. Green *et al.*, Use of Akt inhibitor and a drug-resistant mutant validates a critical role for protein kinase B/Akt in the insulin-dependent regulation of glucose and system A amino acid uptake. *The Journal of biological chemistry* **283**, 27653 (Oct 10, 2008).

179. H. Cho, J. L. Thorvaldsen, Q. Chu, F. Feng, M. J. Birnbaum, Akt1/PKBalpha is required for normal growth but dispensable for maintenance of glucose homeostasis in mice. *J Biol Chem* **276**, 38349 (Oct 19, 2001).
180. H. Cho *et al.*, Insulin resistance and a diabetes mellitus-like syndrome in mice lacking the protein kinase Akt2 (PKB beta). *Science* **292**, 1728 (Jun 1, 2001).
181. R. S. Garofalo *et al.*, Severe diabetes, age-dependent loss of adipose tissue, and mild growth deficiency in mice lacking Akt2/PKB beta. *J Clin Invest* **112**, 197 (Jul, 2003).
182. O. Tschopp *et al.*, Essential role of protein kinase B gamma (PKB gamma/Akt3) in postnatal brain development but not in glucose homeostasis. *Development* **132**, 2943 (Jul, 2005).
183. B. Dummler *et al.*, Life with a single isoform of Akt: mice lacking Akt2 and Akt3 are viable but display impaired glucose homeostasis and growth deficiencies. *Mol Cell Biol* **26**, 8042 (Nov, 2006).
184. H. Sano *et al.*, Insulin-stimulated phosphorylation of a Rab GTPase-activating protein regulates GLUT4 translocation. *J Biol Chem* **278**, 14599 (Apr 25, 2003).
185. S. Chen *et al.*, Complementary regulation of TBC1D1 and AS160 by growth factors, insulin and AMPK activators. *Biochem J* **409**, 449 (Jan 15, 2008).
186. S. Kane *et al.*, A method to identify serine kinase substrates. Akt phosphorylates a novel adipocyte protein with a Rab GTPase-activating protein (GAP) domain. *J Biol Chem* **277**, 22115 (Jun 21, 2002).
187. W. G. Roach, J. A. Chavez, C. P. Miinea, G. E. Lienhard, Substrate specificity and effect on GLUT4 translocation of the Rab GTPase-activating protein Tbc1d1. *Biochem J* **403**, 353 (Apr 15, 2007).
188. L. Eguez *et al.*, Full intracellular retention of GLUT4 requires AS160 Rab GTPase activating protein. *Cell Metab* **2**, 263 (Oct, 2005).
189. X. W. Chen *et al.*, A Ral GAP complex links PI 3-kinase/Akt signaling to RalA activation in insulin action. *Molecular biology of the cell* **22**, 141 (Jan 1, 2011).
190. S. Gridley, J. A. Chavez, W. S. Lane, G. E. Lienhard, Adipocytes contain a novel complex similar to the tuberous sclerosis complex. *Cell Signal* **18**, 1626 (Oct, 2006).
191. D. Leto, M. Uhm, A. Williams, X. W. Chen, A. R. Saltiel, Negative regulation of the RalGAP complex by 14-3-3. *The Journal of biological chemistry* **288**, 9272 (Mar 29, 2013).
192. X. Xie *et al.*, C2 domain-containing phosphoprotein CDP138 regulates GLUT4 insertion into the plasma membrane. *Cell Metab* **14**, 378 (Sep 7).
193. S. J. Isakoff *et al.*, The inability of phosphatidylinositol 3-kinase activation to stimulate GLUT4 translocation indicates additional signaling pathways are required for insulin-stimulated glucose uptake. *Proc Natl Acad Sci U S A* **92**, 10247 (Oct 24, 1995).
194. T. Jiang *et al.*, Membrane-permeant esters of phosphatidylinositol 3,4,5-trisphosphate. *J Biol Chem* **273**, 11017 (May 1, 1998).
195. R. J. Wiese, C. C. Mastick, D. F. Lazar, A. R. Saltiel, Activation of mitogen-activated protein kinase and phosphatidylinositol 3'-kinase is not sufficient for the hormonal stimulation of glucose uptake, lipogenesis, or glycogen synthesis in 3T3-L1 adipocytes. *J Biol Chem* **270**, 3442 (Feb 17, 1995).
196. C. C. Mastick, M. J. Brady, J. A. Printen, V. Ribon, A. R. Saltiel, Spatial determinants of specificity in insulin action. *Mol Cell Biochem* **182**, 65 (May, 1998).

197. J. Gustavsson *et al.*, Localization of the insulin receptor in caveolae of adipocyte plasma membrane. *FASEB J* **13**, 1961 (Nov, 1999).
198. R. G. Anderson, The caveolae membrane system. *Annual review of biochemistry* **67**, 199 (1998).
199. A. Krook *et al.*, Two naturally occurring insulin receptor tyrosine kinase domain mutants provide evidence that phosphoinositide 3-kinase activation alone is not sufficient for the mediation of insulin's metabolic and mitogenic effects. *The Journal of biological chemistry* **272**, 30208 (Nov 28, 1997).
200. J. Hu, J. Liu, R. Ghirlando, A. R. Saltiel, S. R. Hubbard, Structural basis for recruitment of the adaptor protein APS to the activated insulin receptor. *Molecular cell* **12**, 1379 (Dec, 2003).
201. Z. Ahmed, B. J. Smith, K. Kotani, P. Wilden, T. S. Pillay, APS, an adapter protein with a PH and SH2 domain, is a substrate for the insulin receptor kinase. *Biochem J* **341 (Pt 3)**, 665 (Aug 1, 1999).
202. Z. Ahmed, B. J. Smith, T. S. Pillay, The APS adapter protein couples the insulin receptor to the phosphorylation of c-Cbl and facilitates ligand-stimulated ubiquitination of the insulin receptor. *FEBS Lett* **475**, 31 (Jun 9, 2000).
203. M. Y. Ahn, K. D. Katsanakis, F. Bheda, T. S. Pillay, Primary and essential role of the adaptor protein APS for recruitment of both c-Cbl and its associated protein CAP in insulin signaling. *J Biol Chem* **279**, 21526 (May 14, 2004).
204. J. Liu, A. Kimura, C. A. Baumann, A. R. Saltiel, APS facilitates c-Cbl tyrosine phosphorylation and GLUT4 translocation in response to insulin in 3T3-L1 adipocytes. *Mol Cell Biol* **22**, 3599 (Jun, 2002).
205. C. A. Baumann *et al.*, CAP defines a second signalling pathway required for insulin-stimulated glucose transport. *Nature* **407**, 202 (Sep 14, 2000).
206. A. Kimura, C. A. Baumann, S. H. Chiang, A. R. Saltiel, The sorbin homology domain: a motif for the targeting of proteins to lipid rafts. *Proc Natl Acad Sci U S A* **98**, 9098 (Jul 31, 2001).
207. V. Ribon, S. Hubbell, R. Herrera, A. R. Saltiel, The product of the cbl oncogene forms stable complexes in vivo with endogenous Crk in a tyrosine phosphorylation-dependent manner. *Mol Cell Biol* **16**, 45 (Jan, 1996).
208. B. S. Knudsen, S. M. Feller, H. Hanafusa, Four proline-rich sequences of the guanine-nucleotide exchange factor C3G bind with unique specificity to the first Src homology 3 domain of Crk. *J Biol Chem* **269**, 32781 (Dec 30, 1994).
209. S. Tanaka *et al.*, C3G, a guanine nucleotide-releasing protein expressed ubiquitously, binds to the Src homology 3 domains of CRK and GRB2/ASH proteins. *Proc Natl Acad Sci U S A* **91**, 3443 (Apr 12, 1994).
210. S. H. Chiang, J. C. Hou, J. Hwang, J. E. Pessin, A. R. Saltiel, Cloning and functional characterization of related TC10 isoforms, a subfamily of Rho proteins involved in insulin-stimulated glucose transport. *J Biol Chem* **277**, 13067 (Apr 12, 2002).
211. T. Katome *et al.*, Use of RNA interference-mediated gene silencing and adenoviral overexpression to elucidate the roles of AKT/protein kinase B isoforms in insulin actions. *The Journal of biological chemistry* **278**, 28312 (Jul 25, 2003).
212. M. J. Quon *et al.*, Insulin receptor substrate 1 mediates the stimulatory effect of insulin on GLUT4 translocation in transfected rat adipose cells. *The Journal of biological chemistry* **269**, 27920 (Nov 11, 1994).

213. L. Chang, S. H. Chiang, A. R. Saltiel, TC10alpha is required for insulin-stimulated glucose uptake in adipocytes. *Endocrinology* **148**, 27 (Jan, 2007).
214. Y. Takai, T. Sasaki, T. Matozaki, Small GTP-binding proteins. *Physiological reviews* **81**, 153 (Jan, 2001).
215. J. S. Bogan, Regulation of glucose transporter translocation in health and diabetes. *Annual review of biochemistry* **81**, 507 (2012).
216. H. R. Bourne, D. A. Sanders, F. McCormick, The GTPase superfamily: conserved structure and molecular mechanism. *Nature* **349**, 117 (Jan 10, 1991).
217. Y. Takai, K. Kaibuchi, A. Kikuchi, M. Kawata, Small GTP-binding proteins. *International review of cytology* **133**, 187 (1992).
218. A. Valencia, P. Chardin, A. Wittinghofer, C. Sander, The ras protein family: evolutionary tree and role of conserved amino acids. *Biochemistry* **30**, 4637 (May 14, 1991).
219. P. J. Casey, M. C. Seabra, Protein prenyltransferases. *The Journal of biological chemistry* **271**, 5289 (Mar 8, 1996).
220. J. A. Glomset, C. C. Farnsworth, Role of protein modification reactions in programming interactions between ras-related GTPases and cell membranes. *Annual review of cell biology* **10**, 181 (1994).
221. A. I. Magee *et al.*, Lipid modifications and function of the ras superfamily of proteins. *Biochemical Society transactions* **20**, 497 (May, 1992).
222. F. L. Zhang, P. J. Casey, Protein prenylation: molecular mechanisms and functional consequences. *Annual review of biochemistry* **65**, 241 (1996).
223. M. Paduch, F. Jelen, J. Otlewski, Structure of small G proteins and their regulators. *Acta Biochim Pol* **48**, 829 (2001).
224. J. L. Bos, H. Rehmann, A. Wittinghofer, GEFs and GAPs: critical elements in the control of small G proteins. *Cell* **129**, 865 (Jun 1, 2007).
225. G. I. Welsh, I. Hers, M. Wherlock, J. M. Tavare, Regulation of small GTP-binding proteins by insulin. *Biochem Soc Trans* **34**, 209 (Apr, 2006).
226. N. van den Berghe *et al.*, Activation of the Ras/mitogen-activated protein kinase signaling pathway alone is not sufficient to induce glucose uptake in 3T3-L1 adipocytes. *Mol Cell Biol* **14**, 2372 (Apr, 1994).
227. S. F. Hausdorff, J. V. Frangioni, M. J. Birnbaum, Role of p21ras in insulin-stimulated glucose transport in 3T3-L1 adipocytes. *J Biol Chem* **269**, 21391 (Aug 26, 1994).
228. D. F. Lazar *et al.*, Mitogen-activated protein kinase kinase inhibition does not block the stimulation of glucose utilization by insulin. *J Biol Chem* **270**, 20801 (Sep 1, 1995).
229. L. Pang, D. F. Lazar, D. E. Moller, J. S. Flier, A. R. Saltiel, The stimulation of pp42mapkinase by insulin does not correlate with its metabolic actions in cells overexpressing mutant insulin receptors. *Biochemical and biophysical research communications* **196**, 301 (Oct 15, 1993).
230. K. L. Houseknecht *et al.*, Overexpression of Ha-ras selectively in adipose tissue of transgenic mice. Evidence for enhanced sensitivity to insulin. *J Biol Chem* **271**, 11347 (May 10, 1996).
231. A. W. Harmon, D. S. Paul, Y. M. Patel, MEK inhibitors impair insulin-stimulated glucose uptake in 3T3-L1 adipocytes. *Am J Physiol Endocrinol Metab* **287**, E758 (Oct, 2004).

232. C. N. Antonescu *et al.*, Reduction of insulin-stimulated glucose uptake in L6 myotubes by the protein kinase inhibitor SB203580 is independent of p38MAPK activity. *Endocrinology* **146**, 3773 (Sep, 2005).
233. L. A. Feig, Ral-GTPases: approaching their 15 minutes of fame. *Trends Cell Biol* **13**, 419 (Aug, 2003).
234. X. W. Chen *et al.*, Exocyst function is regulated by effector phosphorylation. *Nature cell biology* **13**, 580 (May, 2011).
235. S. J. Heasman, A. J. Ridley, Mammalian Rho GTPases: new insights into their functions from in vivo studies. *Nature reviews. Molecular cell biology* **9**, 690 (Sep, 2008).
236. Z. A. Khayat, P. Tong, K. Yaworsky, R. J. Bloch, A. Klip, Insulin-induced actin filament remodeling colocalizes actin with phosphatidylinositol 3-kinase and GLUT4 in L6 myotubes. *J Cell Sci* **113 Pt 2**, 279 (Jan, 2000).
237. J. Dorrestijn, J. L. Bos, G. C. Van der Zon, J. A. Maassen, Changes in the signalling status of the small GTP-binding proteins Rac and Rho do not influence insulin-stimulated hexose transport. *Exp Clin Endocrinol Diabetes* **105**, 254 (1997).
238. M. Standaert *et al.*, Comparative effects of GTPgammaS and insulin on the activation of Rho, phosphatidylinositol 3-kinase, and protein kinase N in rat adipocytes. Relationship to glucose transport. *J Biol Chem* **273**, 7470 (Mar 27, 1998).
239. G. Schmid *et al.*, Inhibition of insulin-stimulated glucose transport in 3T3-L1 cells by Clostridium difficile toxin B, Clostridium sordellii lethal toxin, and Clostridium botulinum C2 toxin. *Naunyn Schmiedebergs Arch Pharmacol* **357**, 385 (Apr, 1998).
240. L. JeBailey *et al.*, Skeletal muscle cells and adipocytes differ in their reliance on TC10 and Rac for insulin-induced actin remodeling. *Mol Endocrinol* **18**, 359 (Feb, 2004).
241. I. Usui, T. Imamura, J. Huang, H. Satoh, J. M. Olefsky, Cdc42 is a Rho GTPase family member that can mediate insulin signaling to glucose transport in 3T3-L1 adipocytes. *J Biol Chem* **278**, 13765 (Apr 18, 2003).
242. G. Joberty, R. R. Perlungher, I. G. Macara, The Borgs, a new family of Cdc42 and TC10 GTPase-interacting proteins. *Mol Cell Biol* **19**, 6585 (Oct, 1999).
243. C. L. Neudauer, G. Joberty, N. Tatsis, I. G. Macara, Distinct cellular effects and interactions of the Rho-family GTPase TC10. *Curr Biol* **8**, 1151 (Oct 22, 1998).
244. G. A. Murphy *et al.*, Signaling mediated by the closely related mammalian Rho family GTPases TC10 and Cdc42 suggests distinct functional pathways. *Cell Growth Differ* **12**, 157 (Mar, 2001).
245. D. Michaelson *et al.*, Differential localization of Rho GTPases in live cells: regulation by hypervariable regions and RhoGDI binding. *J Cell Biol* **152**, 111 (Jan 8, 2001).
246. L. Chang, R. D. Adams, A. R. Saltiel, The TC10-interacting protein CIP4/2 is required for insulin-stimulated Glut4 translocation in 3T3L1 adipocytes. *Proc Natl Acad Sci U S A* **99**, 12835 (Oct 1, 2002).
247. M. Kanzaki, S. Mora, J. B. Hwang, A. R. Saltiel, J. E. Pessin, Atypical protein kinase C (PKCzeta/lambda) is a convergent downstream target of the insulin-stimulated phosphatidylinositol 3-kinase and TC10 signaling pathways. *J Cell Biol* **164**, 279 (Jan 19, 2004).
248. I. J. Lodhi *et al.*, Gapex-5, a Rab31 guanine nucleotide exchange factor that regulates Glut4 trafficking in adipocytes. *Cell Metab* **5**, 59 (Jan, 2007).
249. I. J. Lodhi *et al.*, Insulin stimulates phosphatidylinositol 3-phosphate production via the activation of Rab5. *Mol Biol Cell* **19**, 2718 (Jul, 2008).

250. X. Mao *et al.*, APPL1 binds to adiponectin receptors and mediates adiponectin signalling and function. *Nat Cell Biol* **8**, 516 (May, 2006).
251. T. Saito, C. C. Jones, S. Huang, M. P. Czech, P. F. Pilch, The interaction of Akt with APPL1 is required for insulin-stimulated Glut4 translocation. *The Journal of biological chemistry* **282**, 32280 (Nov 2, 2007).
252. G. Bandyopadhyay, Y. Kanoh, M. P. Sajan, M. L. Standaert, R. V. Farese, Effects of adenoviral gene transfer of wild-type, constitutively active, and kinase-defective protein kinase C-lambda on insulin-stimulated glucose transport in L6 myotubes. *Endocrinology* **141**, 4120 (Nov, 2000).
253. G. Bandyopadhyay, M. L. Standaert, L. Galloway, J. Moscat, R. V. Farese, Evidence for involvement of protein kinase C (PKC)-zeta and noninvolvement of diacylglycerol-sensitive PKCs in insulin-stimulated glucose transport in L6 myotubes. *Endocrinology* **138**, 4721 (Nov, 1997).
254. G. Bandyopadhyay *et al.*, Activation of protein kinase C (alpha, beta, and zeta) by insulin in 3T3/L1 cells. Transfection studies suggest a role for PKC-zeta in glucose transport. *J Biol Chem* **272**, 2551 (Jan 24, 1997).
255. K. Kotani *et al.*, Requirement of atypical protein kinase clambda for insulin stimulation of glucose uptake but not for Akt activation in 3T3-L1 adipocytes. *Molecular and cellular biology* **18**, 6971 (Dec, 1998).
256. S. K. Kim, Cell polarity: new PARtners for Cdc42 and Rac. *Nat Cell Biol* **2**, E143 (Aug, 2000).
257. M. Zerial, H. McBride, Rab proteins as membrane organizers. *Nature reviews. Molecular cell biology* **2**, 107 (Feb, 2001).
258. P. van der Sluijs *et al.*, The small GTP-binding protein rab4 controls an early sorting event on the endocytic pathway. *Cell* **70**, 729 (Sep 4, 1992).
259. M. Deneka *et al.*, Rabaptin-5alpha/rabaptin-4 serves as a linker between rab4 and gamma(1)-adaptin in membrane recycling from endosomes. *EMBO J* **22**, 2645 (Jun 2, 2003).
260. M. W. McCaffrey *et al.*, Rab4 affects both recycling and degradative endosomal trafficking. *FEBS Lett* **495**, 21 (Apr 20, 2001).
261. M. Cormont *et al.*, Potential role of Rab4 in the regulation of subcellular localization of Glut4 in adipocytes. *Molecular and cellular biology* **16**, 6879 (Dec, 1996).
262. M. Cormont, N. Gautier, K. Ilc, Y. le Marchand-Brustel, Expression of a prenylation-deficient Rab4 inhibits the GLUT4 translocation induced by active phosphatidylinositol 3-kinase and protein kinase B. *Biochem J* **356**, 143 (May 15, 2001).
263. M. Mari *et al.*, The Rab4 effector Rabip4 plays a role in the endocytotic trafficking of Glut 4 in 3T3-L1 adipocytes. *J Cell Sci* **119**, 1297 (Apr 1, 2006).
264. T. Imamura *et al.*, Insulin-induced GLUT4 translocation involves protein kinase C-lambda-mediated functional coupling between Rab4 and the motor protein kinesin. *Mol Cell Biol* **23**, 4892 (Jul, 2003).
265. J. Huang, T. Imamura, J. M. Olefsky, Insulin can regulate GLUT4 internalization by signaling to Rab5 and the motor protein dynein. *Proc Natl Acad Sci U S A* **98**, 13084 (Nov 6, 2001).
266. M. Ren *et al.*, Hydrolysis of GTP on rab11 is required for the direct delivery of transferrin from the pericentriolar recycling compartment to the cell surface but not from sorting endosomes. *Proc Natl Acad Sci U S A* **95**, 6187 (May 26, 1998).

267. M. Wilcke *et al.*, Rab11 regulates the compartmentalization of early endosomes required for efficient transport from early endosomes to the trans-golgi network. *J Cell Biol* **151**, 1207 (Dec 11, 2000).
268. A. Kessler *et al.*, Rab11 is associated with GLUT4-containing vesicles and redistributes in response to insulin. *Diabetologia* **43**, 1518 (Dec, 2000).
269. M. Uhlig, W. Passlack, J. Eckel, Functional role of Rab11 in GLUT4 trafficking in cardiomyocytes. *Mol Cell Endocrinol* **235**, 1 (May 12, 2005).
270. C. P. Miinea *et al.*, AS160, the Akt substrate regulating GLUT4 translocation, has a functional Rab GTPase-activating protein domain. *Biochem J* **391**, 87 (Oct 1, 2005).
271. H. Sano *et al.*, Rab10, a target of the AS160 Rab GAP, is required for insulin-stimulated translocation of GLUT4 to the adipocyte plasma membrane. *Cell Metab* **5**, 293 (Apr, 2007).
272. H. Sano, W. G. Roach, G. R. Peck, M. Fukuda, G. E. Lienhard, Rab10 in insulin-stimulated GLUT4 translocation. *Biochem J* **411**, 89 (Apr 1, 2008).
273. S. Ishikura, P. J. Bilan, A. Klip, Rabs 8A and 14 are targets of the insulin-regulated Rab-GAP AS160 regulating GLUT4 traffic in muscle cells. *Biochem Biophys Res Commun* **353**, 1074 (Feb 23, 2007).
274. S. Karunanithi *et al.*, A Rab10:RalA G protein cascade regulates insulin-stimulated glucose uptake in adipocytes. *Molecular biology of the cell* **25**, 3059 (Oct 1, 2014).
275. M. Kawasaki, K. Nakayama, S. Wakatsuki, Membrane recruitment of effector proteins by Arf and Rab GTPases. *Current opinion in structural biology* **15**, 681 (Dec, 2005).
276. J. Gaschet, V. W. Hsu, Distribution of ARF6 between membrane and cytosol is regulated by its GTPase cycle. *The Journal of biological chemistry* **274**, 20040 (Jul 9, 1999).
277. L. V. Li, K. V. Kandror, Golgi-localized, gamma-ear-containing, Arf-binding protein adaptors mediate insulin-responsive trafficking of glucose transporter 4 in 3T3-L1 adipocytes. *Mol Endocrinol* **19**, 2145 (Aug, 2005).
278. R. T. Watson *et al.*, Entry of newly synthesized GLUT4 into the insulin-responsive storage compartment is GGA dependent. *EMBO J* **23**, 2059 (May 19, 2004).
279. J. Shi, G. Huang, K. V. Kandror, Self-assembly of Glut4 storage vesicles during differentiation of 3T3-L1 adipocytes. *J Biol Chem* **283**, 30311 (Oct 31, 2008).
280. B. Doray, P. Ghosh, J. Griffith, H. J. Geuze, S. Kornfeld, Cooperation of GGAs and AP-1 in packaging MPRs at the trans-Golgi network. *Science* **297**, 1700 (Sep 6, 2002).
281. A. K. Gillingham, F. Koumanov, P. R. Pryor, B. J. Reaves, G. D. Holman, Association of AP1 adaptor complexes with GLUT4 vesicles. *J Cell Sci* **112 (Pt 24)**, 4793 (Dec, 1999).
282. S. Martin *et al.*, Biogenesis of insulin-responsive GLUT4 vesicles is independent of brefeldin A-sensitive trafficking. *Traffic* **1**, 652 (Aug, 2000).
283. J. Li *et al.*, An ACAP1-containing clathrin coat complex for endocytic recycling. *J Cell Biol* **178**, 453 (Jul 30, 2007).
284. H. Hacker, M. Karin, Regulation and function of IKK and IKK-related kinases. *Science's STKE : signal transduction knowledge environment* **2006**, re13 (Oct 17, 2006).
285. G. Bonizzi, M. Karin, The two NF-kappaB activation pathways and their role in innate and adaptive immunity. *Trends in immunology* **25**, 280 (Jun, 2004).
286. M. S. Hayden, S. Ghosh, Signaling to NF-kappaB. *Genes & development* **18**, 2195 (Sep 15, 2004).
287. T. Shimada *et al.*, IKK-i, a novel lipopolysaccharide-inducible kinase that is related to IkappaB kinases. *International immunology* **11**, 1357 (Aug, 1999).

288. R. T. Peters, S. M. Liao, T. Maniatis, IKKepsilon is part of a novel PMA-inducible IkappaB kinase complex. *Molecular cell* **5**, 513 (Mar, 2000).
289. Y. Tojima *et al.*, NAK is an IkappaB kinase-activating kinase. *Nature* **404**, 778 (Apr 13, 2000).
290. J. L. Pomerantz, D. Baltimore, NF-kappaB activation by a signaling complex containing TRAF2, TANK and TBK1, a novel IKK-related kinase. *The EMBO journal* **18**, 6694 (Dec 1, 1999).
291. R. R. Shen, W. C. Hahn, Emerging roles for the non-canonical IKKs in cancer. *Oncogene* **30**, 631 (Feb 10, 2011).
292. J. A. DiDonato, M. Hayakawa, D. M. Rothwarf, E. Zandi, M. Karin, A cytokine-responsive IkappaB kinase that activates the transcription factor NF-kappaB. *Nature* **388**, 548 (Aug 7, 1997).
293. F. Mercurio *et al.*, IKK-1 and IKK-2: cytokine-activated IkappaB kinases essential for NF-kappaB activation. *Science* **278**, 860 (Oct 31, 1997).
294. D. M. Rothwarf, E. Zandi, G. Natoli, M. Karin, IKK-gamma is an essential regulatory subunit of the IkappaB kinase complex. *Nature* **395**, 297 (Sep 17, 1998).
295. Z. Chen *et al.*, Signal-induced site-specific phosphorylation targets I kappa B alpha to the ubiquitin-proteasome pathway. *Genes & development* **9**, 1586 (Jul 1, 1995).
296. M. Shirane, S. Hatakeyama, K. Hattori, K. Nakayama, Common pathway for the ubiquitination of IkappaBalpha, IkappaBbeta, and IkappaBepsilon mediated by the F-box protein FWD1. *The Journal of biological chemistry* **274**, 28169 (Oct 1, 1999).
297. M. Karin, Y. Ben-Neriah, Phosphorylation meets ubiquitination: the control of NF-[kappa]B activity. *Annual review of immunology* **18**, 621 (2000).
298. V. J. Palombella, O. J. Rando, A. L. Goldberg, T. Maniatis, The ubiquitin-proteasome pathway is required for processing the NF-kappa B1 precursor protein and the activation of NF-kappa B. *Cell* **78**, 773 (Sep 9, 1994).
299. J. A. Gustin *et al.*, Cell type-specific expression of the IkappaB kinases determines the significance of phosphatidylinositol 3-kinase/Akt signaling to NF-kappa B activation. *The Journal of biological chemistry* **279**, 1615 (Jan 16, 2004).
300. A. M. Pham, B. R. Tenoever, The IKK Kinases: Operators of Antiviral Signaling. *Viruses* **2**, 55 (Jan, 2010).
301. S. Ghosh, M. Karin, Missing pieces in the NF-kappaB puzzle. *Cell* **109 Suppl**, S81 (Apr, 2002).
302. S. Saccani, S. Pantano, G. Natoli, Modulation of NF-kappaB activity by exchange of dimers. *Molecular cell* **11**, 1563 (Jun, 2003).
303. J. F. Clement, S. Meloche, M. J. Servant, The IKK-related kinases: from innate immunity to oncogenesis. *Cell research* **18**, 889 (Sep, 2008).
304. S. H. Chiang *et al.*, The protein kinase IKKepsilon regulates energy balance in obese mice. *Cell* **138**, 961 (Sep 4, 2009).
305. M. Bonnard *et al.*, Deficiency of T2K leads to apoptotic liver degeneration and impaired NF-kappaB-dependent gene transcription. *The EMBO journal* **19**, 4976 (Sep 15, 2000).
306. H. Buss *et al.*, Constitutive and interleukin-1-inducible phosphorylation of p65 NF-{kappa}B at serine 536 is mediated by multiple protein kinases including I{kappa}B kinase (IKK)-{alpha}, IKK{beta}, IKK{epsilon}, TRAF family member-associated (TANK)-binding kinase 1 (TBK1), and an unknown kinase and couples p65 to TATA-

binding protein-associated factor II31-mediated interleukin-8 transcription. *The Journal of biological chemistry* **279**, 55633 (Dec 31, 2004).
307. T. Kawai, S. Akira, Signaling to NF-kappaB by Toll-like receptors. *Trends in molecular medicine* **13**, 460 (Nov, 2007).
308. Q. Li, G. Estepa, S. Memet, A. Israel, I. M. Verma, Complete lack of NF-kappaB activity in IKK1 and IKK2 double-deficient mice: additional defect in neurulation. *Genes & development* **14**, 1729 (Jul 15, 2000).
309. V. V. Kravchenko, J. C. Mathison, K. Schwamborn, F. Mercurio, R. J. Ulevitch, IKKi/IKKepsilon plays a key role in integrating signals induced by pro-inflammatory stimuli. *The Journal of biological chemistry* **278**, 26612 (Jul 18, 2003).
310. K. Clark *et al.*, Novel cross-talk within the IKK family controls innate immunity. *The Biochemical journal* **434**, 93 (Feb 15, 2011).
311. S. Sharma *et al.*, Triggering the interferon antiviral response through an IKK-related pathway. *Science* **300**, 1148 (May 16, 2003).
312. K. A. Fitzgerald *et al.*, IKKepsilon and TBK1 are essential components of the IRF3 signaling pathway. *Nature immunology* **4**, 491 (May, 2003).
313. H. Hemmi *et al.*, The roles of two IkappaB kinase-related kinases in lipopolysaccharide and double stranded RNA signaling and viral infection. *The Journal of experimental medicine* **199**, 1641 (Jun 21, 2004).
314. S. M. McWhirter *et al.*, IFN-regulatory factor 3-dependent gene expression is defective in Tbk1-deficient mouse embryonic fibroblasts. *Proceedings of the National Academy of Sciences of the United States of America* **101**, 233 (Jan 6, 2004).
315. A. K. Miyahira, A. Shahangian, S. Hwang, R. Sun, G. Cheng, TANK-binding kinase-1 plays an important role during in vitro and in vivo type I IFN responses to DNA virus infections. *Journal of immunology* **182**, 2248 (Feb 15, 2009).
316. A. K. Perry, E. K. Chow, J. B. Goodnough, W. C. Yeh, G. Cheng, Differential requirement for TANK-binding kinase-1 in type I interferon responses to toll-like receptor activation and viral infection. *The Journal of experimental medicine* **199**, 1651 (Jun 21, 2004).
317. H. Chen *et al.*, Activation of STAT6 by STING is critical for antiviral innate immunity. *Cell* **147**, 436 (Oct 14, 2011).
318. Y. H. Ou *et al.*, TBK1 directly engages Akt/PKB survival signaling to support oncogenic transformation. *Molecular cell* **41**, 458 (Feb 18, 2011).
319. S. M. Joung *et al.*, Akt contributes to activation of the TRIF-dependent signaling pathways of TLRs by interacting with TANK-binding kinase 1. *Journal of immunology* **186**, 499 (Jan 1, 2011).
320. X. Xie *et al.*, IkappaB kinase epsilon and TANK-binding kinase 1 activate AKT by direct phosphorylation. *Proceedings of the National Academy of Sciences of the United States of America* **108**, 6474 (Apr 19, 2011).
321. M. Delhase, M. Hayakawa, Y. Chen, M. Karin, Positive and negative regulation of IkappaB kinase activity through IKKbeta subunit phosphorylation. *Science* **284**, 309 (Apr 9, 1999).
322. C. Wang *et al.*, TAK1 is a ubiquitin-dependent kinase of MKK and IKK. *Nature* **412**, 346 (Jul 19, 2001).
323. K. Clark, L. Plater, M. Peggie, P. Cohen, Use of the pharmacological inhibitor BX795 to study the regulation and physiological roles of TBK1 and IkappaB kinase epsilon: a

distinct upstream kinase mediates Ser-172 phosphorylation and activation. *The Journal of biological chemistry* **284**, 14136 (May 22, 2009).
324. N. Kishore *et al.*, IKK-i and TBK-1 are enzymatically distinct from the homologous enzyme IKK-2: comparative analysis of recombinant human IKK-i, TBK-1, and IKK-2. *The Journal of biological chemistry* **277**, 13840 (Apr 19, 2002).
325. F. Fujita *et al.*, Identification of NAP1, a regulatory subunit of IkappaB kinase-related kinases that potentiates NF-kappaB signaling. *Molecular and cellular biology* **23**, 7780 (Nov, 2003).
326. G. Ryzhakov, F. Randow, SINTBAD, a novel component of innate antiviral immunity, shares a TBK1-binding domain with NAP1 and TANK. *The EMBO journal* **26**, 3180 (Jul 11, 2007).
327. H. Ishikawa, Z. Ma, G. N. Barber, STING regulates intracellular DNA-mediated, type I interferon-dependent innate immunity. *Nature* **461**, 788 (Oct 8, 2009).
328. S. S. Kim *et al.*, DOK3 is required for IFN-beta production by enabling TRAF3/TBK1 complex formation and IRF3 activation. *Journal of immunology* **193**, 840 (Jul 15, 2014).
329. D. Tu *et al.*, Structure and ubiquitination-dependent activation of TANK-binding kinase 1. *Cell reports* **3**, 747 (Mar 28, 2013).
330. V. V. Saul, R. Niedenthal, A. Pich, F. Weber, M. L. Schmitz, SUMO modification of TBK1 at the adaptor-binding C-terminal coiled-coil domain contributes to its antiviral activity. *Biochimica et biophysica acta* **1853**, 136 (Jan, 2015).
331. M. Zhang *et al.*, Regulation of IkappaB kinase-related kinases and antiviral responses by tumor suppressor CYLD. *The Journal of biological chemistry* **283**, 18621 (Jul 4, 2008).
332. Y. Chien *et al.*, RalB GTPase-mediated activation of the IkappaB family kinase TBK1 couples innate immune signaling to tumor cell survival. *Cell* **127**, 157 (Oct 6, 2006).

Chapter 2

Novel function of the protein kinase TBK1 in insulin-stimulated glucose transport

Introduction

Insulin maintains glucose homeostasis by stimulating glucose uptake and storage in skeletal muscle and adipose tissue and reducing hepatic glucose production. Dysregulation of insulin-stimulated glucose transport into muscle and fat cells is one of the primary defects underlying insulin resistance, which is a hallmark of Type 2 diabetes (*1, 2*). Insulin stimulates glucose uptake in muscle and fat cells via the translocation of the facilitative transporter Glut4 from intracellular sites to the plasma membrane. Although there has been significant progress in the identification of insulin signaling pathways leading to GLUT4 translocation and glucose uptake, the connections between insulin signaling pathways and the trafficking machineries involved in GLUT4 vesicle translocation and targeting have not been fully defined (*3, 4*). Previous studies demonstrate that the exocyst complex plays a pivotal role in insulin-stimulated GLUT4 translocation by facilitating the docking of GLUT4 vesicles to the plasma membrane (*5, 6*). This tethering complex mediates the initial recognition between GLUT4 vesicles and the plasma membrane, under the control of integrated signal inputs from different insulin-sensitive small G proteins (*4, 7-9*). While the details of signaling pathways that regulate this process remain incomplete, a recent study suggest that the protein kinase TBK1 is found in the exocyst complex,

and RalB GTPases-mediated activation of TBK1 couples innate immune signaling to tumor cell survival (*10*). Given the important roles of the exocyst and Ral GTPases in insulin-stimulated glucose transport, these observations prompted us to examine the role of TBK1 in the regulation of glucose transport in 3T3-L1 adipocytes.

Results and Discussion

TBK1 is required for insulin-stimulated glucose uptake.

While the IκB kinases (IKK), IKKα, IKKβ, IKKε and TBK1, are structurally similar, their physiologically relevant substrates and mode of activation appear to differ (*11, 12*). Recent studies suggest that the activation of NFκB by high fat diet induces the expression of the noncanonical kinases IKKε and TBK1, and further that these kinases can co-opt insulin targets, such as Akt and PDE3B, to counteract inflammation in adipose tissue and promote anabolic process in obesity (*13-17*). Interestingly, a recent study suggests that TBK1 is associated with the exocyst subunit Sec5 (*10*). This prompted us to examine the potential role of this kinase and its family members in the regulation of glucose uptake in adipocytes.

We first evaluated the expression of TBK1 and related IKKs during adipogenesis of 3T3-L1 adipocytes (**Figure 2.1**). TBK1 protein was expressed at low levels in 3T3-L1 preadipocytes, but was induced approximately 2-3 fold after differentiation of these cells into mature adipocytes, mirroring the increased expression of the adipogenic markers PPARγ, C/EBPα, and C/EBPδ, but appearing prior to GLUT4 and perilipin. Expression of the other IKK family members were less

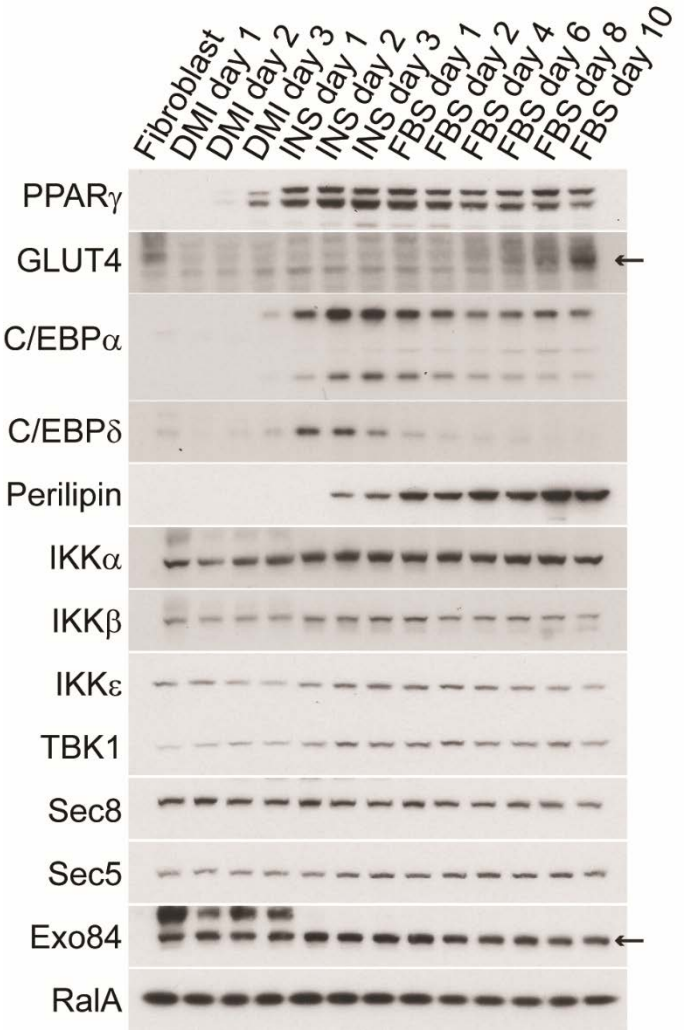

Figure 2.1 Differentiation of 3T3-L1 fibroblasts under different conditions.
3T3-L1 fibroblasts were induced to undergo differentiation with different combinations of dexamethasone (D), insulin (I), and isobutylmethylxanthine (M) in the culture media. Cells were lysed at several stages during adipogenesis. Cell lysates were subjected to immunoblot analysis and probed using specific antibodies as indicated. Arrows indicate the specific band corresponding to the expected molecular weight of the proteins.

dependent on differentiation state, and expression of the exocyst subunits, Sec8, Sec5, and Exo84 remained unchanged during adipogenesis.

To evaluate the potential role of these kinases in insulin-stimulated glucose uptake, we used siRNA oligos to knock down TBK1, IKKε, α, and β in 3T3-L1 adipocytes, followed by measurement of [^{14}C]2-deoxyglucose (DG) uptake in response to insulin (**Figure 2.2**). Insulin treatment produced an approximately 7-8 fold increase in the uptake of 2-DG; electroporation with scrambled control siRNA was without effect. Greater than 80% knockdown of IKKε, α, and β was achieved with specific siRNAs (**Figure 2.2A**), but there was no discernable effect on 2-DG uptake in the basal or insulin-stimulated state. The level of TBK1 was not affected by the knockdown of other related kinases. However, siRNA-mediated knockdown of TBK1 produced an approximately 50% reduction in insulin-stimulated glucose uptake, comparable to what has been reported with Akt knockdown (*18*), without affecting basal transport activity (**Figure 2.2B**). The knockdown of TBK1 appeared to be greater than 90%, and was accompanied by a modest decrease in the stimulation of Akt phosphorylation by insulin, while knockdown of other kinases was without effect on Akt phosphorylation (**Figure 2.2A**).

In addition to its role as a protein kinase, TBK1 can form multiple hetero- and homo-dimeric complexes with other signaling proteins, and thus can serve as a molecular scaffold in addition to its activity as a protein kinase (*19-24*). To explore the role of the kinase activity of TBK1 in insulin-stimulated glucose uptake, we overexpressed both wild type (WT) and a kinase-inactive mutant of TBK1 (K38A) in 3T3-L1 adipocytes, followed by measurement of [^{14}C]2-deoxyglucose (DG) uptake (**Figure 2.3**).

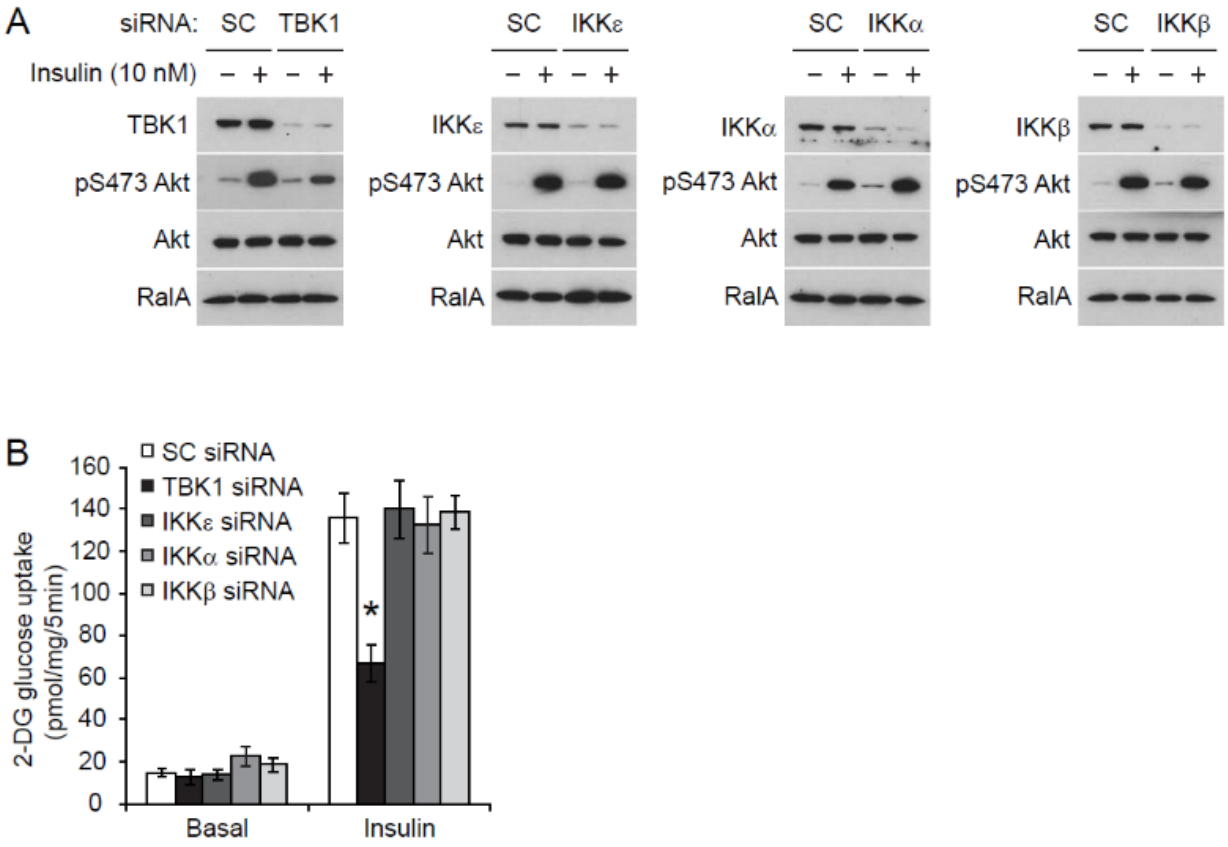

Figure 2.2 SiRNA-mediated knockdown of TBK1 inhibits insulin-stimulated glucose uptake.

(A) SiRNA-mediated knockdown of IKKα, IKKβ, IKKε, and TBK1 in 3T3-L1 adipocytes. 3T3-L1 adipocytes were electroporated with duplex siRNA against IKKα, IKKβ, IKKε, TBK1 or their scrambled control, and stimulated with 10 nM insulin for 30 minutes. Lysates were run on SDS-PAGE and immunoblotted with indicated antibodies. (B) SiRNA-mediated knockdown of TBK1 inhibits insulin-stimulated glucose uptake. Cells from Figure 2.2A were subjected to 2-deoxyglucose uptake assay. Data are shown as the mean ± SEM. *$p < 0.05$; n=3.

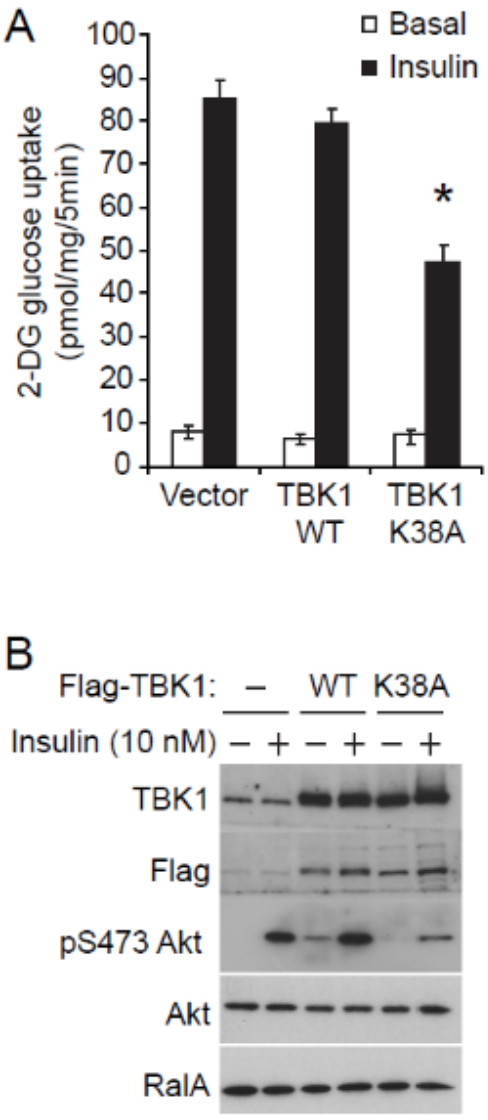

Figure 2.3 Ectopic overexpression of a kinase-inactive mutant of TBK1 reduces insulin-stimulated glucose uptake.
(A) Ectopic overexpression of a kinase-inactive mutant of TBK1 reduces insulin-stimulated glucose uptake. 3T3-L1 adipocytes were ectopically transfected with WT TBK1 or a kinase-inactive mutant of TBK1 (K38A) as indicated and stimulated with 10 nM insulin for 30 minutes. Cells were subjected to 2-deoxyglucose uptake assay. Data are shown as the mean ± SEM. *$p < 0.05$; $n = 3$. (B) Ectopic overexpression of WT TBK1 and its kinase-inactive mutant in 3T3-L1 adipocytes. Levels of indicated proteins in 3T3-L1 adipocytes under conditions in Figure 2.3A were assessed by immunoblots.

While overexpression of WT TBK1 was without effect on basal or insulin-stimulated glucose uptake, overexpression of its kinase-inactive mutant produced an approximately 40-50% inhibition of insulin-stimulated glucose uptake without impacting basal levels (**Figure 2.3A**). In these experiments, approximately 2-3 fold overexpression was achieved relative to endogenous protein levels (**Figure 2.3B**). In addition, overexpression of WT TBK1 increased Akt phosphorylation in the basal and insulin-stimulated state, consistent with previous reports that TBK1 is an upstream kinase of Akt (*14-16*). Consistent with this, expression of the catalytically inactive kinase partially blocked insulin-stimulated Akt phosphorylation but was without effect on basal activity.

To test further if TBK1 kinase activity is required for insulin-stimulated glucose uptake, we blocked TBK1 activity with the selective, but structurally unrelated inhibitors of TBK1 and IKKε, Amlexanox or CAY10576 (Cay) (*25, 26*) (**Figure 2.4**). Insulin-stimulated glucose uptake was inhibited in a dose-dependent manner with both inhibitors.

We also examined the translocation of GLUT4 to the plasma membrane in 3T3-L1 adipocytes stably expressing a dual tagged-GLUT4, in which the exofacial loop of GLUT4 is tagged with MYC, while the cytoplasmic tail is tagged with enhanced green fluorescent protein (eGFP) (*27*). As previously described (*9, 27, 28*), insulin treatment produced a large increase in the translocation of the GLUT4 fusion protein to the plasma membrane, along with the appearance of the exofacial MYC epitope signal. Compared to cells electroporated with scrambled control siRNA, knockdown of TBK1 blocked the appearance of the MYC epitope signal on the plasma

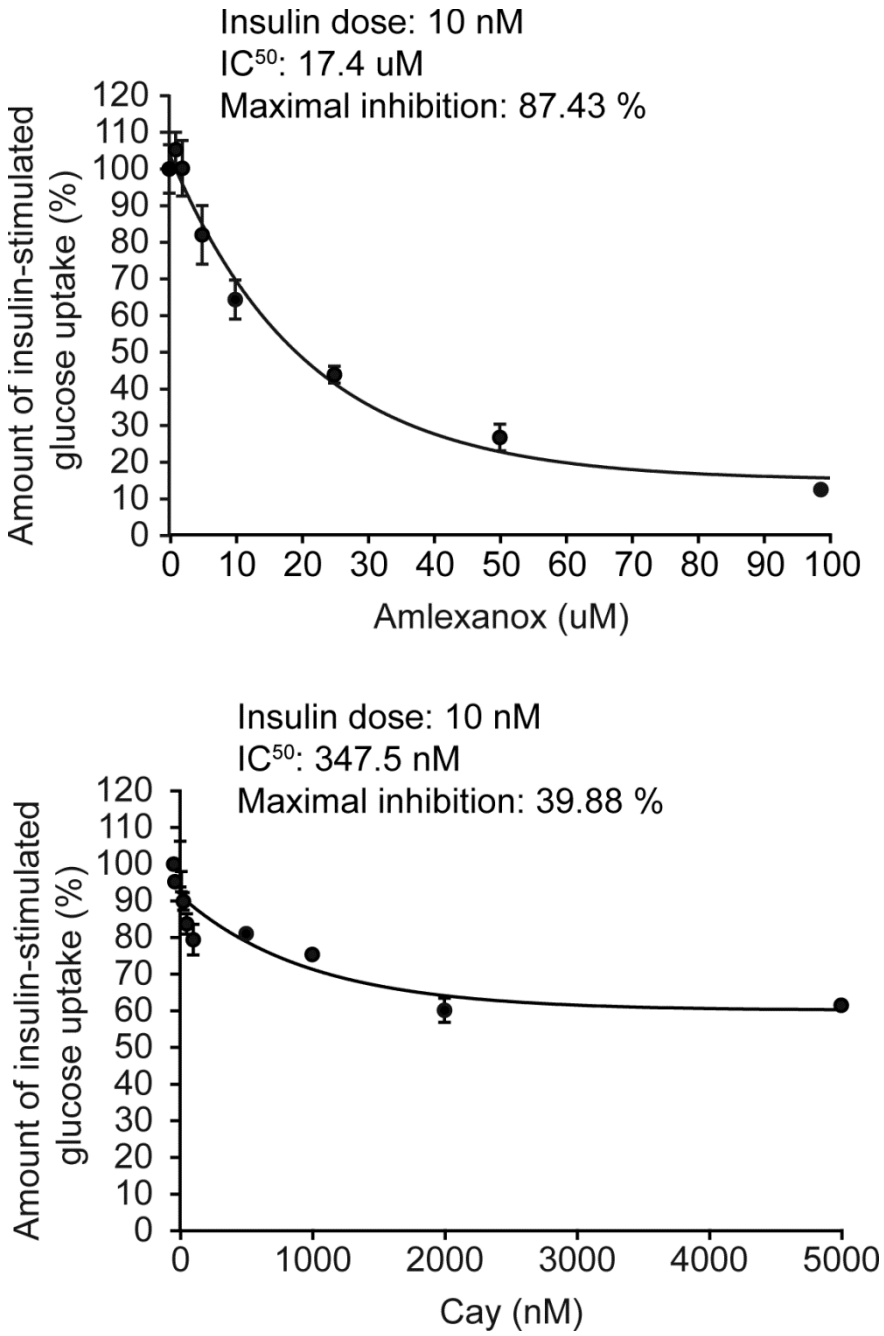

Figure 2.4 TBK1 activity is required for insulin-stimulated glucose uptake.
Inhibition of insulin-stimulated glucose uptake in a dose-dependent manner with TBK1 inhibitors. Insulin-stimulated glucose uptake was performed as described in materials and methods in 3T3-L1 adipocytes pretreated with different doses of amlexanox or cay. Percentage of insulin-stimulated glucose uptake was calculated and the values of IC^{50} and maximal inhibition were produced with GraphPad Prism 6 software. Data are shown as the mean ± SEM. n = 3.

membrane in response to insulin, without affecting the localization of the GLUT4 fusion protein in the basal state (**Figure 2.5A**). Quantitation of these data revealed that knockdown of TBK1 produced an approximate 40% reduction in the appearance of the MYC epitope signal on the plasma membrane in response to insulin (**Figure 2.5B**). Although it was difficult to assess the knockdown efficiency of TBK1 by immunohistochemistry due to autofluorescence (data not shown), the knockdown of TBK1 appeared to be approximately 50% as assessed by western blotting, with little effect on the stimulation of Akt phosphorylation by insulin (**Figure 2.5C**). These studies demonstrate that TBK1 is required for insulin-stimulated glucose transport and GLUT4 translocation in adipocytes in a cell-autonomous manner.

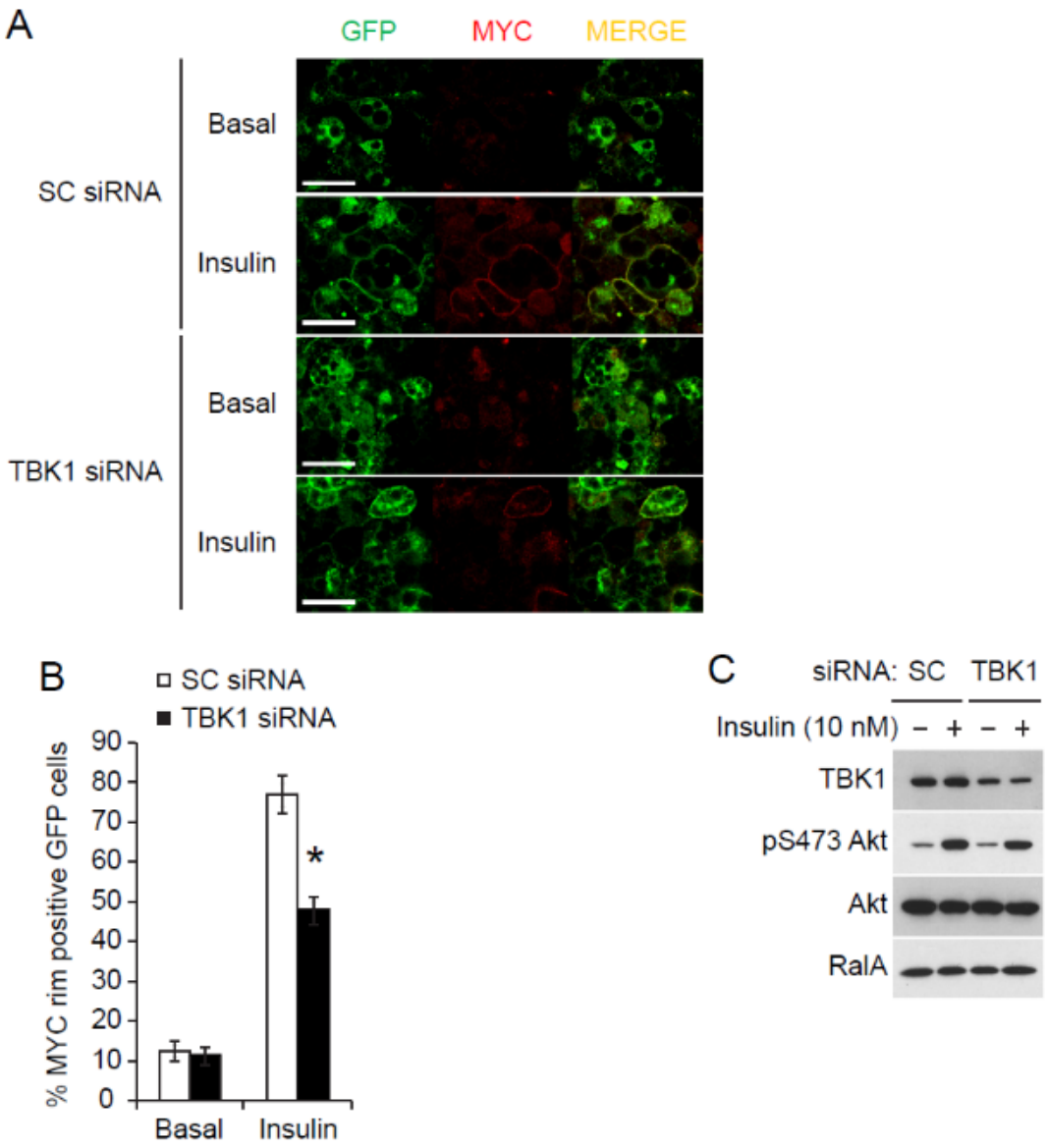

Figure 2.5 SiRNA-mediated knockdown of TBK1 inhibits insulin-stimulated GLUT4 translocation.

(A) SiRNA-mediated knockdown of TBK1 inhibits insulin-stimulated GLUT4 translocation. 3T3-L1 adipocytes stably expressing MYC-GLUT4-eGFP were electroporated with duplex siRNA against TBK1 and stimulated with 10 nM insulin for 15 minutes. Immunostaining for MYC (red) in nonpermeabilized cells indicates GLUT4 translocation to the plasma membrane. GFP levels in cells indicate total GLUT4 expressed. A merge of GFP and MYC is shown. Bar, 200 μm. (B) Quantification of GLUT4 translocation as shown in Figure 2.5A. Number of cells that show MYC staining at the rim in the total number of GFP-positive cells was counted for scrambled and TBK1 knockdown. Percentage of cells that undergo GLUT4 translocation is graphed. Error bars are indicative of at least three independent experiments. Data are shown as the mean ± SEM. *$p < 0.05$; $n = 97$. (C) SiRNA-mediated knockdown of TBK1 in 3T3-L1 adipocytes. Levels of indicated proteins in 3T3-L1 adipocytes under conditions in Figure 2.5A were assessed by immunoblots.

The impact of TBK1 on insulin-stimulated glucose uptake occurs in parallel with Akt.

TBK1 serves as an important component of multiple signaling pathways, including the innate immune response, autophagy, cell proliferation and growth, and insulin signaling (*12*). However, how TBK1 is activated, as well as the identity of its physiologically relevant substrates remain uncertain. The observation that knockdown of TBK1 reduced insulin-stimulated GLUT4 translocation, with little effect on Akt phosphorylation (**Figure 2.5**), suggests that the kinase might regulate glucose uptake through a mechanism independent of Akt. To explore the relative role of Akt and TBK1 in insulin-stimulated glucose transport, 3T3-L1 adipocytes were pretreated with Akti-1/2 (Akti), an inhibitor with high specificity for Akt kinases by targeting the PH domain (*29*), the TBK1 inhibitor amlexanox, or the two inhibitors together, followed by measurement of [^{14}C]2-deoxyglucose (DG) uptake (**Figure 2.6**). Pretreatment of 3T3-L1 adipocytes with Akti or amlexanox produced an approximately 80% and 70% inhibition of insulin-stimulated glucose uptake, respectively (**Figure 2.6A and Figure 2.6C**). However, insulin-stimulated glucose uptake was completely suppressed by a combination of pretreatment with both inhibitors. Stimulation of Akt phosphorylation by insulin was partially inhibited by Akti, amlexanox, and a combination of both inhibitors, but not completely inhibited to the basal state (**Figure 2.6B**). These data indicate that complete inhibition of insulin-stimulated glucose uptake by the combination of Akti and amlexanox can only be partially explained by inhibition of Akt activation.

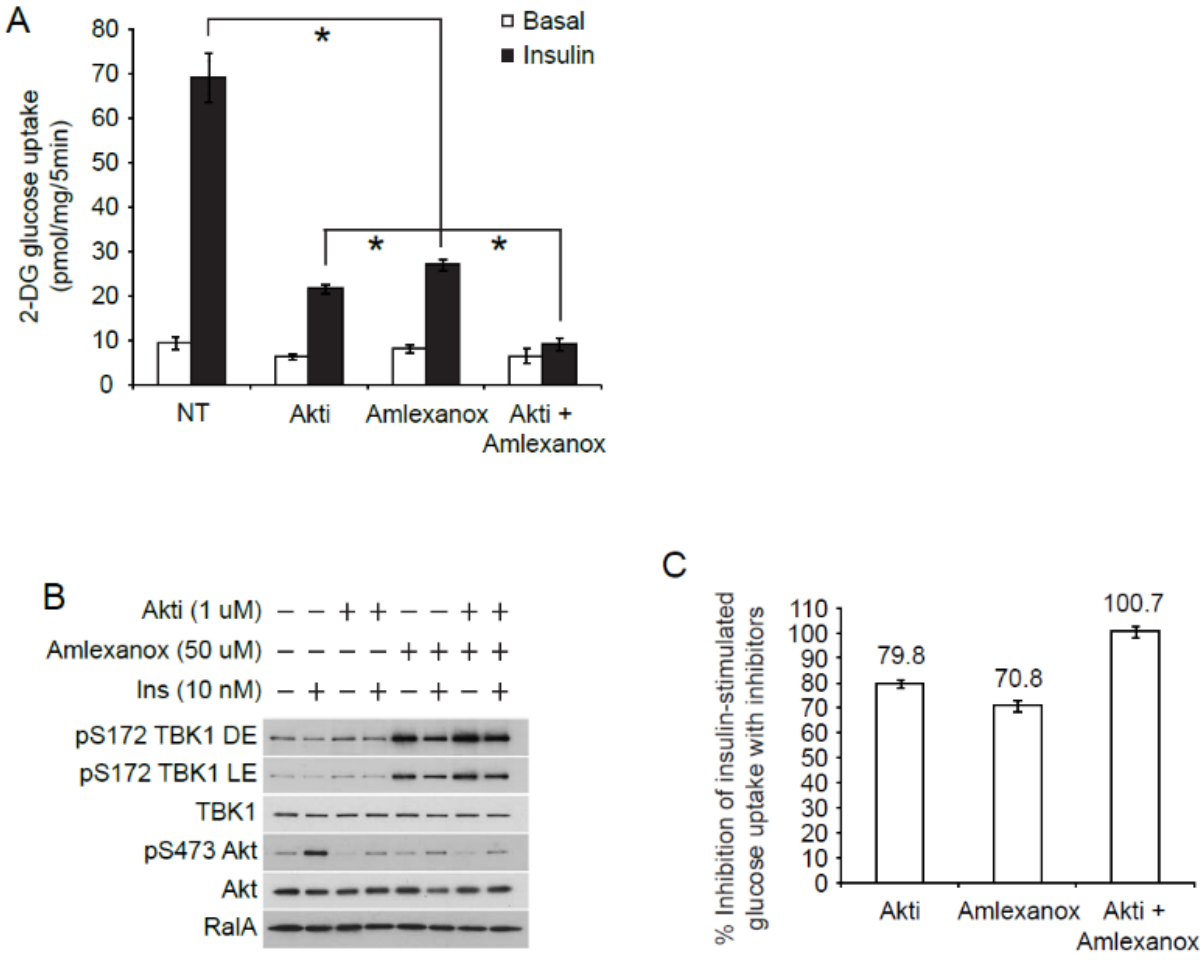

Figure 2.6 TBK1 regulates insulin-stimulated glucose uptake in parallel with Akt.
(A) Inhibition of Akt and TBK1 blocks insulin-stimulated glucose uptake. Insulin-stimulated glucose uptake in 3T3-L1 adipocytes pretreated with inhibitors of Akt and TBK1. Data are shown as the mean ± SEM. *$p < 0.05$; n=3. (B) Stimulation of Akt phosphorylation by insulin was inhibited by Akti and amlexanox. Cells from Figure 2.6A were lysed and subjected to immunoblot analysis with indicated antibodies. DE and LE stand for dark exposure and light exposure, respectively. (C) Quantification of inhibition of insulin-stimulated glucose uptake as shown in Figure 2.6A. Percent inhibition of insulin-stimulated glucose uptake was calculated. Data are shown as the mean ± SEM. n = 3.

To further evaluate whether TBK1 regulates insulin-stimulated glucose uptake in parallel with Akt, we tested another structurally unrelated inhibitor of TBK1, Cay (**Figure 2.7**). Pretreatment of 3T3-L1 adipocytes with Akti or Cay produced an approximately 70% or 45% inhibition of insulin-stimulated glucose uptake, respectively (**Figure 2.7A** and **Figure 2.7C**). Stimulation of Akt phosphorylation by insulin was partially inhibited by Akti, Cay, and a combination of both inhibitors (**Figure 2.7B**). Similar to amlexanox, Akti and Cay synergistically blocked insulin-stimulated glucose uptake in 3T3-L1 adipocytes, suggesting that TBK1 and Akt parallel pathways may be involved.

We also examined the effects of these inhibitors in a GLUT4 translocation assay (**Figure 2.8**). Pretreatment of 3T3-L1 adipocytes with Akti and amlexanox had no effect on the localization of GLUT4 fusion protein in the basal state, but blocked the effect of insulin, since the appearance of the MYC epitope signal on the plasma membrane in response to insulin was significantly reduced. Pretreatment with Akti in combination with amlexanox synergistically blocked the appearance of the MYC epitope signal on the plasma membrane in response to insulin, without affecting the localization of the GLUT4 fusion protein under basal conditions (**Figure 2.8A**). Quantitation of these data showed that approximately 70% of the appearance of the plasma membrane MYC epitope signal in response to insulin was blocked by a combination of pretreatment with both inhibitors (**Figure 2.8B**). These data demonstrate that synergistic inhibition of insulin-stimulated glucose uptake by pretreatment of Akti in combination with amlexanox (or Cay) is likely due to inhibition of the translocation of GLUT4 to the plasma membrane (**Figure 2.9**).

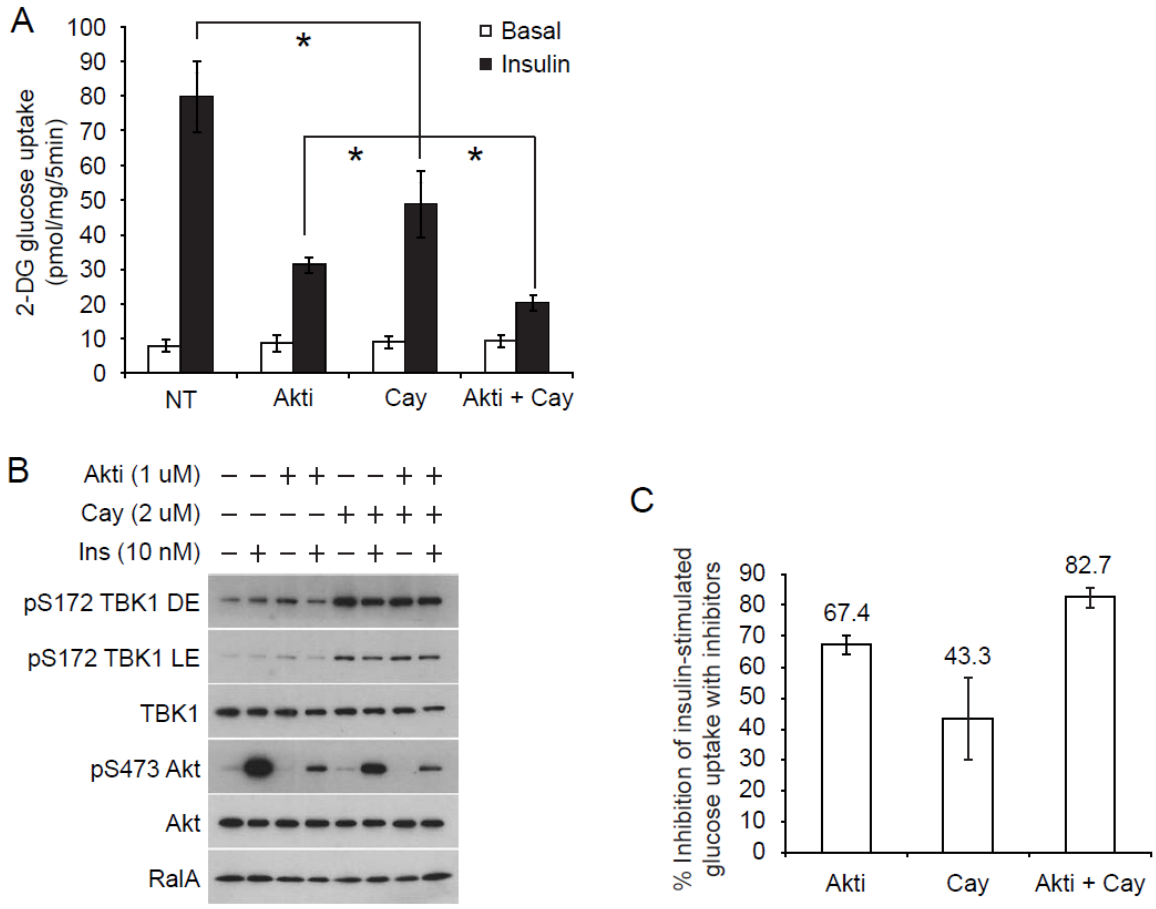

Figure 2.7 TBK1 and Akt parallel pathways are required for insulin-stimulated glucose uptake.
(A) Inhibition of Akt and TBK1 blocks insulin-stimulated glucose uptake. Insulin-stimulated glucose uptake in 3T3-L1 adipocytes pretreated with inhibitors of Akt and TBK1. Data are shown as the mean ± SEM. *$p < 0.05$; n=3. (B) Stimulation of Akt phosphorylation by insulin was inhibited by Akti and Cay. Cells from Figure 2.7A were lysed and subjected to immunoblot analysis with specific antibodies as indicated. DE and LE stand for dark exposure and light exposure, respectively. (C) Quantification of inhibition of insulin-stimulated glucose uptake as shown in Figure 2.7A. Percent inhibition of insulin-stimulated glucose uptake was calculated. Data are shown as the mean ± SEM. n = 3.

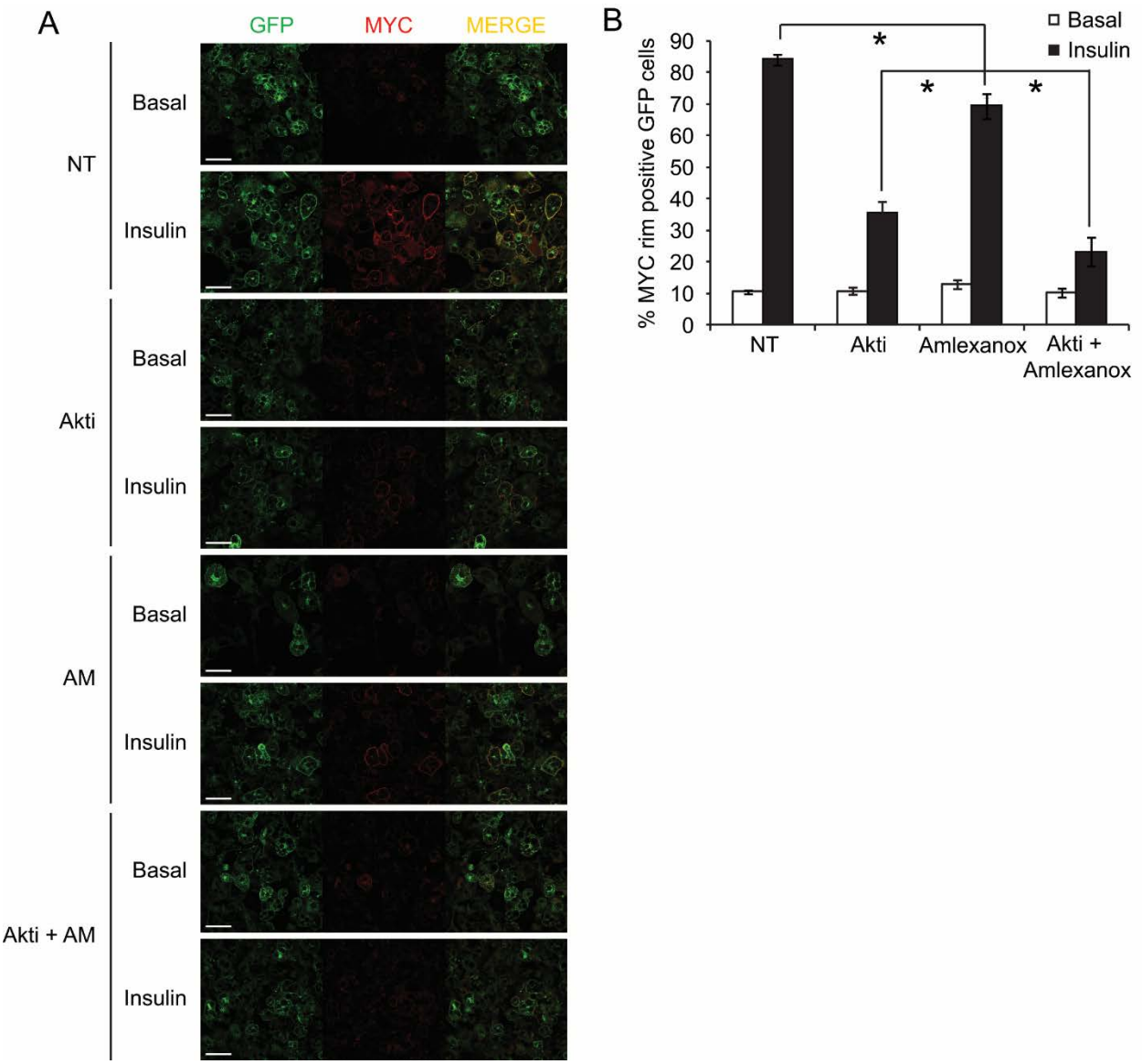

Figure 2.8 TBK1 regulates insulin-stimulated GLUT4 translocation in parallel with Akt. (A) Inhibition of Akt and TBK1 blocks insulin-stimulated GLUT4 translocation. 3T3-L1 adipocytes stably expressing MYC-GLUT4-eGFP were pretreated with Akti (1 μM) and amlexanox (50 μM) for 1 hour and stimulated with 10 nM insulin for 15 minutes. Immunostaining for MYC (red) in nonpermeabilized cells indicates GLUT4 translocation to the plasma membrane. GFP levels in cells indicate total GLUT4 expressed. A merge of GFP and MYC is shown. Bar, 50 μm. (B) Quantification of GLUT4 translocation as shown in Figure 2.8A. Number of cells that show MYC staining at the rim in the total number of GFP-positive cells was counted for each condition. Percentage of cells that undergo GLUT4 translocation is graphed. Error bars are indicative of three independent experiments. Data are shown as the mean ± SEM. *$p < 0.05$; At least 100 cells per condition were counted for anti-MYC rim staining.

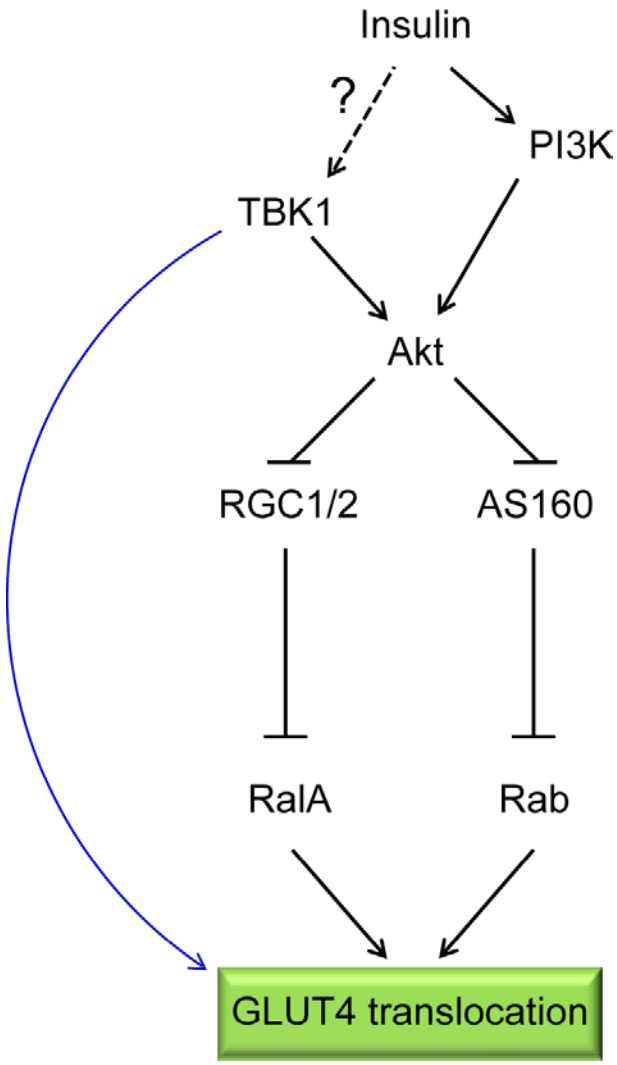

Figure 2.9 Hypothetical model of the role of TBK1 in insulin-stimulated GLUT4 translocation.
Insulin activates the PI3K/Akt pathway, which in turn phosphorylates the Ral GAP complex RGC1/2 and Rab GAP AS160, in the process reducing the inactivation of their cognate GTPases and thus increasing the activity of RalA and Rab10. Once activated, RalA and Rab10 control GLUT4 translocation via the interaction with its effectors involved in GLUT4 trafficking machineries (*4*). While it is not known that insulin regulates the intrinsic kinase activity of TBK1, TBK1 also regulates insulin-stimulated GLUT4 translocation in parallel with Akt.

Materials and Methods

Materials and reagents

All chemicals were obtained from Sigma-Aldrich unless stated otherwise. 2-deoxy-D-[^{14}C]glucose and [γ-^{32}P]ATP were obtained from Perkin Elmer Life Sciences. Stealth™ duplex siRNAs were obtained from Life Technologies and their sequences are listed below.

5’-AGAACAGUGUAUAAACUCCCACAGG-3’and

5’-CCUGUGGGAGUUUAUACACUGUUCU-3’ in combination with

5’-GAUAAGUCGGAAGAGUGGAUGAGAA-3’and

5’-UUCUCAUCCACUCUUCCGACUUAUC-3’ against mouse *Tbk1*.

5’-UGGACAUGCUGAACAGAGUUAGAGG-3’ and

5’-CCUCUAACUCUGUUCAGCAUGUCCA-3’ in combination with

5’-CAGAAGGUGCUAAUCAUGGAGUACU-3’ and

5’-AGUACUCCAUGAUUAGCACCUUCUG-3’ against mouse *Ikbke*.

5’-UGGCACCCAAUGAUUUGCCACUGCU-3’ and

5’-AGCAGUGGCAAAUCAUUGGGUGCCA-3’ in combination with

5’-CAGACAGCAUGAAUGUGUCUCGACU-3’ and

5’-AGUCGAGACACAUUCAUGCUGUCUG-3’ against mouse *Ikbkb*.

5’-CCUCUUCUGGCAAUGGAGUACUGUU-3’ and

5’-AACAGUACUCCAUUGCCAGAAGAGG-3’ in combination with

5’-CCGCUCUCUUGUAGGAUACAGUCUA-3’ and

5’-UAGACUGUAUCCUACAAGAGAGCGG-3’ against mouse *Ikbka*. SiRNAs together with their respective scrambled negative controls were designed using the Block-IT™ program from Life Technologies. Enhanced chemiluminescence (ECL) reagents were purchased from Thermo Scientific. EDTA-free protease inhibitor tablet was purchased from Roche Diagnostics. Amlexanox was purchased from Ontario Chemical Inc. The TBK1/IKKε inhibitor CAY10576 (Cay) was purchased from Cayman Chemical. Akti-1/2 was purchased from EMD Millipore. BenchMark™ Pre-stained protein ladder was purchased from Life Technologies.

Antibodies

Anti-Exo84 was obtained from Santa Cruz Biotechnology. Anti-IKKε, anti-TBK1, anti-phospho-TBK1 (Ser172), anti-AKT, anti-phospho-AKT (Ser473), anti-IKKβ, anti-IKKα, anti-PPARγ, anti-C/EBPα, anti-C/EBPδ, anti-perilipin were purchased from Cell Signaling Technology. Anti-RalA and anti-Sec8 antibodies were purchased from BD Bioscience. Anti-GLUT4 was purchased from Alpha Diagnostics. Anti-Sec5 was purchased from Proteintech Group.

Plasmids

The Flag-tagged human TBK1 WT and TBK1 K38A cDNAs were kindly provided by Dr. Tom Maniatis (Columbia University).

Cell culture and transfection

3T3-L1 fibroblasts (American Type Culture Collection) were cultured and differentiated as described previously (*30*). Cells were routinely used within 10 days after completion of the differentiation process; only cultures in which > 90% of cells displayed adipocyte morphology were used. 3T3-L1 adipocytes were routinely transfected with plasmids and siRNAs by electroporation as described previously (*31*). Electroporation into mature adipocytes was done within 1-4 days post-differentiation at 160 kV, 950 uF. Electroporation with siRNAs to knockdown the gene of interest was continued for 4 days after electroportation unless specified otherwise. 3T3-L1 preadipocytes stably expressing MYC-GLUT4-eGFP were maintained and differentiated as described previously (*9, 28*). 3T3-L1 adipocytes were starved in reduced serum (0.5% FBS) medium for 12 hours. After serum starvation, cells were pretreated for 1 hour with amlexanox or Cay at the given concentrations and stimulated with 10 nM insulin for indicated time.

Glucose uptake assay

3T3-L1 adipocytes grown in 12-well plates were subjected to a glucose uptake assay as described previously (*6*). Briefly, siRNA-electroporated 3T3-L1 adipocytes were cultured until 8 days post-differentiation. For overexpression experiments, 3T3-L1 adipocytes were cultured until 7 days post-differentiation to obtain maximal expression of WT TBK1 and its K38A mutant. After serum starvation, cells were incubated with or without 10 nM insulin for 30 minutes in Krebs-Ringer buffer (*6*). Glucose uptake was initiated by addition of 2-deoxy-D-[^{14}C]glucose and the ^{14}C-labeled glucose incorporation in 5 minutes was measured by scintillation counting.

GLUT4 translocation assay

GLUT4 translocation was measured as described previously (*6*). Briefly, differentiated 3T3-L1 adipocytes stably expressing MYC-GLUT4-eGFP were used at 10 days post-differentiation. After serum starvation, cells were pretreated with or without amlexanox or Cay and stimulated with or without 10 nM insulin for 15 minutes. Cells were then washed once with ice-cold PBS, fixed for 10 minutes in 4% paraformaldehyde (PFA; Electron Microscopy Sciences), neutralized with 100 mM glycine-PBS, followed by blocking in 2% bovine serum albumin (BSA) in PBS for 1 hour at room temperature. Monoclonal anti-MYC antibodies were used at 1:300 dilution. GLUT4 translocation to the plasma membrane was measured by staining with MYC antibodies in nonpermeabilized cells. Alexa-Fluor 568 conjugated goat anti-mouse secondary antibody (Life Technologies) was used as indicated at 1:500 dilution. Confocal images were obtained using an inverted Olympus confocal microscope operated with the Fluoview300 program (Olympus America Inc.). Percentage of cells with insulin-stimulated GLUT4 translocation was calculated as the percentage of cells with MYC staining in the GFP-positive pool.

Immunoblotting

Cells were washed once with ice-cold PBS before lysis with SDS buffer (100 mM Tris-HCL (pH 8.0), 130 mM NaCl, 1% Nonidet P-40 (NP-40), 0.2% Sodium deoxycholate, 0.1% SDS, 10 mM Sodium Pyrophosphate, 1 mM Na_3VO_4, 10 mM NaF) supplemented with an EDTA-free protease inhibitor tablet (Roche), followed by sonication. The crude lysates were centrifuged at13,000 xg for 15 minutes and determined the protein concentration using Protein Assay Reagent (Bio-Rad).

Samples were diluted in 4X SDS sample buffer and boiled for 5 minutes at 95 °C. Proteins were resolved by SDS-polyacrylamide gel electrophoresis (PAGE; Life Technologies) and transferred to nitrocellulose membranes (Bio-Rad). Individual proteins were detected with the specific antibodies and visualized on X-ray film using horseradish peroxidase-conjugated secondary antibodies (Bio-Rad) and Western Lightning Enhanced Chemiluminescence (Perkin Elmer Life Sciences).

Statistical analyses

Averaged values are presented as the mean ± standard error of the mean (s.e.m). When comparing two groups, we performed Student's *t*-test to determine statistical significance. When more than two groups and two factors were investigated, we first performed a two-way analysis of variance (ANOVA) to establish that not all groups were equal. After a statistically significant ANOVA result, we performed between-group comparisons using the Tukey *post hoc* analysis for comparisons of all means and Sidak for comparisons of within factor main effect means. ANOVA and Tukey/Sidak tests were performed using GraphPad Prism version 6.

References

1. A. R. Saltiel, New perspectives into the molecular pathogenesis and treatment of type 2 diabetes. *Cell* 104, 517 (Feb 23, 2001).
2. A. R. Saltiel, C. R. Kahn, Insulin signalling and the regulation of glucose and lipid metabolism. *Nature* 414, 799 (Dec 13, 2001).
3. L. Chang, S. H. Chiang, A. R. Saltiel, Insulin signaling and the regulation of glucose transport. *Mol Med* 10, 65 (Jul-Dec, 2004).
4. D. Leto, A. R. Saltiel, Regulation of glucose transport by insulin: traffic control of GLUT4. *Nature reviews. Molecular cell biology* 13, 383 (Jun, 2012).
5. M. Inoue, L. Chang, J. Hwang, S. H. Chiang, A. R. Saltiel, The exocyst complex is required for targeting of Glut4 to the plasma membrane by insulin. *Nature* 422, 629 (Apr 10, 2003).
6. M. Inoue, S. H. Chiang, L. Chang, X. W. Chen, A. R. Saltiel, Compartmentalization of the exocyst complex in lipid rafts controls Glut4 vesicle tethering. *Mol Biol Cell* 17, 2303 (May, 2006).
7. M. Kanzaki, J. E. Pessin, Insulin signaling: GLUT4 vesicles exit via the exocyst. *Current biology : CB* 13, R574 (Jul 15, 2003).
8. S. Ishikura, A. Koshkina, A. Klip, Small G proteins in insulin action: Rab and Rho families at the crossroads of signal transduction and GLUT4 vesicle traffic. *Acta physiologica* 192, 61 (Jan, 2008).
9. X. W. Chen, D. Leto, S. H. Chiang, Q. Wang, A. R. Saltiel, Activation of RalA is required for insulin-stimulated Glut4 trafficking to the plasma membrane via the exocyst and the motor protein Myo1c. *Dev Cell* 13, 391 (Sep, 2007).
10. Y. Chien *et al.*, RalB GTPase-mediated activation of the IkappaB family kinase TBK1 couples innate immune signaling to tumor cell survival. *Cell* 127, 157 (Oct 6, 2006).
11. R. R. Shen, W. C. Hahn, Emerging roles for the non-canonical IKKs in cancer. *Oncogene* 30, 631 (Feb 10, 2011).
12. E. Helgason, Q. T. Phung, E. C. Dueber, Recent insights into the complexity of Tank-binding kinase 1 signaling networks: the emerging role of cellular localization in the activation and substrate specificity of TBK1. *FEBS letters* 587, 1230 (Apr 17, 2013).
13. S. H. Chiang *et al.*, The protein kinase IKKepsilon regulates energy balance in obese mice. *Cell* 138, 961 (Sep 4, 2009).
14. S. M. Joung *et al.*, Akt contributes to activation of the TRIF-dependent signaling pathways of TLRs by interacting with TANK-binding kinase 1. *Journal of immunology* 186, 499 (Jan 1, 2011).
15. Y. H. Ou *et al.*, TBK1 directly engages Akt/PKB survival signaling to support oncogenic transformation. *Molecular cell* 41, 458 (Feb 18, 2011).
16. X. Xie *et al.*, IkappaB kinase epsilon and TANK-binding kinase 1 activate AKT by direct phosphorylation. *Proceedings of the National Academy of Sciences of the United States of America* 108, 6474 (Apr 19, 2011).
17. J. Mowers *et al.*, Inflammation produces catecholamine resistance in obesity via activation of PDE3B by the protein kinases IKKepsilon and TBK1. *eLife* 2, e01119 (2013).

18. Z. Y. Jiang *et al.*, Insulin signaling through Akt/protein kinase B analyzed by small interfering RNA-mediated gene silencing. *Proceedings of the National Academy of Sciences of the United States of America* 100, 7569 (Jun 24, 2003).
19. H. Hacker, M. Karin, Regulation and function of IKK and IKK-related kinases. *Science's STKE : signal transduction knowledge environment* 2006, re13 (Oct 17, 2006).
20. F. Fujita *et al.*, Identification of NAP1, a regulatory subunit of IkappaB kinase-related kinases that potentiates NF-kappaB signaling. *Molecular and cellular biology* 23, 7780 (Nov, 2003).
21. G. Ryzhakov, F. Randow, SINTBAD, a novel component of innate antiviral immunity, shares a TBK1-binding domain with NAP1 and TANK. *The EMBO journal* 26, 3180 (Jul 11, 2007).
22. H. Ishikawa, Z. Ma, G. N. Barber, STING regulates intracellular DNA-mediated, type I interferon-dependent innate immunity. *Nature* 461, 788 (Oct 8, 2009).
23. S. S. Kim *et al.*, DOK3 is required for IFN-beta production by enabling TRAF3/TBK1 complex formation and IRF3 activation. *Journal of immunology* 193, 840 (Jul 15, 2014).
24. J. L. Pomerantz, D. Baltimore, NF-kappaB activation by a signaling complex containing TRAF2, TANK and TBK1, a novel IKK-related kinase. *The EMBO journal* 18, 6694 (Dec 1, 1999).
25. P. Bamborough *et al.*, 5-(1H-Benzimidazol-1-yl)-3-alkoxy-2-thiophenecarbonitriles as potent, selective, inhibitors of IKK-epsilon kinase. *Bioorganic & medicinal chemistry letters* 16, 6236 (Dec 15, 2006).
26. S. M. Reilly *et al.*, An inhibitor of the protein kinases TBK1 and IKK-varepsilon improves obesity-related metabolic dysfunctions in mice. *Nature medicine* 19, 313 (Mar, 2013).
27. R. T. Watson, J. E. Pessin, Bridging the GAP between insulin signaling and GLUT4 translocation. *Trends in biochemical sciences* 31, 215 (Apr, 2006).
28. I. J. Lodhi *et al.*, Gapex-5, a Rab31 guanine nucleotide exchange factor that regulates Glut4 trafficking in adipocytes. *Cell Metab* 5, 59 (Jan, 2007).
29. C. W. Lindsley *et al.*, Allosteric Akt (PKB) inhibitors: discovery and SAR of isozyme selective inhibitors. *Bioorganic & medicinal chemistry letters* 15, 761 (Feb 1, 2005).
30. J. Liu, S. M. DeYoung, M. Zhang, A. Cheng, A. R. Saltiel, Changes in integrin expression during adipocyte differentiation. *Cell metabolism* 2, 165 (Sep, 2005).
31. S. Karunanithi *et al.*, A Rab10:RalA G protein cascade regulates insulin-stimulated glucose uptake in adipocytes. *Molecular biology of the cell* 25, 3059 (Oct 1, 2014).

CHAPTER 3

Exo84, a *bona fide* direct substrate of TBK1

Introduction

Our previous studies showed that the exocyst plays a pivotal role in insulin-stimulated GLUT4 translocation in 3T3-L1 adipocytes by facilitating the docking of GLUT4 vesicles to the plasma membrane (*1, 2*). Earlier findings showed that TBK1 can be associated with the Sec5 subunit of the exocyst, in a manner crucial for cancer cell survival (*3*). In Chapter 2, our studies demonstrate that TBK1 is required for insulin-stimulated glucose transport and GLUT4 translocation in adipocytes in a cell-autonomous manner. To explore the mechanism by which TBK1 regulates insulin-stimulated glucose uptake, we sought to identify potential downstream targets of TBK1. A *Scansite* database search (http://scansite.mit.edu/) to predict potential substrates of TBK1 revealed that the exocyst subunit Exo84 contains TBK1 consensus phosphorylation sites (*4, 5*). Mammalian Exo84 has a Ral binding domain (RBD) that interacts with the small G proteins RalA and RalB, and a putative helical domain potentially important for its interaction with other exocyst subunits (*6-10*). Since knockdown of either Sec5 or Exo84 attenuated insulin-stimulated glucose transport (*11*), we examined whether TBK1 directly phosphorylates Exo84.

Results and Discussion

TBK1 directly phosphorylates Exo84 both *in vitro* and *in vivo*.

Rat Exo84 cDNA (**Figure 3.1A**) was cloned into mammalian and bacterial expression vectors. We purified a glutathione *S*-transferase (GST)-tagged full-length wild type or RBD of Exo84 (**Figure 3.1B**). Recombinant TBK1 was incubated *in vitro* with [γ-^{32}P]ATP and the purified GST-tagged WT Exo84 or myelin basic protein (MBP) as a substrate (**Figure 3.1C**). Phosphorylation was assessed by SDS PAGE, followed by autoradiography. TBK1 directly catalyzed the phosphorylation of recombinant Exo84, as well as MBP. TBK1 autophosphorylation was also detected. To eliminate the possibility that TBK1 phosphorylates GST rather than Exo84, purified GST, GST-tagged Exo84 WT, and Exo84 RBD were incubated *in vitro* with [γ-^{32}P]ATP and recombinant TBK1 (**Figure 3.1D**). TBK1 directly catalyzed the phosphorylation of both WT Exo84 and Exo84 RBD, but not GST itself.

We also made GST-free Exo84 RBD by cleaving GST from GST-tagged Exo84 RBD to use as a substrate in the kinase assay (**Figure 3.2A**). We performed an *in vitro* kinase assay using baculoviral-expressed TBK1 fused to maltose binding protein (MBP-TBK1) and either GST-tagged Exo84 WT or GST-free Exo84 RBD, detecting phosphorylation by incorporation of [γ-^{32}P]ATP (**Figure 3.2B**). Phosphorylation was dose-dependent, suggesting that recombinant TBK1 was capable of stoichiometric phosphorylation of Exo84 *in vitro*.

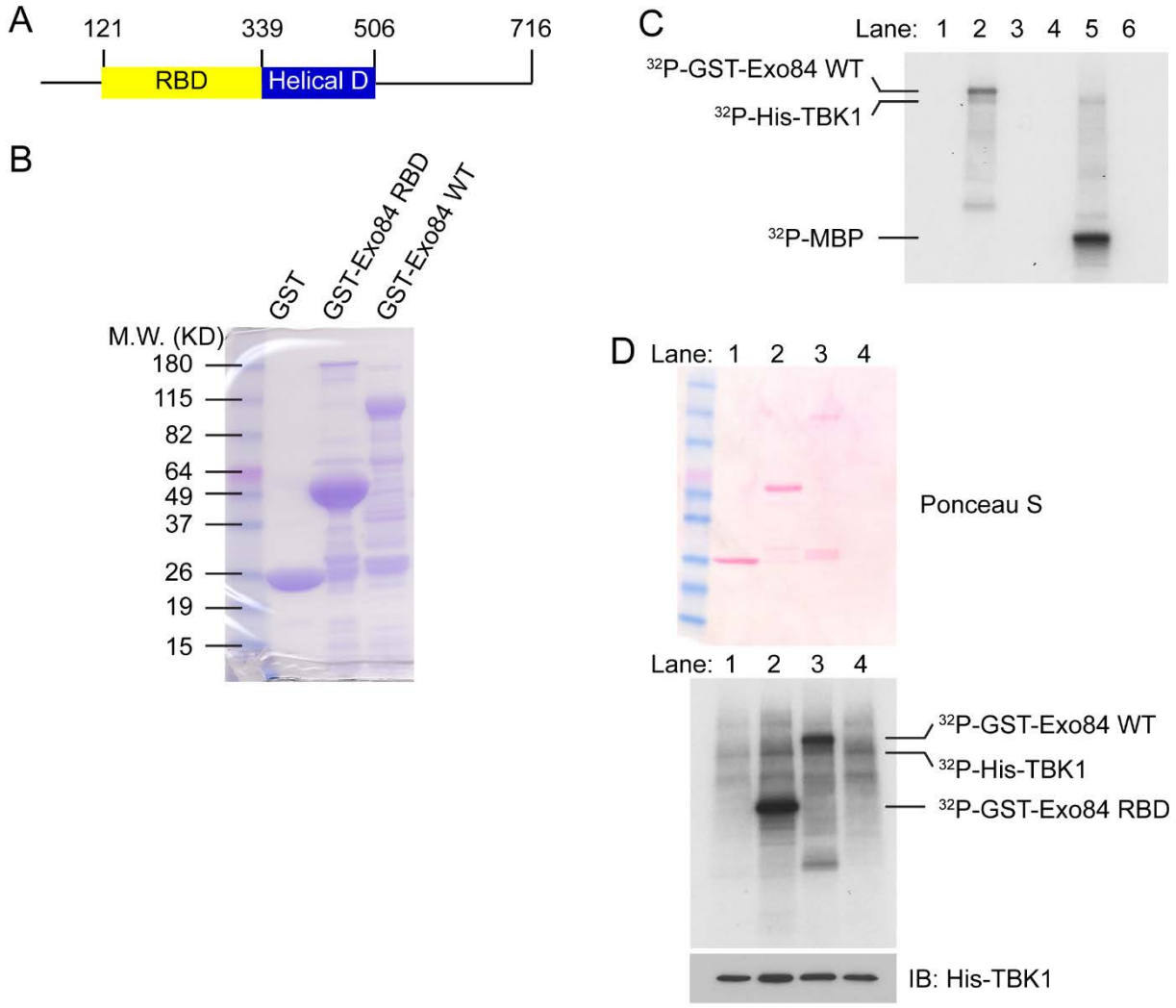

Figure 3.1 TBK1 phosphorylates Exo84 *in vitro*.
(A) Schematic representation of *Rattus norvegicus (Rat)* Exo84. (B) Purification of GST fusion proteins. GST, GST-tagged full-length Exo84 (WT) or Exo84 Ral binding domain (RBD) was purified from bacteria and used as a substrate for an *in vitro* kinase assay. (C) TBK1 phosphorylates Exo84 *in vitro*. Recombinant His-tagged TBK1 WT was incubated with MBP or GST-Exo84 WT for an *in vitro* kinase assay. Lane 1: GST-Exo84 WT, Lane 2: His-TBK1 + GST-Exo84 with [γ-^{32}P]-ATP, Lane 3: His-TBK1 + GST-Exo84 without [γ-^{32}P]-ATP, Lane 4: MBP, Lane 5: His-TBK1 + MBP with [γ-^{32}P]-ATP, and Lane 6: His-TBK1 + MBP without [γ-^{32}P]-ATP. (D) TBK1 phosphorylates Exo84 *in vitro*. GST-tagged full-length Exo84 (WT) or Exo84 Ral binding domain (RBD) was purified from bacteria and used as a substrate. Recombinant His-tagged TBK1 WT was used for an *in vitro* kinase assay. Ponceau S (top panel) staining shows the amount of substrates used. Lane 1: GST, Lane 2: GST-Exo84 RBD, Lane 3: GST-Exo84 WT, and Lane 4: none. Amount of His-TBK1 WT used for an *in vitro* kinase assay was assessed by immunoblots. Phosphorylation of proteins was observed in the autoradiograph (bottom panel).

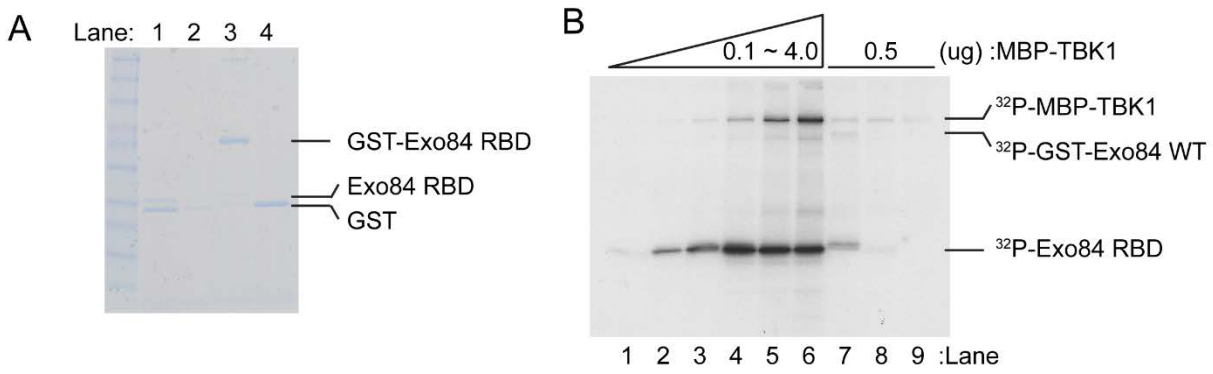

Figure 3.2 TBK1 phosphorylates Exo84 *in vitro* in a dose-dependent manner.
(A) Generation of GST-free Exo84 RBD. GST-Exo84 RBD was cleaved with thrombin. Lane 1: 1 ug of GST-Exo84 RBD with thrombin, Lane 2: 500 ng of GST-Exo84 RBD with thrombin, Lane 3: 1 ug of GST-Exo84 RBD, and Lane 4: GST. (B) TBK1 phosphorylates Exo84 *in vitro* in a dose-dependent manner. GST-tagged full-length Exo84 (WT) or GST-free Exo84 RBD (GST-Exo84 RBD cleaved with thrombin) was used as a substrate. TBK1 fused to maltose binding protein (MBP-TBK1) was purified from insect SF9 cells by baculovirus expression system. Increasing amount of MBP-TBK1 was used in Lane 1 ~ Lane 6 and 0.5 ug of MBP-TBK1 was used in Lane 7 ~ Lane 9. Lane 1 ~ 6: 1 ug of GST-free Exo84 RBD, Lane 7: GST-Exo84 WT, Lane 8: GST, and Lane 9: none. Phosphorylation of proteins was observed in the autoradiograph.

To determine the specificity of Exo84 phosphorylation, purified Exo84 or MBP were incubated with [γ-^{32}P]ATP and various kinases *in vitro* (**Figure 3.3**). Phosphorylation of Exo84 was detected only with TBK1 but not the other kinases.

To determine whether TBK1 can phosphorylate Exo84 in cells, we co-overexpressed increasing amounts of Flag-tagged WT TBK1 or its inactive K38A mutant with MYC-tagged Exo84 in COS-1 cells, followed by SDS PAGE (**Figure 3.4A**). Expression of WT TBK1 but not its inactive mutant reduced the electrophoretic mobility of Exo84, indicative of Exo84 phosphorylation. This phosphorylation was specific for TBK1, as co-transfection of Exo84 with the related protein kinase IKKε caused little shift (**Figure 3.4B**, bottom panel). To determine whether this molecular shift was dependent on phosphorylation of Exo84, MYC-Exo84 was co-expressed in COS-1 cells along with TBK1 and IKKε or their kinase inactive mutants, followed by immunoprecipitation (IP) with anti-MYC antibodies. Anti-MYC immunoprecipitates were then treated with or without calf intestinal phosphatase (CIP) (**Figure 3.4B**, top panel). Expression of TBK1 reduced the electrophoretic mobility of Exo84, which could be reversed by treatment with the phosphatase (**Figure 3.4B**, compare lane 3 to lane 7 in top panel). The kinase-inactive mutant of TBK1 was without effect (**Figure 3.4B**, compare lane 4 to lane 8 in top panel). Additionally, phosphorylation of Exo84 was detected by blotting with antibodies that recognize a 14-3-3 binding motif, as previously reported (*12*). Expression of WT TBK1 increased the phosphorylation of Exo84 as determined by immunoblotting with this antibody, and was reduced by treatment with the phosphatase (**Figure 3.4B**, compare lane 3 to lane 7 in top panel). Expression of WT IKKε was less effective (**Figure 3.4B**, compare lane 3 to lane 5 in top panel).

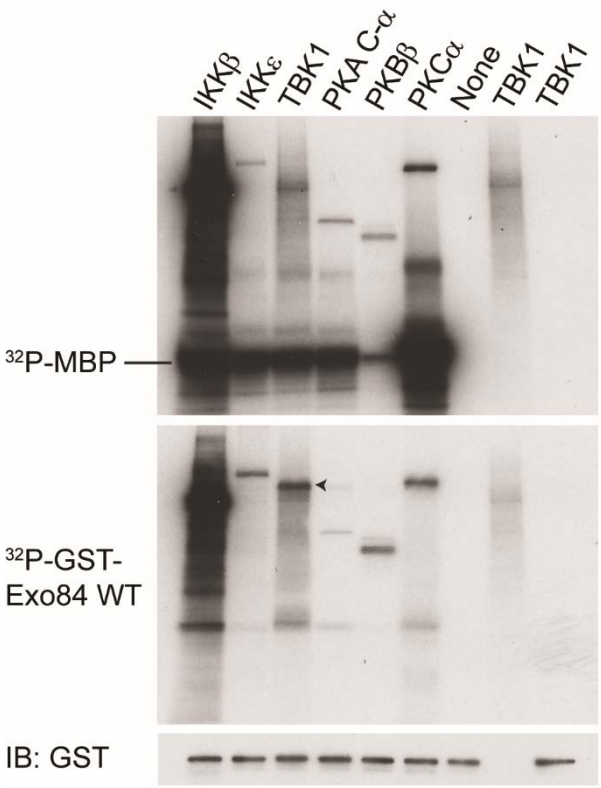

Figure 3.3 TBK1 but not other kinases phosphorylates Exo84 *in vitro*.
Arrow head indicates phosphorylated GST-Exo84 WT. Various kinases were used for an *in vitro* kinase assay. Levels of myelin basic protein (MBP) phosphorylation show the activity of various kinases (Top panel). Amount of GST-Exo84 WT used for an *in vitro* kinase assay was assessed by immunoblots.

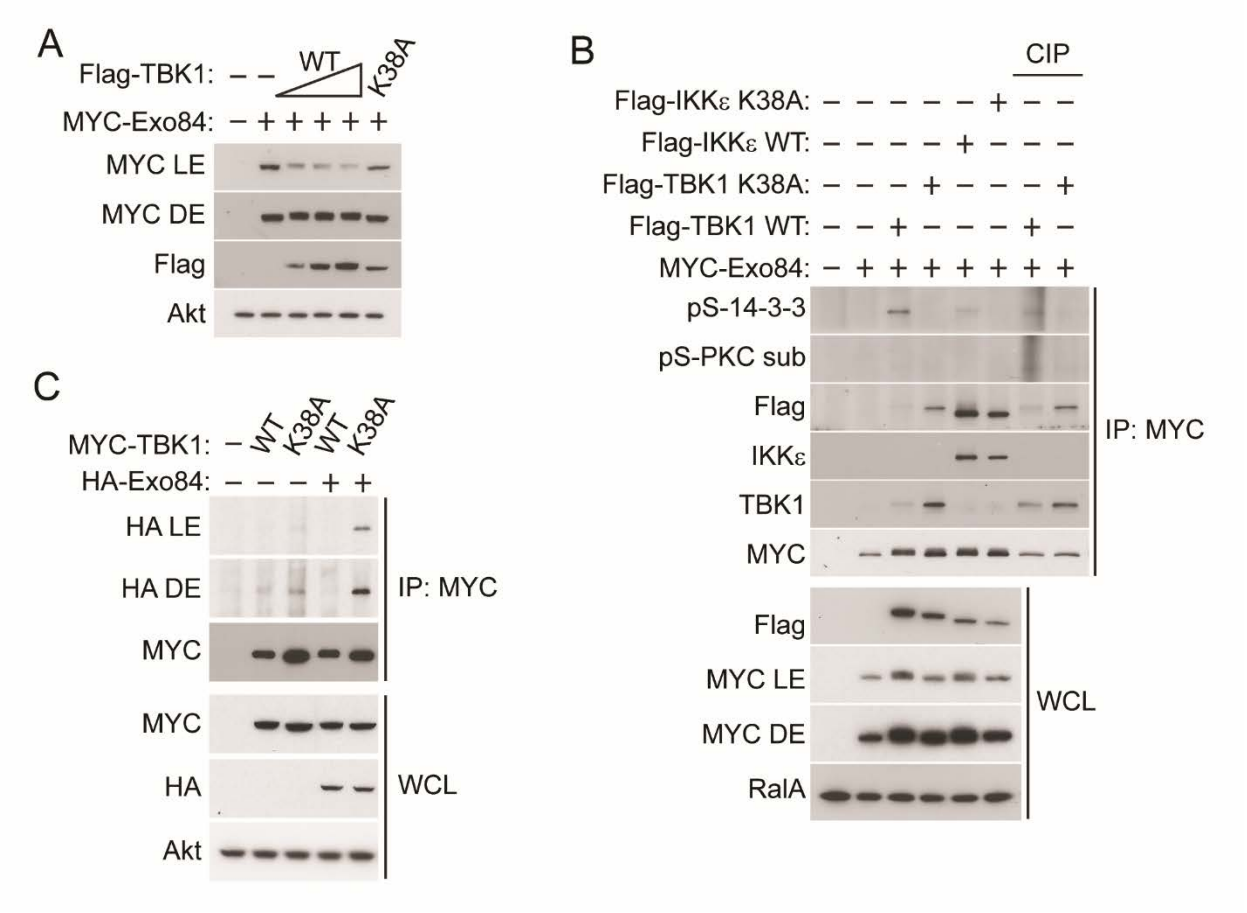

Figure 3.4 TBK1 phosphorylates Exo84 *in vivo*.
(A) TBK1 phosphorylates Exo84 in COS-1 cells. Levels of indicated proteins in the whole cell lysates are shown. DE and LE stand for dark exposure and light exposure, respectively. (B) Exo84 is a substrate of TBK1. MYC-tagged Exo84 was immunoprecipitated from COS-1 cells co-expressing TBK1 and IKKε or their kinase-inactive mutants. Anti-MYC immunoprecipitates were then treated with or without calf intestinal phosphatase (CIP). Levels of indicated proteins in the whole cell lysates (WCL) and the immunoprecipitates are shown. DE and LE stand for dark exposure and light exposure, respectively. (C) Exo84 directly interacts with TBK1. HA-tagged Exo84 was immunoprecipitated from COS-1 cells co-expressing TBK1 or its kinase-inactive mutant. Levels of indicated proteins in WCL and the immunoprecipitates are shown. DE and LE stand for dark exposure and light exposure, respectively.

To explore whether TBK1 directly phosphorylates Exo84, anti-MYC immunoprecipitates were blotted with antibodies that recognize Flag, TBK1, or IKKε (**Figure 3.4B**, top panel). Kinase-inactive TBK1 preferentially co-immunoprecipitated with Exo84, whereas the interaction of Exo84 with WT TBK1 was barely detected. Interestingly, the interaction of Exo84 with WT TBK1 was rescued by treatment with CIP. These data are consistent with our previous findings (*12*), demonstrating that TBK1 associates with its substrates, and subsequently dissociates upon phosphorylation. However, the interaction of Exo84 with IKKε was constitutive and not dependent upon kinase activity, further confirming that Exo84 is not a target of IKKε. It has been suggested that TBK1 can form a heterodimer with IKKε (*13, 14*). Therefore, it is possible that IKKε does not function as a kinase but rather as a scaffolding protein to recruit Exo84 to TBK1 in this case. We also performed a reciprocal IP with anti-MYC antibodies in COS-1 cells co-expressing MYC-tagged WT TBK1 and its K38A mutant with HA-tagged Exo84 (**Figure 3.4C**). We detected the interaction of Exo84 with the kinase-inactive mutant of TBK1 K38A but not the wild type enzyme.

To test further whether the interaction between Exo84 and TBK1 is specific, we prepared several GST-tagged fusion proteins, including the Ral binding protein 1 (RalBP1) RBD, Exo84 RBD, and WT Exo84, and incubated these with lysates from COS-1 cells expressing Flag-tagged WT TBK1 or its kinase-inactive mutant (**Figure 3.5**). The inactive mutant K38A but not WT TBK1 was preferentially pulled down by GST-Exo84 WT but not by other fusion proteins, suggesting that the catalytically inactive kinase TBK1 specifically interacts with its substrate Exo84.

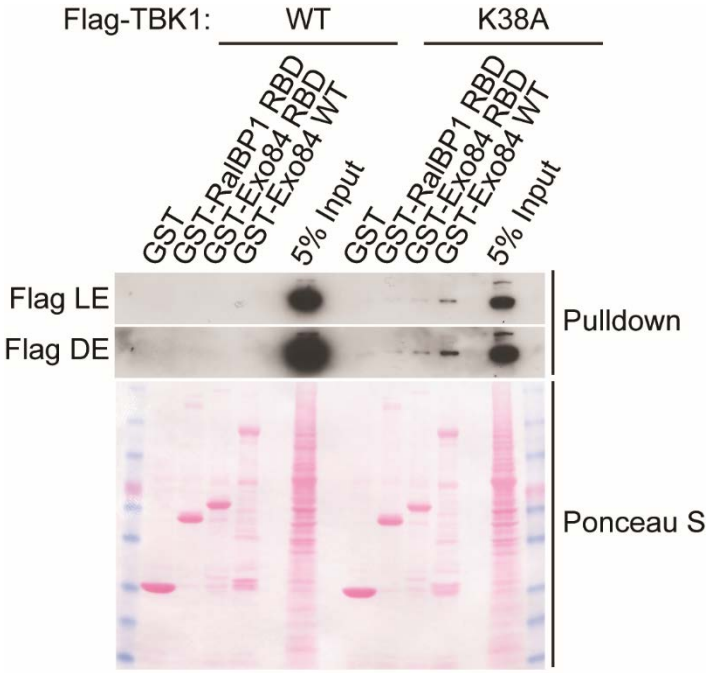

Figure 3.5 The interaction between Exo84 and TBK1 is specific.
COS-1 cell lysates overexpressing Flag-TBK1 WT and its kinase-inactive mutant were incubated with GST fusion proteins as indicated. Pull downs were subjected to immunoblot analysis with anti-Flag antibody. Amount of GST fusion proteins used in the pull down assay was visualized with Ponceau S. DE and LE stand for dark exposure and light exposure, respectively.

TBK1 is also known to phosphorylate the exocyst subunit Sec5 (*3*). HA-tagged Sec5 WT or its phospho-defective mutant S89A (*15*) were co-expressed in COS-1 cells along with Flag-tagged WT TBK1 and its K38A mutant, and HA immunoprecipitates were treated with or without CIP (**Figure 3.6**). Both Sec5 and its S89A mutant were phosphorylated by WT TBK1, as detected by blotting with antibodies that recognize the phospho-S89 PKC substrate motif, as well as the 14-3-3 binding motif; phosphorylation was reduced with CIP treatment. While the kinase-inactive mutant of TBK1 phosphorylated neither Sec5 construct, both were preferentially co-immunoprecipitated with the kinase-inactive TBK1, whereas the interaction of Sec5 with WT TBK1 was not detected, even with CIP treatment. These data suggest that both Sec5 and Exo84 are *bona fide* substrates of TBK1 both *in vitro* and *in vivo,* and furthermore that TBK1 directly interacts with Exo84 when the kinase is inactive, and subsequently dissociates upon phosphorylation.

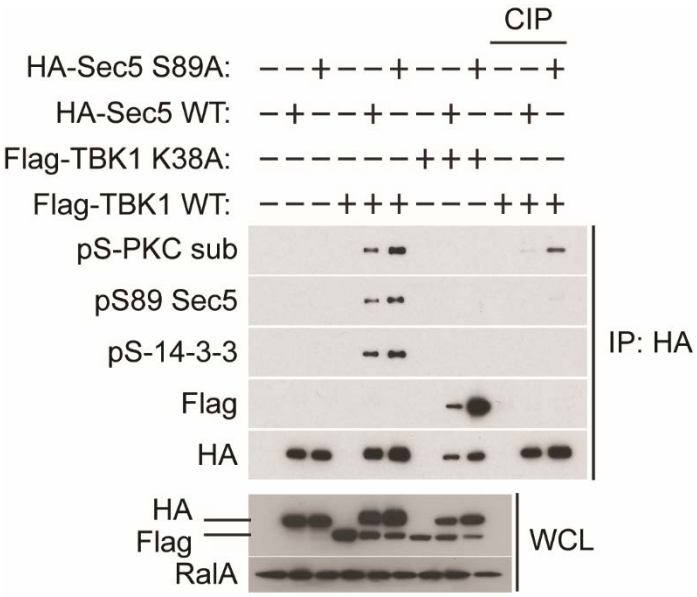

Figure 3.6 Sec5 is a substrate of TBK1.
HA-tagged Sec5 was immunoprecipitated from COS-1 cells coexpressing TBK1 or its kinase-inactive mutant. Anti-HA immunoprecipitates were then treated with or without calf intestinal phosphatase (CIP). Levels of indicated proteins in WCL and the immunoprecipitates are shown.

TBK1 directly interacts with Exo84 via the coiled-coil domain of TBK1 and helical domain of Exo84.

In order to understand how TBK1 might control the function of the exocyst, we generated various mammalian Exo84 truncation mutants to identify the domain required for its interaction with TBK1 (**Figure 3.7A**). We co-expressed in COS-1 cells WT TBK1 and its K38A mutant with HA-tagged full-length Exo84, its RBD or the various deletion mutants, and immunoprecipitated the protein with anti-HA antibodies (**Figure 3.7B**). Kinase-inactive TBK1 preferentially co-immunoprecipitated with Exo84 WT and its Del 1 mutant, whereas the interaction with Exo84 RBD was significantly reduced, suggesting that the domain of Exo84 required for the interaction with TBK1 is located in the C-terminal region. Phosphorylation of Exo84 and its truncation mutants were also detected after expression with TBK1 by blotting with antibodies that recognize the 14-3-3 binding motif. Phosphorylation of both Exo84 truncation mutants by TBK1 was significantly reduced, suggesting that there are multiple sites on Exo84 phosphorylated by TBK1. To further map out the domain of Exo84 required for the interaction with TBK1, we co-expressed WT TBK1 and its K38A mutant with HA-tagged Exo84 WT, deletion 1, 2, 3, or 4 mutants in COS-1 cells, and immunoprecipitated with anti-HA antibodies (**Figure 3.7C**). Kinase-inactive TBK1 preferentially co-immunoprecipitated with Exo84 WT and the Del 1 mutant, whereas the interaction of Exo84 Del 2, Del 3, and Del 4 with TBK1 K38A was significantly reduced, suggesting that the helical domain of Exo84 is required for the interaction with TBK1.

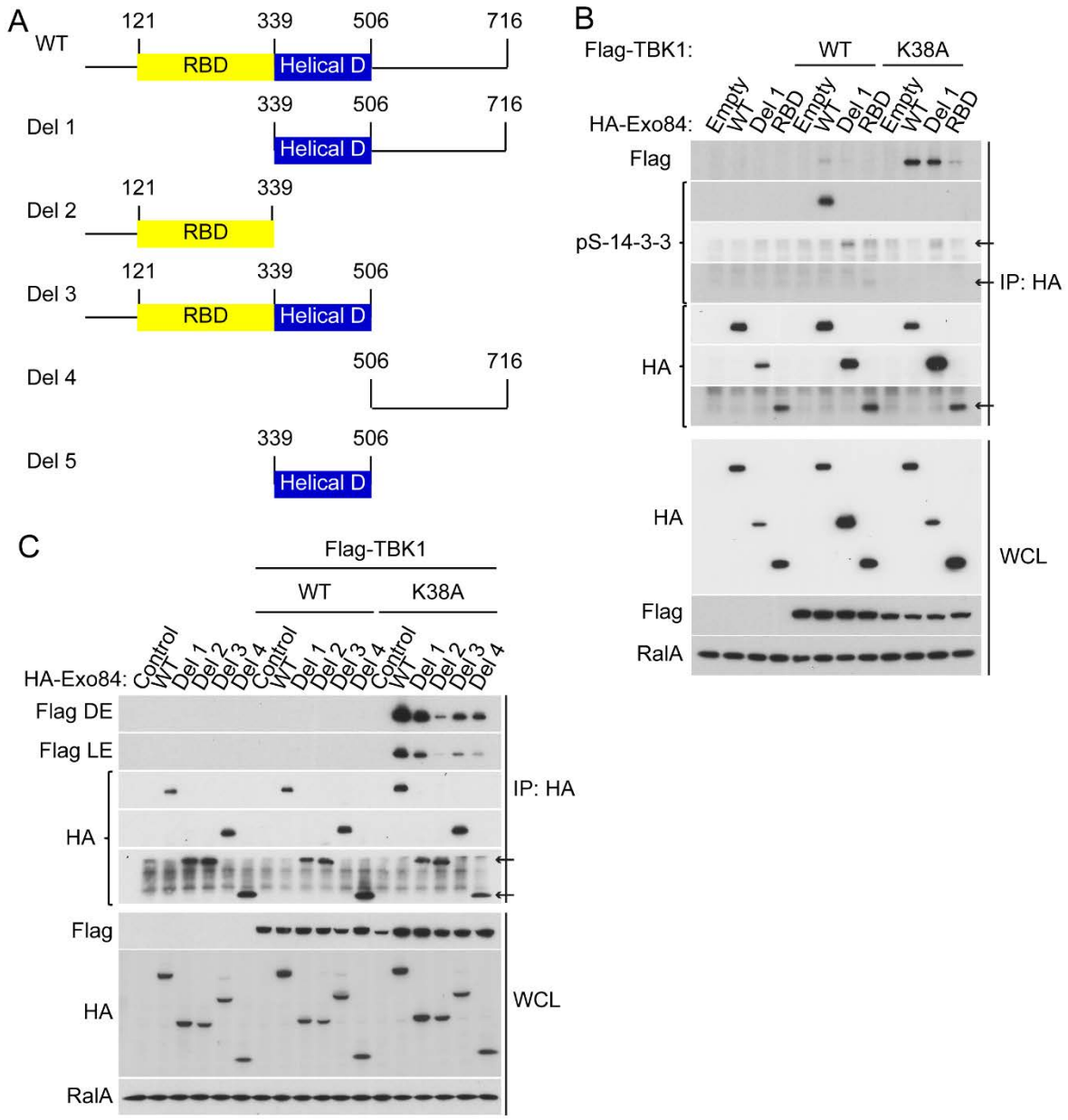

Figure 3.7 The helical domain of Exo84 interacts with TBK1.
(A) Schematic representation of various domains in full-length and truncated Exo84. (B) The C-terminal domain of Exo84 interacts with TBK1. HA-tagged various truncation mutants of Exo84 were immunoprecipitated from COS-1 cells co-expressing TBK1 or its kinase-inactive mutant. Levels of indicated proteins in WCL and the immunoprecipitates are shown. Arrows refer to each immunoprecipitated protein as indicated. (C) The helical domain of Exo84 is required for its interaction with TBK1. HA-tagged various truncation mutants of Exo84 were immunoprecipitated from COS-1 cells co-expressing TBK1 or its kinase-inactive mutant. Levels of indicated proteins in WCL and the immunoprecipitates are shown. Arrows indicate Del 1, Del 2, and Del 4, respectively. DE and LE stand for dark exposure and light exposure, respectively.

Several scaffolding proteins have been identified that interact with TBK1, including TANK, NAP1, and SINTBAD, and these appear to play important roles in the activation of the kinase in response to different stimuli (*16*-*18*). It is possible that the phosphorylation of Exo84 by TBK1 might require scaffolding proteins, exocyst subunits or other associated proteins. To test whether the interaction of TBK1 with Exo84 is direct or indirect, we performed an *in vitro* protein interaction assay. cDNAs encoding Flag-tagged WT TBK1 or its K38A mutant, along with HA-tagged WT Exo84, and the deletion 1, 2, 3, 4, and 5 mutants (Del 1, 2, 3, 4, and 5 as shown in **Figure 3.7A**) were translated *in vitro*, and the translation products were then immunoprecipitated with anti-HA antibodies (**Figure 3.8**). *In vitro* translated proteins were detected by SDS PAGE, followed by western blotting with an anti-Flag and anti-HA antibodies (**Figure 3.8**, bottom panel). *In vitro* translated, kinase-inactive TBK1 preferentially co-immunoprecipitated with *in vitro* translated WT Exo84, as shown in cells (**Figure 3.4B**, **Figure 3.7B**, and **C**). *In vitro* translated Exo84 lacking its helical domain (Del 2 and Del 4) showed a significantly reduced interaction with TBK1, whereas *in vitro* translated Exo84 helical domain (Del 5) was sufficient to interact with the kinase-inactive mutant. Thus, the helical domain of Exo84 is required and sufficient for its interaction with TBK1 *in vitro*.

TBK1 has three structurally distinct domains: the kinase domain, the ubiquitin-like domain (ULD), and the scaffold and dimerization domain (coiled-coil domain) (*19*-*21*). Previous studies suggested that TBK1 recognizes its substrates through the ULD domain proximal to its kinase domain (*22*). To confirm that TBK1 directly interacts with Exo84, various truncation mutants of TBK1 were obtained as described previously (*22*) (**Figure 3.9A**).

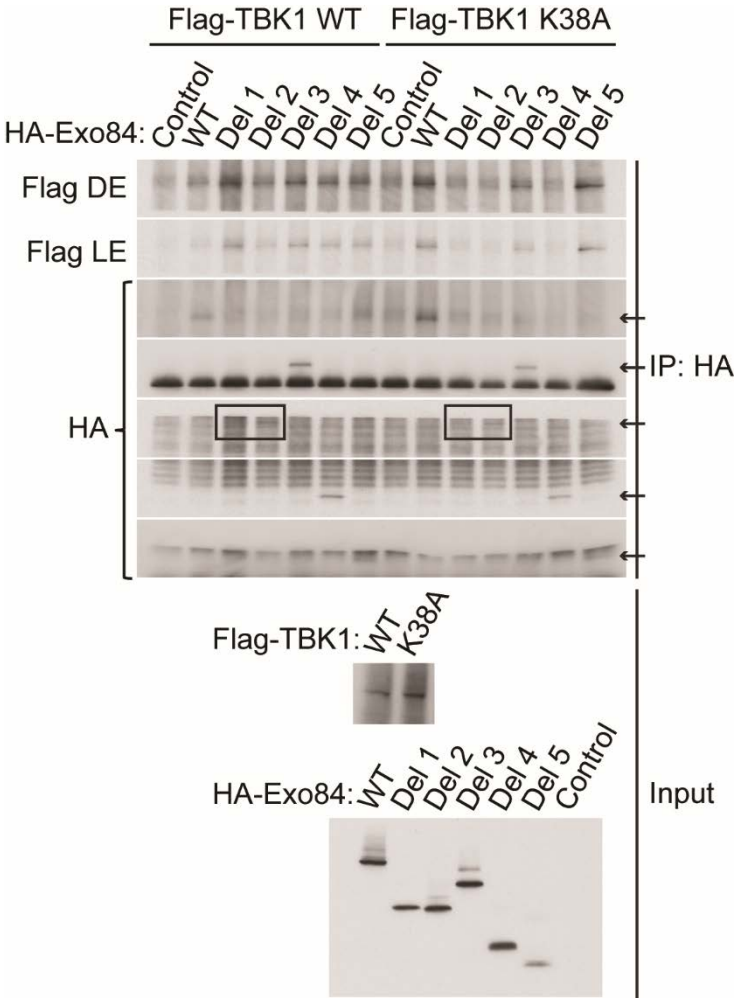

Figure 3.8 TBK1 directly interacts with Exo84 via the helical domain of Exo84 *in vitro*. HA-tagged various truncation mutants of Exo84, Flag-tagged TBK1, and its kinase-inactive mutant were *in vitro* translated. As a control, HA-empty vector was used. Amount of *in vitro* translated proteins used for the immunoprecipitation are shown as input. Anti-HA immunoprecipitates were subjected to immunoblot analysis and probed using specific antibodies as indicated. Arrows indicate WT Exo84 and the Exo84 variants. Signals from immunoprecipitated Exo84 Del 1 and Del 2 were masked by the heavy chain of the IgG as shown in the squares. DE and LE stand for dark exposure and light exposure, respectively.

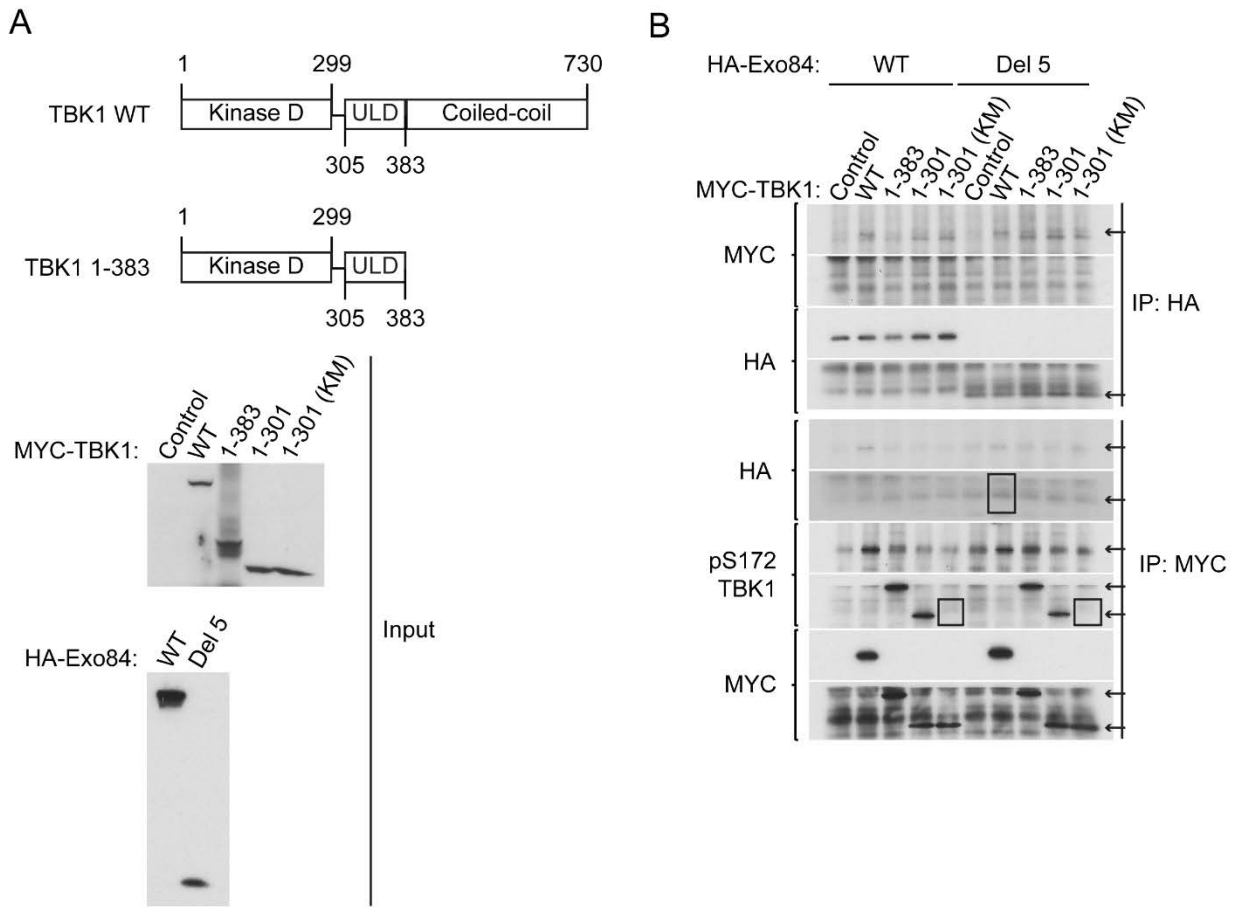

Figure 3.9 TBK1 directly interacts with Exo84 via the coiled-coil domain of TBK1 *in vitro*. (A) Schematic representation of various domains in full-length and truncated TBK1. Amount of *in vitro* translated proteins used for Figure 3.9B are shown as input. (B) TBK1 directly interacts with Exo84 via the coiled-coil domain of TBK1 *in vitro*. MYC-tagged various truncation mutants of TBK1, HA-tagged WT Exo84, and its Del 5 mutant were *in vitro* translated. As a control, MYC-empty vector was used. Anti-HA immunoprecipitates (top panel) or anti-MYC immunoprecipitates (bottom panel) were subjected to immunoblot analysis and probed using specific antibodies as indicated. Arrows (top panel) indicate WT TBK1 and Exo84 Del 5 mutant, respectively. Arrows (bottom panel) indicate each immunoprecipitated protein. Exo84 Del 5 was sufficient to interact with WT TBK1 as shown in the square. TBK1 1-301 (KM) was inactive as shown in the squares.

The plasmids containing cDNAs of MYC-tagged WT TBK1, 1-383, which contains the kinase domain and the ULD, its kinase domain (1-301), and the inactive kinase domain of TBK1 (1-301 (KM)) were translated *in vitro* along with HA-tagged Exo84 WT and the Del 5 mutant. These *in vitro* translated proteins were then immunoprecipitated with anti-HA antibodies. Only the full-length TBK1 (TBK1 WT) co-immunoprecipitated with *in vitro* translated Exo84 or the Del 5 mutant (**Figure 3.9B**, top panel). Similarly, WT Exo84 and the Del 5 mutant were co-immunoprecipitated only with the full-length TBK1 in reciprocal immunoprecipitation of *in vitro* translated proteins with anti-MYC antibodies (**Figure 3.9B**, bottom panel). Active TBK1, 1-383, and 1-301 but not the inactive kinase domain of TBK1 (1-301 (KM)) were detected in the anti-MYC immunoprecipitation by blotting with antibodies that recognize phosphorylation of TBK1 at S172. These data suggest that although TBK1 exists in different complexes depending on cellular response, the kinase directly interacts with Exo84 via binding between the helical domain of Exo84 and the coiled-coil domain of TBK1. TBK1 and its related kinase IKKε both have a kinase domain in the N terminus, and share 64% similarity in amino acid sequences (*23*). It is possible that the differential substrate specificity of these two related kinases might be determined through their C-terminal scaffold and dimerization domain.

Materials and Methods

Materials and reagents

Enhanced chemiluminescence (ECL) reagents were purchased from Thermo Scientific. EDTA-free protease inhibitor tablet was purchased from Roche Diagnostics. BenchMark™ Pre-stained protein ladder was purchased from Life Technologies. CIP was purchased from New England Biolabs Inc. Imperial™ protein stain was purchased from Pierce and SimplyBlue™ SafeStain was purchased from Life Technologies for gel staining. GST-tagged RalBP1 agarose beads were purchased from EMD Millipore. Purified recombinant His-TBK1 was purchased from Life Technologies. Purified recombinant GST-IKKβ, GST-PKA C-α, and GST-PKCα were purchased from Cell Signaling Technology. Purified recombinant His-PKBβ was purchased from Millipore. IKKε and TBK1 fused to MBP (maltose binding protein) were purified from insect SF9 cells by baculovirus expression system by Dr. Stuart J Decker (Life Sciences Institute, University of Michigan).

Antibodies

Anti-Flag antibody was obtained from Sigma, and anti-HA, anti-MYC, and anti-GST antibodies were obtained from Santa Cruz Biotechnology. Anti-IKKε, anti-TBK1, anti-phospho-TBK1 (Ser172), anti-phospho-PKC substrate, and anti-phospho-(Ser) 14-3-3 binding motif (R-X-Y/F-X-pS) antibodies were purchased from Cell Signaling Technology. Anti-RalA antibody was purchased from BD Bioscience. Anti-His was purchased from Life Technologies.

Plasmids

The Flag-tagged human TBK1 WT, TBK1 K38A, IKKε WT, and IKKε K38A cDNAs were kindly provided by Dr. Tom Maniatis (Columbia University). The rat Exo84 cDNA was kindly provided by Dr. Charles Yeaman (University of Iowa) and subcloned into pKH3 and pGEX-4T-1 vectors (GE Healthcare Life Sciences). The Myc-tagged human TBK1 WT, TBK1 1-383, TBK1 1-301 (WT), and TBK1 1-301 (KM) cDNAs were kindly provided by Dr. Ivan Dikic (Goethe University, Germany). Site-directed mutagenesis (QuickChange; Agilent Technologies) was used to generate the phosphomimetic and phosphorylation deficient mutants of Exo84 as well as the truncation mutants (Exo84 Del 2 and Del 3). Del 1, Del 4, and Del 5 mutants of Exo84 was cloned from rat Exo84 WT cDNA by PCR and subcloned into pKH3 vector. HA-tagged Sec5 WT and S89A cDNAs were obtained as previously described (*15*).

Cell culture and transfection

COS-1 cells were cultured in DMEM containing 10% fetal bovine serum (FBS). These cells were cultured to 90% confluence and transfection was carried out using Opti-MEM media and Lipofectamine 2000 (Life Technologies) according to manufacturer's protocol. For overexpression experiments, cells were collected and lysed 18-36 hours after transfection.

Immunoprecipitation and immunoblotting

For immunoprecipitation, cells were washed once with ice-cold PBS before lysis with IP buffer (100 mM Tris-HCL (pH 7.5), 130 mM NaCl, 1% Triton X-100, 1 mM EDTA, 1 mM Na_3VO_4, 10 mM NaF, 5 mM $MgCl_2$) supplemented with an EDTA-free protease inhibitor tablet (Roche). Lysates were cleared by centrifugation at 13,000 xg for 15 minutes and then incubated with 2 ug of antibody for 1 mg of protein for 4 hours to overnight at 4 °C. Immunoprecipitaes were adsorbed on Protein A/G plus agarose (Santa Cruz Biotechnology) for 1.5-2 hours, washed three times in lysis buffer, and eluted in 1.5X sodium dodecyl sulfate (SDS) sample buffer (240 mM Tris-HCL (pH6.8), 40% glycerol, 8% SDS, 0.04% bromophenol blue, and 5% beta-mercaptoethanol) by boiling the samples for 5 minutes at 95 °C. For regular cell lysis, cell were washed once with ice-cold PBS before lysis with SDS buffer (100 mM Tris-HCL (pH 8.0), 130 mM NaCl, 1% Nonidet P-40 (NP-40), 0.2% Sodium deoxycholate, 0.1% SDS, 10 mM Sodium Pyrophosphate, 1 mM Na_3VO_4, 10 mM NaF) supplemented with an EDTA-free protease inhibitor tablet (Roche), followed by sonication. The crude lysates were centrifuged at13,000 xg for 15 minutes and determined the protein concentration using Protein Assay Reagent (Bio-Rad). Samples were diluted in 4X SDS sample buffer and boiled for 5 minutes at 95 °C. Proteins were resolved by SDS-polyacrylamide gel electrophoresis (PAGE; Life Technologies) and transferred to nitrocellulose membranes (Bio-Rad). Individual proteins were detected with the specific antibodies and visualized on X-ray film using horseradish peroxidase-conjugated secondary antibodies (Bio-Rad) and Western Lightning Enhanced Chemiluminescence (Perkin Elmer Life Sciences). Where necessary, blots were incubated in the stripping buffer (50 mM Tris-HCL (pH 6.8), 150 mM NaCl, 110 mM beta-mercaptoethanol, and 2% SDS) and re-probed with the specific antibodies.

Calf-intestinal phosphatase dephosphorylation

Calf intestinal phosphatase (CIP) was obtained from New England Biolabs. Immunoprecipitates were incubated for 1 hour at 37 °C in a 100 μl reaction containing 50 mM Tris pH 7.5, 150 mM NaCl, 1% NP-40, EDTA-free protease inhibitor tablet, and 5 μl CIP.

In vitro kinase assay

In vitro kinase assays were performed by incubating purified kinase (IKKε, TBK1, IKKβ, PKA C-α, PKCα or PKBβ) in kinase buffer containing 25 mM Tris (pH 7.5), 10 mM MgCl2, 1 mM dithiothreitol (DTT), and 50 μM ATP for 30 minutes at 30 °C in the presence of 0.5 μCi γ-[^{32}P]-ATP and 1 μg myelin basic protein (MBP) per sample as a substrate. For PKCα, a PKC lipid activator (EMD Millipore) was added. Purified GST, GST-Exo84 WT, GST-Exo84 RBD, or Exo84 RBD were also used as a substrate. The purification of these proteins is described below. The kinase reaction was stopped by adding 4X SDS sample buffer and boiling for 5 minutes at 95 °C. Supernatants were resolved by SDS-PAGE, transferred to nitrocellulose, and analyzed by autoradiography.

Protein purification and pull-down experiment

GST fusion proteins were expressed in Rosetta™ (DE3)pLysS competent cells (Novagen). GST proteins were induced 50-100 mM Isopropyl β-D-1-thiogalactopyranoside (IPTG) for 16 hours at 25 °C. Cells were pelleted by centrifugation at 4,000 xg for 10 minutes. Cells were lysed with

lysis buffer containing 50 mM Tris (pH 7.5), 0.5 mM EDTA, and 0.3 M NaCl supplemented with an EDTA-free protease inhibitor tablet (Roche). Lysates were mixed with 1:10 dilution of 10 mg/ml lysozyme and 4 mM DTT and then incubated on ice for 15 minutes. 0.2% NP-40 were added to lysates and lysis was further performed by freeze-thaw cycle. To get soluble proteins, lysates were mixed with a buffer containing 1.5 M NaCl, 12 mM $MgCl_2$, and 1:1000 dilution of 10 mg/ml DNase I (Roche) supplemented with an EDTA-free protease inhibitor tablet (Roche). Lysates were passed through syringe with 18 gauge needle (BD Bioscience) every 10-15 minutes for 2 hours at 4 °C. Soluble proteins were collected by centrifugation at 15,000 xg for 20 minutes at 4 °C. Supernatants were incubated with glutathione sepharose beads (GE Healthcare Life Sciences) and washed four times with PBS (pH 8.0). Protein immobilized on beads were stored at -80 °C in PBS containing 10% glycerol and 10 mM DTT. Sometimes, proteins were eluted from glutathione beads by washing the beads with 10 mM glutathione in PBS (pH 8.0). Purified GST-tagged Exo84 RBD proteins were cleaved with thrombin (GE Healthcare Life Sciences) according to manufacturer's protocol. For pull-down experiment, cells were washed once with ice-cold PBS and then lysed in pulldown buffer (100 mM Tris, pH 7.5, 130 mM NaCl, 1% NP-40, 10% glycerol, 1 mM Na_3VO_4, 10 mM NaF, 5 mM $MgCl_2$, 1 mM EDTA, 1 mM DTT) supplemented with a protease inhibitor tablet (Roche). Lysates were cleared by centrifuging at 13,000 xg for 15 minutes and then were incubated with GST fusion proteins bound to glutathione beads (GE Healthcare Life Sciences) for 40 minutes at 4 °C. Beads were washed three times with 1 mL of pull-down lysis buffer and then resuspended in 1.5X SDS sample buffer.

In vitro translation and co-immunoprecipitation

1ug of vector constructs as indicated were used in the T_NT® T7 or SP6 Quick Coupled transcription/Translation Systems (Promega) according to manufacturer's protocol. Before co-IP, all *in vitro* translated proteins were run on SDS-PAGE, transferred to nitrocellulose. *In vitro* translation of epitope-tagged proteins was confirmed by immunoblotting with the specific antibodies as indicated and quantified using Image J. The same amount of proteins were resuspended in a buffer containing 50 mM HEPES (pH 7.5), 150 mM NaCl, 10 mM EDTA, 5 mM DTT, 0.1% Triton X-100 supplemented with a protease inhibitor tablet and combined with each other for 1 hour at room temperature. The solutions were then centrifuged at 13,000 xg for 20 minutes at 4 °C. Following centrifugation, the supernatant was incubated with anti-MYC or anti-HA antibodies for each IP for 4 hours at 4 °C. The resulting immunocomplexes were collected on Protein A/G plus agarose (Santa Cruz Biotechnology) by incubation for 1 hour at 4 °C. The immunoprecipitates were washed three times with a buffer, and eluted in 1.5X SDS sample buffer by boiling the samples for 5 minutes at 95 °C. Samples were run on SDS-PAGE and transferred to nitrocellulose membrane. Proteins were analyzed by immunoblotting with appropriate antibodies as indicated.

References

1. M. Inoue, L. Chang, J. Hwang, S. H. Chiang, A. R. Saltiel, The exocyst complex is required for targeting of Glut4 to the plasma membrane by insulin. *Nature* 422, 629 (Apr 10, 2003).
2. M. Inoue, S. H. Chiang, L. Chang, X. W. Chen, A. R. Saltiel, Compartmentalization of the exocyst complex in lipid rafts controls Glut4 vesicle tethering. *Mol Biol Cell* 17, 2303 (May, 2006).
3. Y. Chien *et al.*, RalB GTPase-mediated activation of the IkappaB family kinase TBK1 couples innate immune signaling to tumor cell survival. *Cell* 127, 157 (Oct 6, 2006).
4. D. Soulat *et al.*, The DEAD-box helicase DDX3X is a critical component of the TANK-binding kinase 1-dependent innate immune response. *The EMBO journal* 27, 2135 (Aug 6, 2008).
5. J. E. Hutti *et al.*, Development of a high-throughput assay for identifying inhibitors of TBK1 and IKKepsilon. *PloS one* 7, e41494 (2012).
6. S. Fukai, H. T. Matern, J. R. Jagath, R. H. Scheller, A. T. Brunger, Structural basis of the interaction between RalA and Sec5, a subunit of the sec6/8 complex. *The EMBO journal* 22, 3267 (Jul 1, 2003).
7. S. Moskalenko *et al.*, Ral GTPases regulate exocyst assembly through dual subunit interactions. *J Biol Chem* 278, 51743 (Dec 19, 2003).
8. G. Dong, A. H. Hutagalung, C. Fu, P. Novick, K. M. Reinisch, The structures of exocyst subunit Exo70p and the Exo84p C-terminal domains reveal a common motif. *Nat Struct Mol Biol* 12, 1094 (Dec, 2005).
9. R. Jin *et al.*, Exo84 and Sec5 are competitive regulatory Sec6/8 effectors to the RalA GTPase. *The EMBO journal* 24, 2064 (Jun 15, 2005).
10. M. Munson, P. Novick, The exocyst defrocked, a framework of rods revealed. *Nat Struct Mol Biol* 13, 577 (Jul, 2006).
11. X. W. Chen, D. Leto, S. H. Chiang, Q. Wang, A. R. Saltiel, Activation of RalA is required for insulin-stimulated Glut4 trafficking to the plasma membrane via the exocyst and the motor protein Myo1c. *Dev Cell* 13, 391 (Sep, 2007).
12. J. Mowers *et al.*, Inflammation produces catecholamine resistance in obesity via activation of PDE3B by the protein kinases IKKepsilon and TBK1. *eLife* 2, e01119 (2013).
13. T. L. Chau *et al.*, Are the IKKs and IKK-related kinases TBK1 and IKK-epsilon similarly activated? *Trends in biochemical sciences* 33, 171 (Apr, 2008).
14. H. Hacker, M. Karin, Regulation and function of IKK and IKK-related kinases. *Science's STKE : signal transduction knowledge environment* 2006, re13 (Oct 17, 2006).
15. X. W. Chen *et al.*, Exocyst function is regulated by effector phosphorylation. *Nature cell biology* 13, 580 (May, 2011).
16. J. L. Pomerantz, D. Baltimore, NF-kappaB activation by a signaling complex containing TRAF2, TANK and TBK1, a novel IKK-related kinase. *The EMBO journal* 18, 6694 (Dec 1, 1999).
17. F. Fujita *et al.*, Identification of NAP1, a regulatory subunit of IkappaB kinase-related kinases that potentiates NF-kappaB signaling. *Molecular and cellular biology* 23, 7780 (Nov, 2003).

18. G. Ryzhakov, F. Randow, SINTBAD, a novel component of innate antiviral immunity, shares a TBK1-binding domain with NAP1 and TANK. *The EMBO journal* 26, 3180 (Jul 11, 2007).
19. A. Larabi *et al.*, Crystal structure and mechanism of activation of TANK-binding kinase 1. *Cell reports* 3, 734 (Mar 28, 2013).
20. C. Shu *et al.*, Structural insights into the functions of TBK1 in innate antimicrobial immunity. *Structure* 21, 1137 (Jul 2, 2013).
21. D. Tu *et al.*, Structure and ubiquitination-dependent activation of TANK-binding kinase 1. *Cell reports* 3, 747 (Mar 28, 2013).
22. F. Ikeda *et al.*, Involvement of the ubiquitin-like domain of TBK1/IKK-i kinases in regulation of IFN-inducible genes. *The EMBO journal* 26, 3451 (Jul 25, 2007).
23. R. R. Shen, W. C. Hahn, Emerging roles for the non-canonical IKKs in cancer. *Oncogene* 30, 631 (Feb 10, 2011).

CHAPTER 4

Regulation of engagement and disengagement of GLUT4 vesicles from the exocyst by TBK1

Introduction

GLUT4 translocation requires the assembly and recognition of the exocyst. Exocyst assembly is controlled by activation of the Rho subfamily G protein TC10 in response to insulin via a PI3K-independent pathway (*1-3*). Exocyst recognition is mediated by the G protein RalA, which is activated by insulin via a PI3K-dependent pathway involving the Akt-catalyzed phosphorylation (*4, 5*) and inhibition of two different GAPs (*5, 6*). Phosphorylation of the Rab GAP AS160 can ultimately target Rab10; among its effectors is the RalA GEF Rgl2, which is required for sustained activation of RalA (*7*). Akt-dependent phosphorylation and subsequent inhibition of the Ral GAP complex (RGC1/2) is also required for activation of RalA (*5, 7-9*). Once activated, the activation of the GLUT4 vesicle-associated small GTPase RalA leads to its engagement with the exocyst complex, via Sec5 and Exo84 (*4*). However, these complexes must also dissociate to permit GLUT4 vesicles to engage SNARE proteins at the plasma membrane for fusion. Recent studies suggest that disengagement between RalA and the exocyst requires phosphorylation of Sec5, thus allowing the continuation of exocytic vesicle cycling events (*10*). This prompted us to investigate the role of Exo84 phosphorylation in this process.

Results and Discussion

Phosphorylation of Exo84 by TBK1 decreases its interaction with RalA.

We first examined the interaction of Exo84, WT TBK1, and its kinase active mutant with GST-RalA fusion proteins (**Figure 4.1**). We loaded GST or GST-RalA fusion proteins with guanosine diphosphate (GDP) or guanosine 5'-O-[γ-thio]triphosphate (GTPγS) to mimic its inactive or stably active state. These fusion proteins were incubated with lysates from COS-1 cells overexpressing MYC-tagged Exo84, WT TBK1 or its K38A mutant. Exo84 was specifically pulled down by GST-RalA loaded with GTPγS but not GDP, whereas GST beads alone did not interact, confirming that the interaction between RalA and Exo84 is specific, and further that TBK1 does not directly interact with RalA.

To explore further the impact of phosphorylation on the interaction of Exo84 with RalA, we co-expressed Flag-tagged WT RalA or its constitutively active (G23V/GV) mutant (*11*) with Exo84 in the presence or absence of WT TBK1 or its K38A mutant in COS-1 cells, and immunoprecipitated with anti-Flag antibodies (**Figure 4.2A**). Exo84 preferentially co-immunoprecipitated with the active mutant of RalA (GV), and WT TBK1 overexpression produced an approximately 50% reduction in this interaction; this reduction was not observed upon overexpression of the K38A kinase-inactive mutant of TBK1. Next, lysates from COS-1 cells co-expressing increasing amounts of WT TBK1 or its K38A mutant with HA-tagged Exo84 were subjected to pulldown with a GST-RalA GV fusion protein (**Figure 4.2B**). Expression of WT TBK1 caused a dose-dependent shift in the electrophoretic mobility of Exo84 both in the

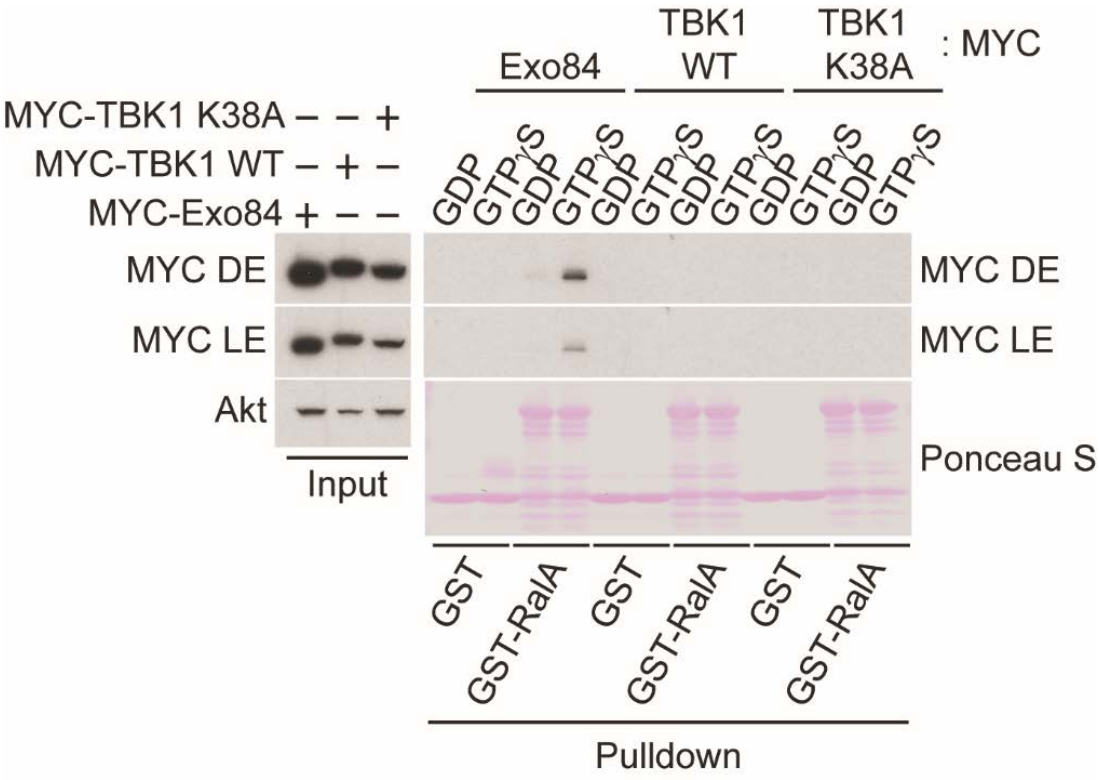

Figure 4.1 TBK1 does not directly interact with RalA.
COS-1 cell lysates overexpressing MYC-tagged Exo84, WT TBK1, and its kinase-inactive mutant were incubated with immobilized GST or GST-RalA bound to GDP or GTPγS as indicated. Pull downs were subjected to immunoblot analysis and probed using anti-MYC antibody. Amount of GST fusion proteins used in the pull down assay was visualized with Ponceau S. DE and LE stand for dark exposure and light exposure, respectively.

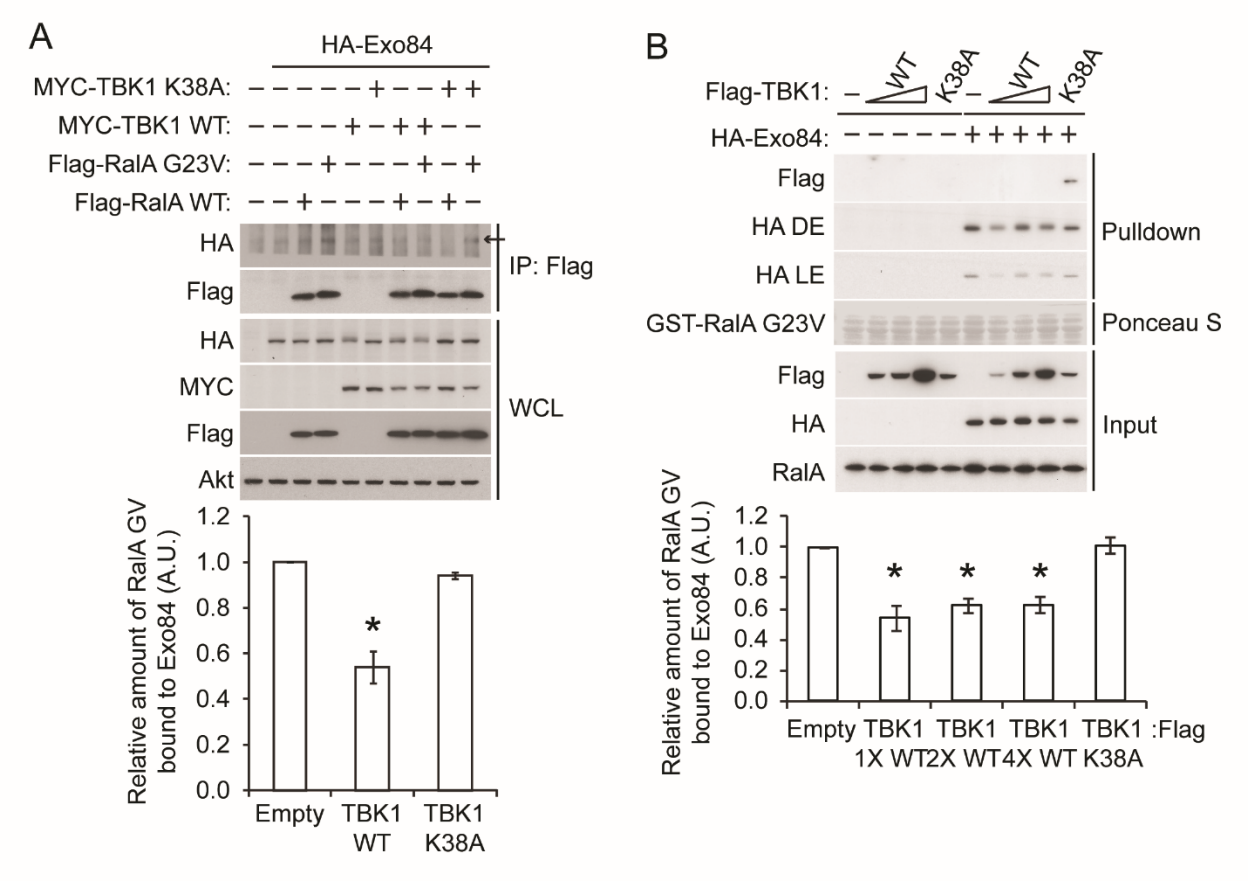

Figure 4.2 The interaction of Exo84 with RalA is impaired by WT TBK1 overexpression. (A) The interaction of Exo84 with RalA is impaired upon overexpression of WT TBK1. Flag-tagged WT RalA and its constitutively active (G23V/GV) mutant were immunoprecipitated from COS-1 cells co-expressing TBK1 or its kinase-inactive mutant along with HA-Exo84. Levels of indicated proteins in WCL and the immunoprecipitates are shown. Arrow indicates immunoprecipitated Exo84. Quantification of the binding of Exo84 with RalA is shown. The levels of binding were normalized to the fourth lane. The normalized ratio is represented in arbitrary units. Data are shown as the mean ± SEM. *$p < 0.05$; $n = 3$. (B) The interaction of active RalA with Exo84 is reduced upon overexpression of WT TBK1. Cell lysates from COS-1 cells co-expressing increasing amounts of Flag-tagged WT TBK1 and its kinase-inactive mutant with HA-Exo84 were incubated with immobilized GST-RalA G23V. Pull downs were subjected to immunoblot analysis and probed using specific antibodies as indicated. Amount of GST fusion proteins used in the pull down assay was visualized with Ponceau S. DE and LE stand for dark exposure and light exposure, respectively. Quantification of the binding of Exo84 with RalA is shown. The levels of binding were normalized to the sixth lane. The normalized ratio is represented in arbitrary units. Data are shown as the mean ± SEM. *$p < 0.05$; $n = 3$.

pulldown product and input lysates, although this shift was not detected when TBK1 K38A was expressed. WT TBK1 overexpression resulted in an approximately 50% reduction in the interaction of active RalA with Exo84, which was not observed after TBK1 K38A overexpression. Furthermore, Exo84 was pulled down with the kinase-inactive mutant of TBK1 but not with WT TBK1 by the GST-RalA GV fusion protein, whereas the fusion protein enriched neither WT TBK1 nor its K38A mutant in the absence of Exo84, confirming that the catalytically inactive TBK1 preferentially interacts with its substrate Exo84 in the pulldown assay.

To examine whether the reduction in the interaction of active RalA with Exo84 is due to changes in RalA activity, we evaluated the activity state of RalA by effector pulldown assay with another effector, RalBP1 (**Figure 4.3**). The Flag-RalA GV mutant preferentially co-precipitated with GST-RalBP1 RBD, whereas neither WT TBK1 nor its K38A mutant overexpression affected this interaction, indicating that TBK1 does not directly affect RalA activity.

To determine whether phosphorylation of Exo84 by TBK1 disengages RalA from the exocyst, HA-Exo84 was co-expressed in COS-1 cells along with WT RalA, RalA GV, or a GDP-locked dominant-negative Ral (S28N/SN) mutant (*11*), in the presence of TBK1 or its kinase inactive mutant, followed by IP with anti-HA antibodies (**Figure 4.4A**). Phosphorylation of Exo84 was detected after expression with WT TBK1 but not its kinase-inactive mutant in cells, as detected by blotting with antibodies that recognize the 14-3-3 binding motif. Interestingly, Exo84 phosphorylation was enhanced by RalA GV expression, whereas it was barely detected after RalA SN expression. Furthermore, the RalA GV mutant preferentially co-immunoprecipitated

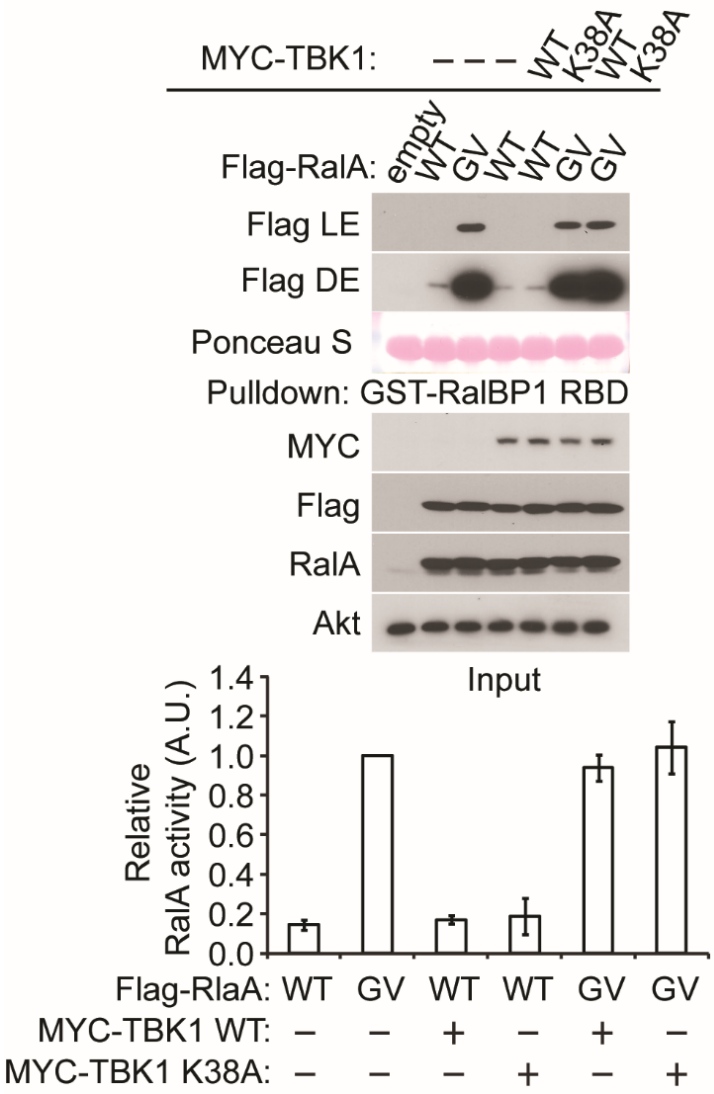

Figure 4.3 TBK1 does not directly affect RalA activity.
Cell lysates from COS-1 cells co-expressing MYC-tagged WT TBK1 and its kinase-inactive mutant with Flag-RalA WT or RalA GV were incubated with GST-RalBP1 RBD beads. Pull downs were subjected to immunoblot analysis and probed using anti-Flag antibody. Amount of GST fusion proteins used in the pull down assay was visualized with Ponceau S. DE and LE stand for dark exposure and light exposure, respectively. Quantification of RalA activity is shown. RalA activity (pull-down/total RalA) was normalized to the third lane. The normalized ratio is represented in arbitrary units. Data are shown as the mean ± SEM. *$p < 0.05$; $n = 3$.

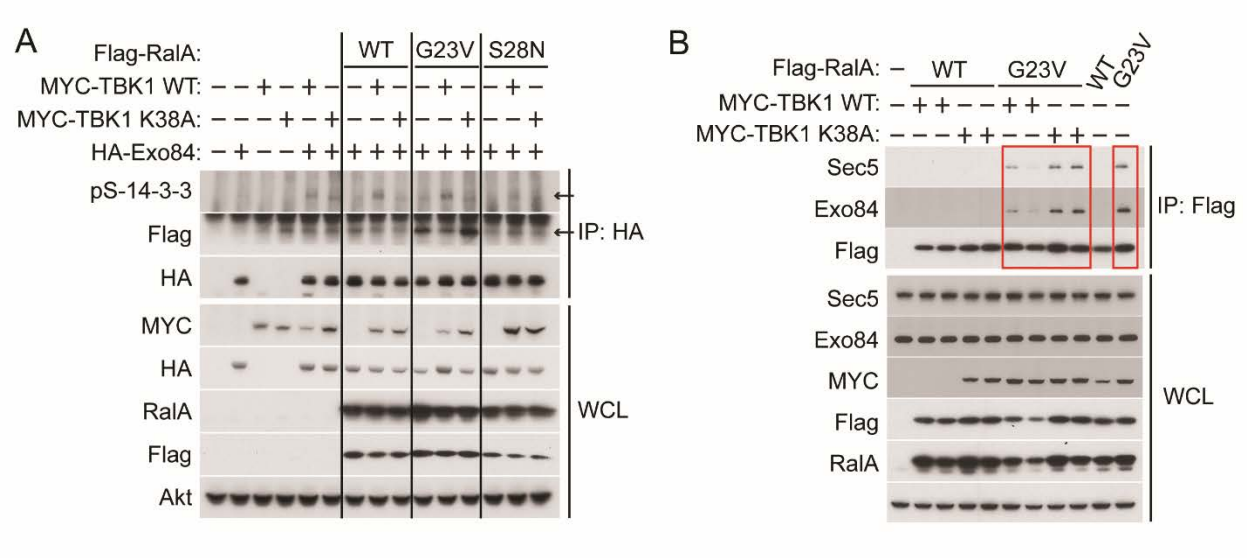

Figure 4.4 Phosphorylation of Exo84 by TBK1 decreases its interaction with RalA.
(A) TBK1-mediated Exo84 phosphorylation decreases the interaction between RalA and Exo84. HA-tagged Exo84 was immunoprecipitated from COS-1 cells co-expressing TBK1 or its kinase-inactive mutant along with Exo84 and RalA, RalA GV, or a GDP-locked dominant-negative Ral (S28N/SN) mutant. Levels of indicated proteins in WCL and the immunoprecipitates are shown. Arrow indicates phosphorylated Exo84 and RalA, respectively. (B) The interaction of endogenous Exo84 and Sec5 with RalA is decreased upon overexpression of WT TBK1. Flag-tagged WT RalA and its constitutively active (G23V/GV) mutant were immunoprecipitated from COS-1 cells co-expressing TBK1 or its kinase-inactive mutant. Levels of indicated proteins in WCL and the immunoprecipitates are shown. The interaction of endogenous Exo84 and Sec5 with RalA GV in the presence or absence of TBK1 is shown in the square.

with Exo84, whereas the interaction of Exo84 with WT RalA and the RalA SN mutant was barely detected. As shown in **Figure 4.2**, the interaction of Exo84 with the RalA GV mutant was significantly decreased by expression of WT TBK1 but not by its inactive K38A mutant. To examine the interaction of endogenous Exo84 and Sec5 with RalA, we also co-expressed WT TBK1 or its K38A mutant along with Flag-tagged WT RalA or its constitutively active GV mutant, followed by IP with anti-Flag antibodies (**Figure 4.4B**). We confirmed that both endogenous Sec5 and Exo84 preferentially immunoprecipitated with RalA GV, whereas the interaction of Sec5 or Exo84 with WT RalA was barely detectable. We also validated that the interaction between active RalA and endogenous Sec5 or Exo84 was significantly decreased only when WT TBK1 but not its K38A mutant was overexpressed. These data confirm that TBK1-mediated Exo84 phosphorylation decreases the interaction between RalA and Exo84 by targeting the effector.

Previous studies suggested that RalB activates TBK1 by promoting Sec5/TBK1 complex assembly (*12*). To explore this possibility, we examined whether the activity status of RalA affects the interaction between TBK1 and Exo84. We co-expressed WT TBK1 and its K38A mutant with HA-tagged Exo84 in the presence or absence of WT RalA, the constitutively active GV or the dominant-negative SN RalA mutant in COS-1 cells, and immunoprecipitated the protein with anti-HA antibodies (**Figure 4.5**). Kinase-inactive TBK1 preferentially co-immunoprecipitated with Exo84, whereas the interaction of Exo84 with WT TBK1 was barely detected. This effect was consistent with the observation that the association of the catalytically inactive TBK1 with Exo84 did not correlate with the activity state of RalA. The constitutively

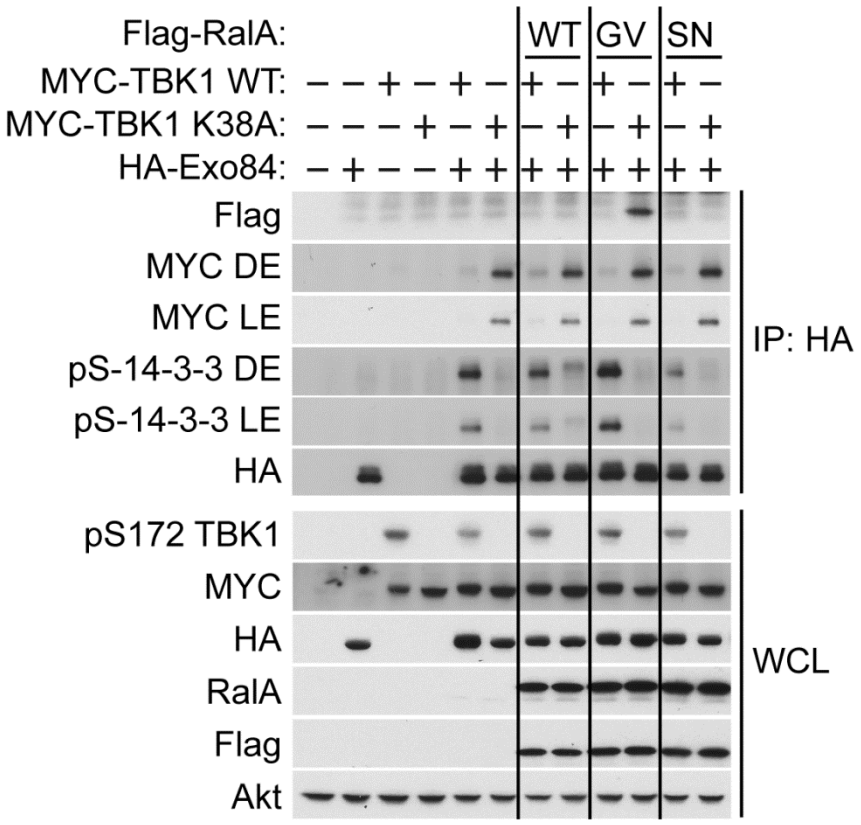

Figure 4.5 The activity state of RalA does not affect the interaction between TBK1 and Exo84.

HA-tagged Exo84 was immunoprecipitated from COS-1 cells co-expressing TBK1 or its kinase-inactive mutant along with Exo84 and RalA, RalA GV, or Ral SN mutant. Levels of indicated proteins in WCL and the immunoprecipitates are shown. DE and LE stand for dark exposure and light exposure, respectively.

active RalA GV mutant also preferentially co-immunoprecipitated with Exo84, unlike the WT or SN RalA mutant. We also confirmed that the interaction between RalA GV and Exo84 was significantly decreased when WT TBK1 but not its K38A mutant was co-expressed. Phosphorylated Exo84 was enriched by IP with anti-HA antibodies and detected by blotting with antibodies that recognize the 14-3-3 binding motif. As shown in **Figure 4.4A**, Exo84 phosphorylation was enhanced by RalA GV expression, whereas it was significantly decreased by RalA SN expression, suggesting that active RalA does not promote Exo84/TBK1 complex assembly but rather may change phosphorylation due to the accessibility of substrate.

To explore this possibility, we generated stable cell lines in HEK293T cells expressing *Aequorea coerulescens* green fluorescent protein (AcGFP1), a dual-tagged WT TBK1, and TBK1 K38A, in which the N-terminus of TBK1 is tagged with MYC and the C-terminus with AcGFP1 (MYC-TBK1 WT-AcGFP1 or MYC-TBK1 K38A-AcGFP1). HEK293T cell lines stably expressing dual MYC and AcGFP1-tagged WT TBK1 or its inactive mutant were overexpressed with RalA WT, GV, SN or a fast cycling mutant (F39L/FL) bearing increased nucleotide dissociation rates that quickly cycles between the GDP- and GTP-bound state of RalA (*13*, *14*). This was followed by an *in vitro* immune complex kinase assay using anti-MYC antibodies or control mouse IgG antibodies, [γ-^{32}P]ATP and MBP as a substrate (**Figure 4.6**). Whole cell lysates were blotted with antibodies that recognize phosphorylation of TBK1 at S172, revealing that WT TBK1 was autoactivated (*15*). Moreover, overexpressed TBK1 (arrow) was phosphorylated to a greater extent than was endogenous TBK1 (arrow head), whereas overexpression of dominant-negative TBK1 K38A completely abolished phosphorylation of TBK1. Overexpression of any of the RalA mutants was without effect on phosphorylation of TBK1 at S172 or on TBK1 activity.

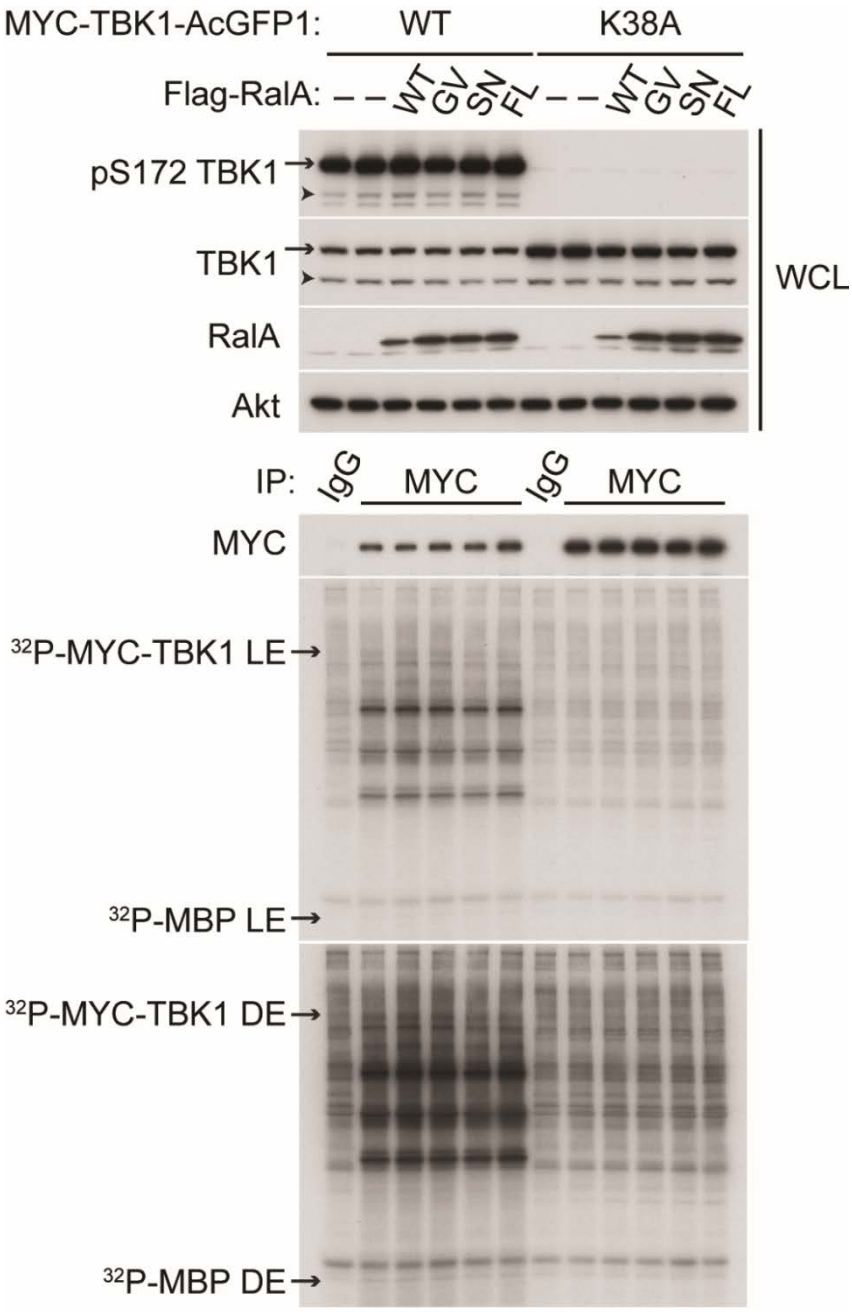

Figure 4.6 The activity state of RalA does not affect TBK1 activity.
MYC-tagged TBK1 or its kinase-inactive mutant was immunoprecipitated from HEK293T cell lines stably expressing dual MYC and AcGFP1-tagged WT TBK1 or its inactive mutant K38A co-expressing RalA, RalA GV, Ral SN, or a fast cycling RalA (F39L/FL) mutant. As a control, IgG was used. Levels of indicated proteins in WCL and the immunoprecipitates are shown. DE and LE stand for dark exposure and light exposure, respectively. Arrows indicate exogenous TBK1 and arrow heads indicate endogenous TBK1 in WCL. Arrows in the immunoprecipitates indicate phosphorylated proteins.

To measure endogenous TBK1 catalytic activity, HEK293T cells were overexpressed with Flag-tagged RalA WT, GV, FL, or RalB WT and FL, or TBK1 WT and K38A, followed by an *in vitro* immune complex kinase assay as described above (**Figure 4.7**). Overexpression of WT TBK1 caused its autophosphorylation, and increased phosphorylation of interferon regulatory factor 3 (IRF3) as a downstream target (*16-20*), as well as overall phosphorylation levels detected by blotting of whole cell lysates with antibodies that recognize the 14-3-3 binding motif, whereas overexpression of TBK1 K38A was without effect. None of the RalA or RalB mutants affected endogenous TBK1 activity. These combined observations indicate that while RalA has no direct effect on either TBK1 activation or Exo84/TBK1 complex assembly, phosphorylation of Exo84 by TBK1 disengages RalA from the exocyst by reducing the affinity of Exo84 for RalA.

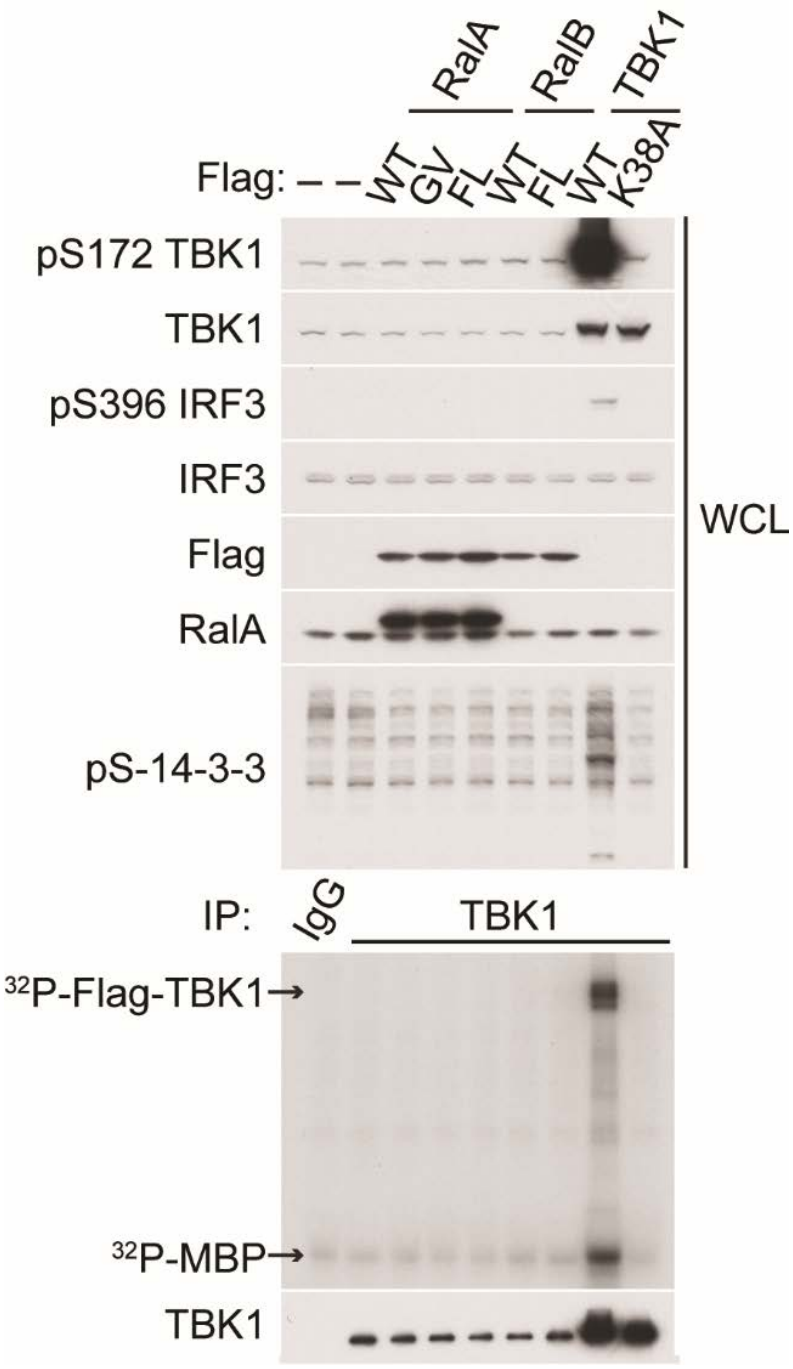

Figure 4.7 RalA or RalB do not affect TBK1 activity.
TBK1 was immunoprecipitated from HEK293T cells expressing RalA WT, GV, FL, or RalB WT and FL, or TBK1 WT and K38A. As a control, IgG was used. *In vitro* immune complex kinase assay was performed as described in materials and methods. Levels of indicated proteins in WCL and the immunoprecipitates are shown. Arrows indicate phosphorylated proteins in the immunoprecipitates.

Exo84 interaction with RalA and other exocyst subunits is dependent upon TBK1 phosphorylation of Exo84.

To identify the phosphorylation sites on Exo84 catalyzed by TBK1, HA-Exo84 was co-expressed in COS-1 cells with WT TBK1 or its K38A mutant, followed by IP with anti-HA antibodies to enrich phosphorylated Exo84. Phosphorylation sites on Exo84 were then determined by LC-MS/MS mass spectrometry. 11 potential phosphorylation sites were identified with a total coverage of 60.2% of the Exo84 amino acid sequence (**Figure 4.8**).

To identify the importance of these phosphorylation events and further validate the mass spectrometry analysis, each of the 11 phosphorylation sites was mutated to alanine by site-directed mutagenesis. The phosphorylation-defective (S/T to A) Exo84 point mutants were HA-tagged and overexpressed in HEK293T stable cell lines expressing AcGFP1 or a dual-tagged WT TBK1 (MYC-TBK1 WT-AcGFP1), and levels of phosphorylation of Exo84 was assayed after anti-HA IP followed by blotting with anti-14-3-3 binding motif antibodies (**Figure 4.9**). While phosphorylation of most of the Exo84 point mutants was increased by WT TBK1 overexpression, the S93A, S96A, S505A, and S670A mutants showed reduced 14-3-3 motif antibody binding.

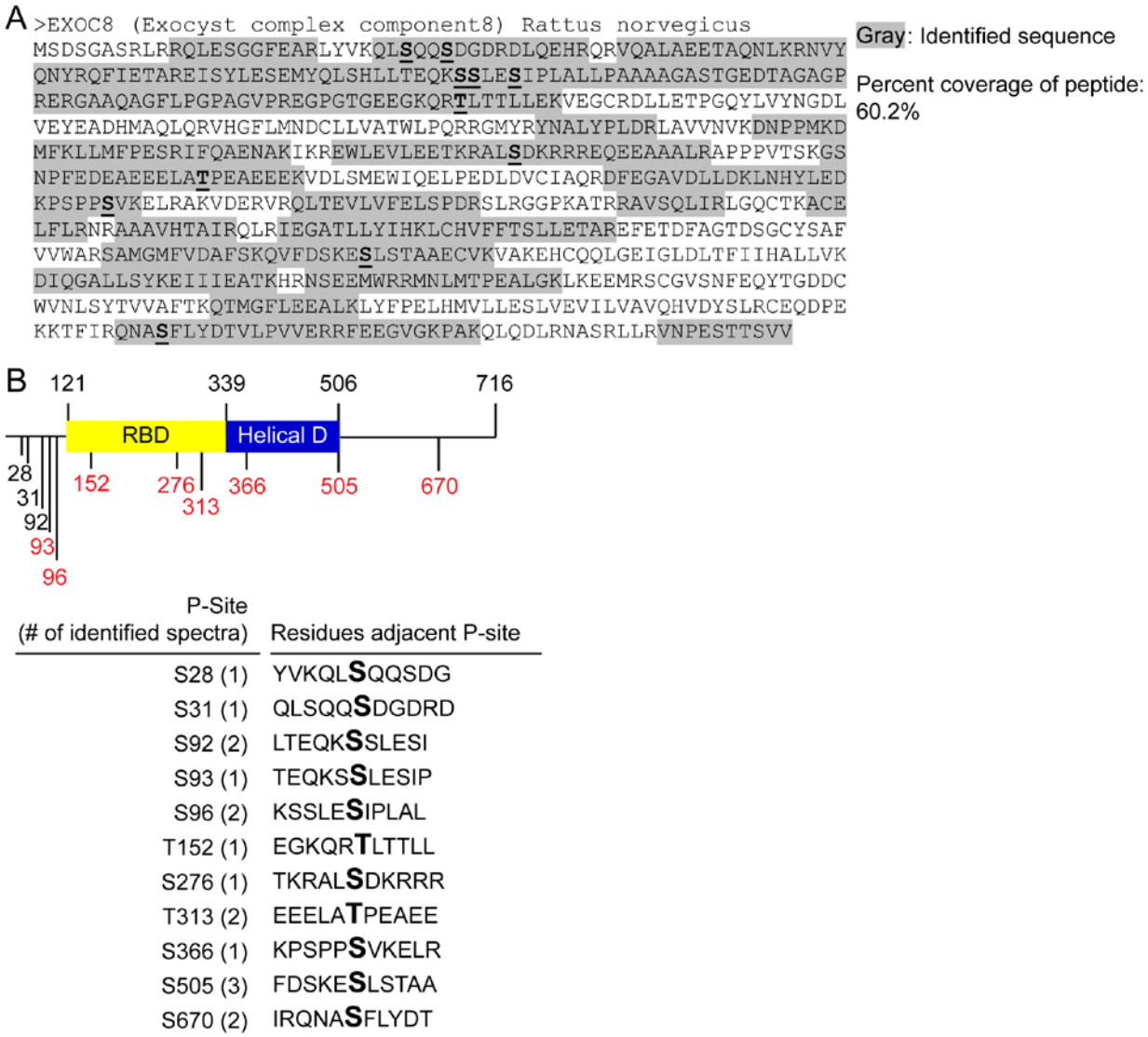

Figure 4.8 Schematic representation of mass spectrometry analysis.
(A) Mass spectrometry sequence coverage of affinity-purified phosphorylated HA-Exo84. Identified sequence from mass spectrometry analysis is shown in gray. S or T indicate amino acid residue modified with phosphorylation. (B) Exo84 undergoes phosphorylation on multiple sites. Schematic diagram of the Exo84 domains is shown. Exo84 phosphorylation sties were identified in two independent mass spectrometry analyses with a total coverage of 60.2% of the Exo84 amino acid sequence (Figure 4.8A). The major functional phosphorylation sites are indicated in red. Each phosphorylation sites and residues adjacent phosphorylation sites are shown.

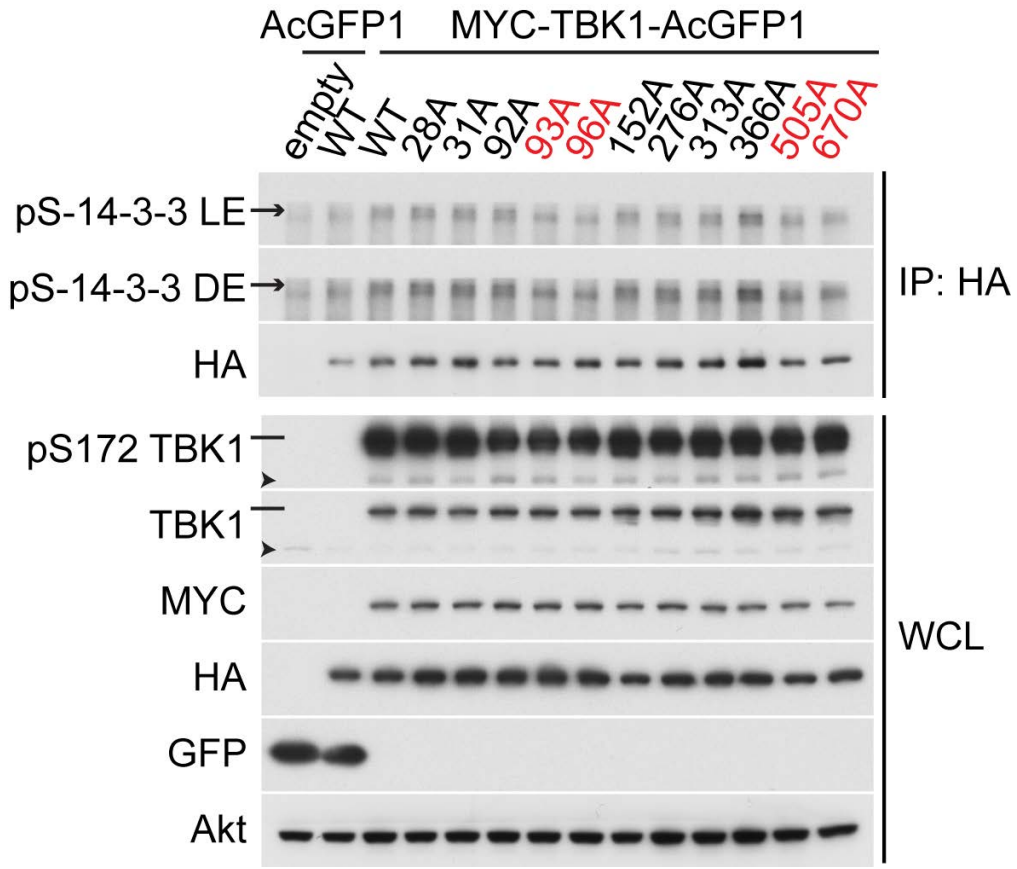

Figure 4.9 Substitution of alanine for serine at position 93, 96, 505, and 670 inhibits phosphorylation of Exo84.
HA-tagged phosphorylation-defective Exo84 point mutants were immunoprecipitated from HEK293T cell lines stably expressing dual MYC and AcGFP1-tagged WT TBK1 or AcGFP1-tagged empty vector. Levels of indicated proteins in WCL and the immunoprecipitates are shown. DE and LE stand for dark exposure and light exposure, respectively. Arrows indicate phosphorylated proteins the immunoprecipitates. Solid lines indicate exogenous TBK1 and arrow heads indicate endogenous TBK1 in WCL.

To test whether these 4 sites are functionally important for Exo84, we generated compound mutants, in which each residue was mutated to either Alanine (4A) or Glutamic acid (4E) to prevent or mimic phosphorylation. Lysates from COS-1 cells co-expressing WT TBK1 or its K38A mutant with HA-tagged Exo84 WT, 4A, or 4E were subjected to a pulldown assay with a GST-RalA GV fusion protein (**Figure 4.10**). Replacement of these 4 phosphorylation sites on Exo84 with glutamate resulted in a mobility shift comparable to what was observed with WT Exo84 phosphorylated by TBK1. Interestingly, the RalA fusion protein precipitated approximately 60% less of the Exo84 4E mutant compared to the WT protein. This reduction in the binding of Exo84 4E with active RalA was not changed by either WT TBK1 or its K38A mutant overexpression, suggesting that these 4 phosphorylation sites on Exo84 reduce the affinity of Exo84 for RalA in response to TBK1. While WT TBK1 overexpression resulted in an approximately 85% reduction in the interaction of active RalA with Exo84 WT or Exo84 4A, this inhibitory effect was not observed after overexpression of TBK1 K38A. Together these data suggest that while Exo84 is phosphorylated by TBK1 on other sites, these phosphorylation sites are not sufficient to influence the binding of the protein to RalA.

To explore the role of other phosphorylation sites, we created more compound mutants from the 11 potential phosphorylation sites identified from the mass spectrometry analysis, including eight (S93, S96, T152, S276, T313, S366, S505, S670) sites that appeared to represent consensus phosphorylation sites (*21*, *22*). We performed a GST pull-down assay using a GST-RalA GV fusion protein with lysates from COS-1 cells co-expressing WT TBK1 and its K38A mutant, along with HA-tagged Exo84 WT, 8A, or 8E (**Figure 4.11**). Similar to the Exo84 4E mutant

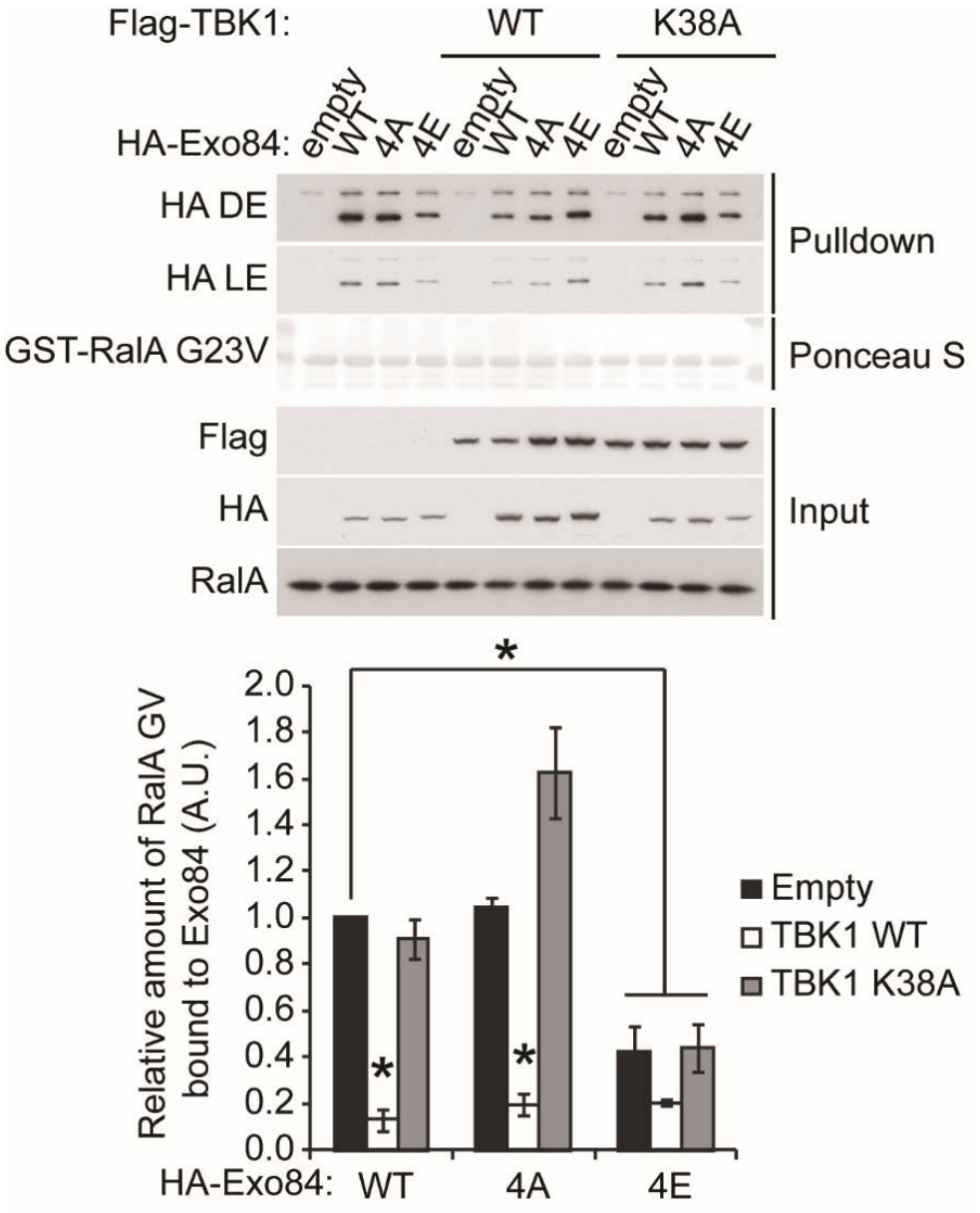

Figure 4.10 TBK1-mediated Exo84 phosphorylation at position 93, 96, 505, and 670 is required for RalA disengagement.
Cell lysates from COS-1 cells co-expressing Flag-tagged WT TBK1 and its kinase-inactive mutant with Exo84 and its phosphorylation-defective 4A or phosphomimetic 4E mutant were incubated with immobilized GST-RalA G23V. Pull downs were subjected to immunoblotting with anti-HA antibody. Amount of GST fusion proteins used in the pull down assay was visualized with Ponceau S. DE and LE stand for dark exposure and light exposure, respectively. Quantification of the binding of Exo84 with RalA is shown. The levels of binding were normalized to the second lane. The normalized ratio is represented in arbitrary units. Data are shown as the mean ± SEM. *$p < 0.05$; $n = 3$.

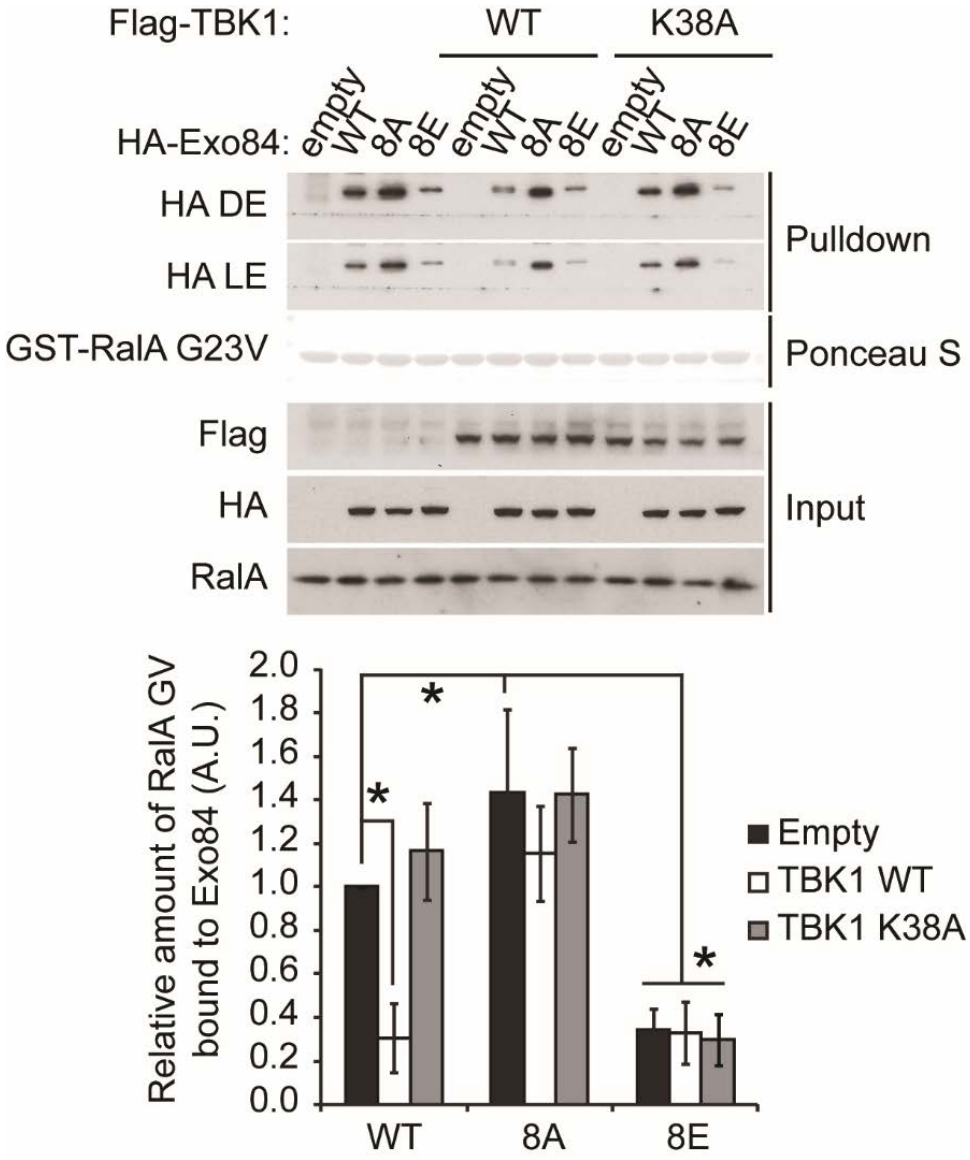

Figure 4.11 TBK1-mediated Exo84 phosphorylation at position 93, 96, 152, 276, 313, 366, 505, and 670 is necessary and sufficient for RalA disengagement.
Cell lysates from COS-1 cells co-expressing Flag-tagged WT TBK1 and its kinase-inactive mutant with Exo84 and its phosphorylation-defective 8A or phosphomimetic 8E mutant were incubated with immobilized GST-RalA G23V. Pull downs were subjected to immunoblot analysis and probed using anti-HA antibody. Amount of GST fusion proteins used in the pull down assay was visualized with Ponceau S. DE and LE stand for dark exposure and light exposure, respectively. Quantification of the binding of Exo84 with RalA is shown. The levels of binding were normalized to the second lane. The normalized ratio is represented in arbitrary units. Data are shown as the mean ± SEM. *$p < 0.05$; $n = 3$.

described above, the 8E mutant displayed reduced mobility on SDS PAGE compared to wild type. The RalA fusion protein precipitated approximately 70% less of the Exo84 8E mutant, but approximately 40% more of the 8A mutant compared to the WT protein. Overexpression of neither WT TBK1 nor its K38A mutant reduced or enhanced the binding between RalA and the Exo84 mutants. Furthermore, WT TBK1 overexpression resulted in an approximately 70% reduction in the interaction of active RalA with Exo84 WT, which was not observed by phosphorylation of the Exo84 8A mutant, or when TBK1 K38A was overexpressed. These data suggest that TBK1-mediated Exo84 phosphorylation on these 8 sites is necessary and sufficient for RalA disengagement, as Exo84 8A was resistant to phosphorylation-dependent RalA disengagement, whereas Exo84 8E exhibited a lower affinity for RalA.

To understand whether TBK1-dependent phosphorylation of Exo84 influences other interactions, we investigated binding to other exocyst subunits. We co-expressed WT TBK1 and its K38A mutant with HA-tagged Exo84 WT, 4A, or 4E in COS-1 cells, followed by IP with anti-HA antibodies (**Figure 4.12**). HA immunoprecipitates were blotted with antibodies against two other exocyst subunits, Sec5 and Sec8, which were previously shown to interact with Exo84 in the exocyst complex (*23*). The phosphorylation-defective Exo84 4A mutant bound more strongly to Sec5 and Sec8 than did the WT Exo84 or its phosphomimetic 4E mutant. WT TBK1 overexpression reduced the binding of WT Exo84 to Sec5 and Sec8, while overexpression of the kinase-inactive mutant enhanced this interaction. The stronger binding of the Exo84 4A mutant

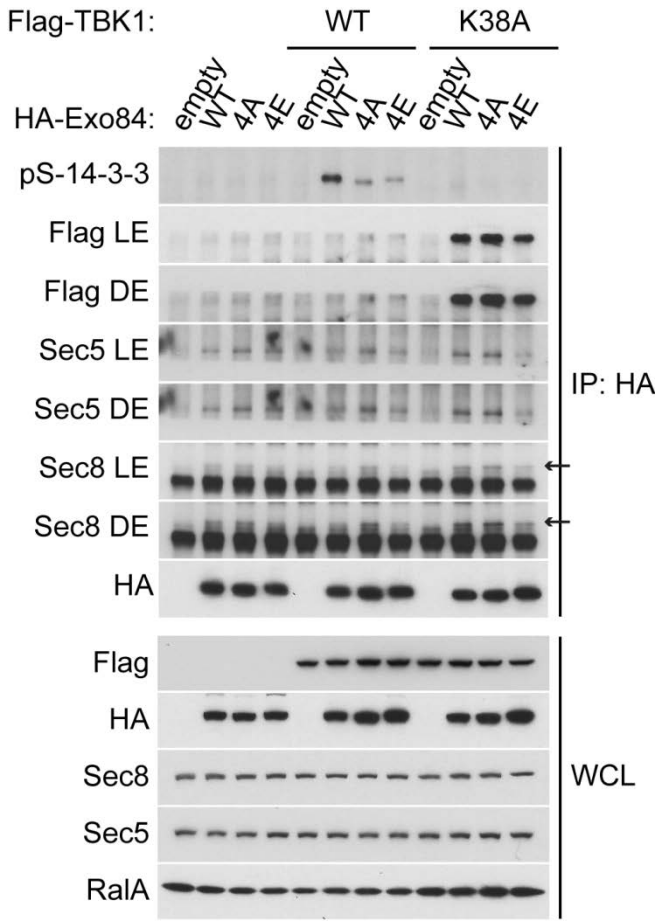

Figure 4.12 Phosphorylation of Exo84 by TBK1 induces its disengagement from other exocyst components.
HA-tagged Exo84 WT, 4A, and 4E were immunoprecipitated from COS-1 cells co-expressing Flag-tagged WT TBK1 and its kinase-inactive mutant. Levels of indicated proteins in WCL and the immunoprecipitates are shown. DE and LE stand for dark exposure and light exposure, respectively. Arrows point to Sec8.

to Sec5 and Sec8 was not affected by WT TBK1 overexpression; however, the binding of Exo84 4E to Sec5 and Sec8 was significantly reduced, even in the presence of the kinase-inactive mutant of TBK1. Anti-HA immunoprecipitation of lysates followed by blotting with antibodies that recognize the 14-3-3 binding motif revealed that WT Exo84 was phosphorylated upon TBK1 but not K38A overexpression. Exo84 mutants were less phosphorylated upon TBK1 but not K38A overexpression. However, the kinase-inactive mutant of TBK1 K38A and Exo84 still interacted with Exo84 4A and Exo84 4E.

We performed similar experiments with the 8A and phosphomimetic Exo84 8E mutants (**Figure 4.13**). The phosphorylation-defective Exo84 8A mutant interacted well with Sec5 and Sec8, whereas binding with the phosphomimetic 8E mutant was reduced. WT TBK1 overexpression blocked the binding of WT Exo84 but not the mutant forms of the protein to Sec5 and Sec8. Both Exo84 8A and 8E also underwent less phosphorylation by TBK1 overexpression. Interestingly, while the interaction of Exo84 with WT TBK1 was barely detected, it was easily visualized for the Exo84 8A mutant. Taken together, these data suggest that phosphorylation of Exo84 by TBK1 induces its disengagement from both RalA and other exocyst components. Exo84 sites S93, S96, S505, and S670 are crucial for the regulation of exocyst binding, whereas S93, S96, T152, S276, T313, S366, S505 and S670 appeared to negatively regulate both RalA and exocyst binding. These data suggest that these are independent processes mediated by TBK1 phosphorylation on Exo84 at different amino acids.

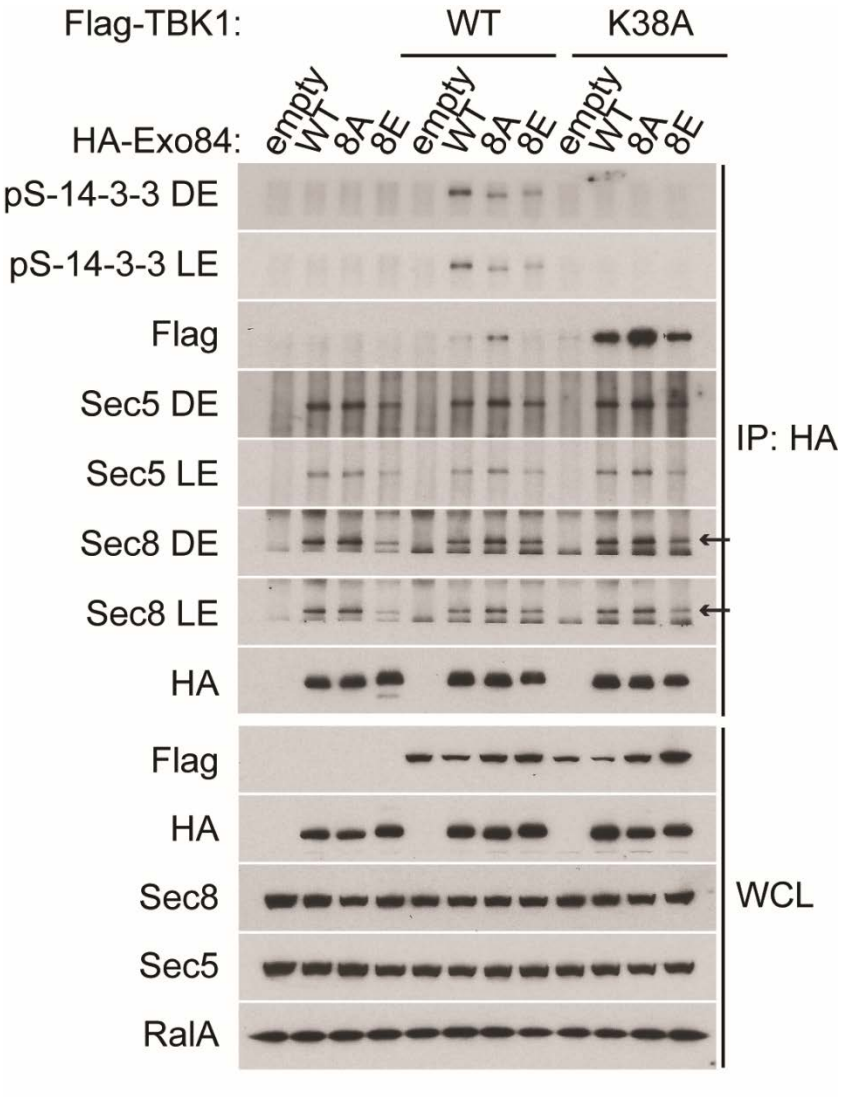

Figure 4.13 Phosphorylation of Exo84 by TBK1 induces its disengagement from other exocyst components.
HA-tagged Exo84 WT, 8A, and 8E were immunoprecipitated from COS-1 cells co-expressing Flag-tagged WT TBK1 and its kinase-inactive mutant. Levels of indicated proteins in WCL and the immunoprecipitates are shown. DE and LE stand for dark exposure and light exposure, respectively. Arrows indicate Sec8.

Exo84 phosphorylation by TBK1 results in disengagement of RalA and disassociation of the exocyst for insulin-stimulated glucose transport.

We speculate that GLUT4 vesicle recognition at the plasma membrane is triggered by RalA activation, but once bound, the phosphorylation of Exo84 and Sec5 releases the GLUT4 vesicle from the exocyst to permit fusion. To examine whether this process is triggered by TBK1-mediated Exo84 phosphorylation in 3T3-L1 adipocytes, endogenous Exo84 was immunoprecipitated from cell lysates of 3T3-L1 adipocytes treated with or without insulin, in the presence or absence of the TBK1 inhibitor amlexanox, and the interaction of Exo84 with various proteins was assessed by western blotting (**Figure 4.14A** and **Figure 4.15A**). Endogenous RalA rapidly associated with Exo84 in response to insulin. This effect was maximal 2 minutes after insulin stimulation and declined thereafter. Assessment of RalA activity by pull-down assay with a GST-RalBP1 RBD fusion protein (**Figure 4.14B** and **Figure 4.15B**) revealed that RalA was maximally activated by 2 minutes, and maintained throughout 30 minutes. While amlexanox pretreatment was without effect on RalA activity, it prevented the decline in RalA-Exo84 binding, suggesting that inhibition of TBK1 delays the rate of dissociation of RalA-Exo84 interaction. To examine whether the disengagement phase is due to TBK1-mediated Exo84 phosphorylation, Exo84 immunoprecipitates were blotted with antibodies that recognize the 14-3-3 binding motif during the time course. Phosphorylation of Exo84 reached maximal levels 2 minutes after insulin stimulation and declined by 30 minutes. It is likely that disruption of the exocyst complex might also be crucial to initiate another round of vesicle fusion. To examine this possibility, Exo84 immunoprecipitates were blotted with anti-Sec8 and anti-Sec5 antibodies. The interaction of Exo84 with Sec5 and Sec8 reached maximal levels 2 minutes after insulin

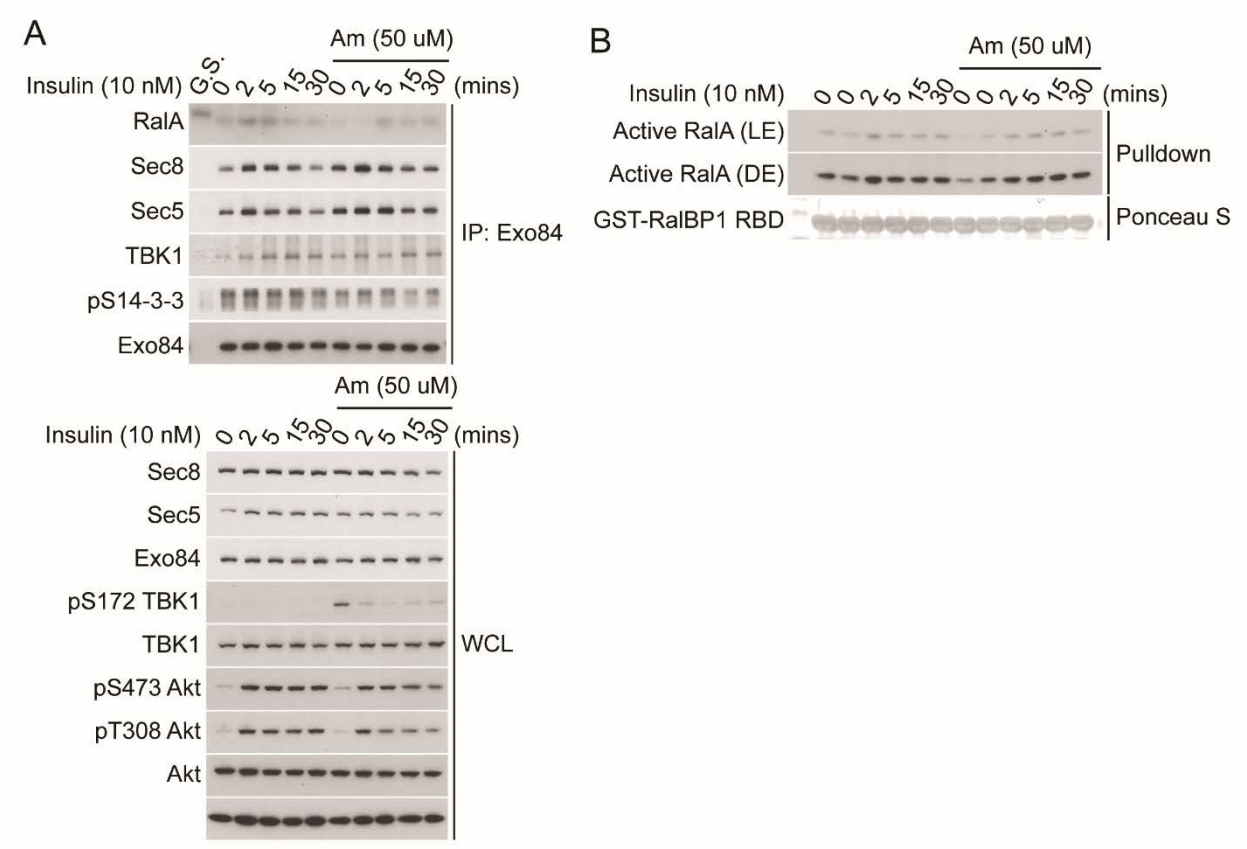

Figure 4.14 Disengagement of TBK1, Exo84, and RalA in insulin-stimulated GLUT4 trafficking.

(A) Disengagement of TBK1, Exo84, and RalA in insulin-stimulated GLUT4 trafficking is due to TBK1-mediated Exo84 phosphorylation. Exo84 was immunoprecipitated from 3T3-L1 adipocytes treated with or without insulin (10 nM) in the presence or absence of pretreatment with amlexanox (50 μM). As a control, goat serum (G.S) was used. Levels of indicated proteins in WCL and the immunoprecipitates are shown. (B) TBK1 does not directly affect RalA activity. Cell lysates from 3T3-L1 adipocytes treated with or without insulin (10 nM) in the presence or absence of pretreatment with amlexanox (50 μM) were incubated with GST-RalBP1 RBD beads. Pull downs were subjected to immunoblot analysis using anti-RalA antibody. Amount of GST fusion proteins used in the pull down assay was visualized with Ponceau S. DE and LE stand for dark exposure and light exposure, respectively.

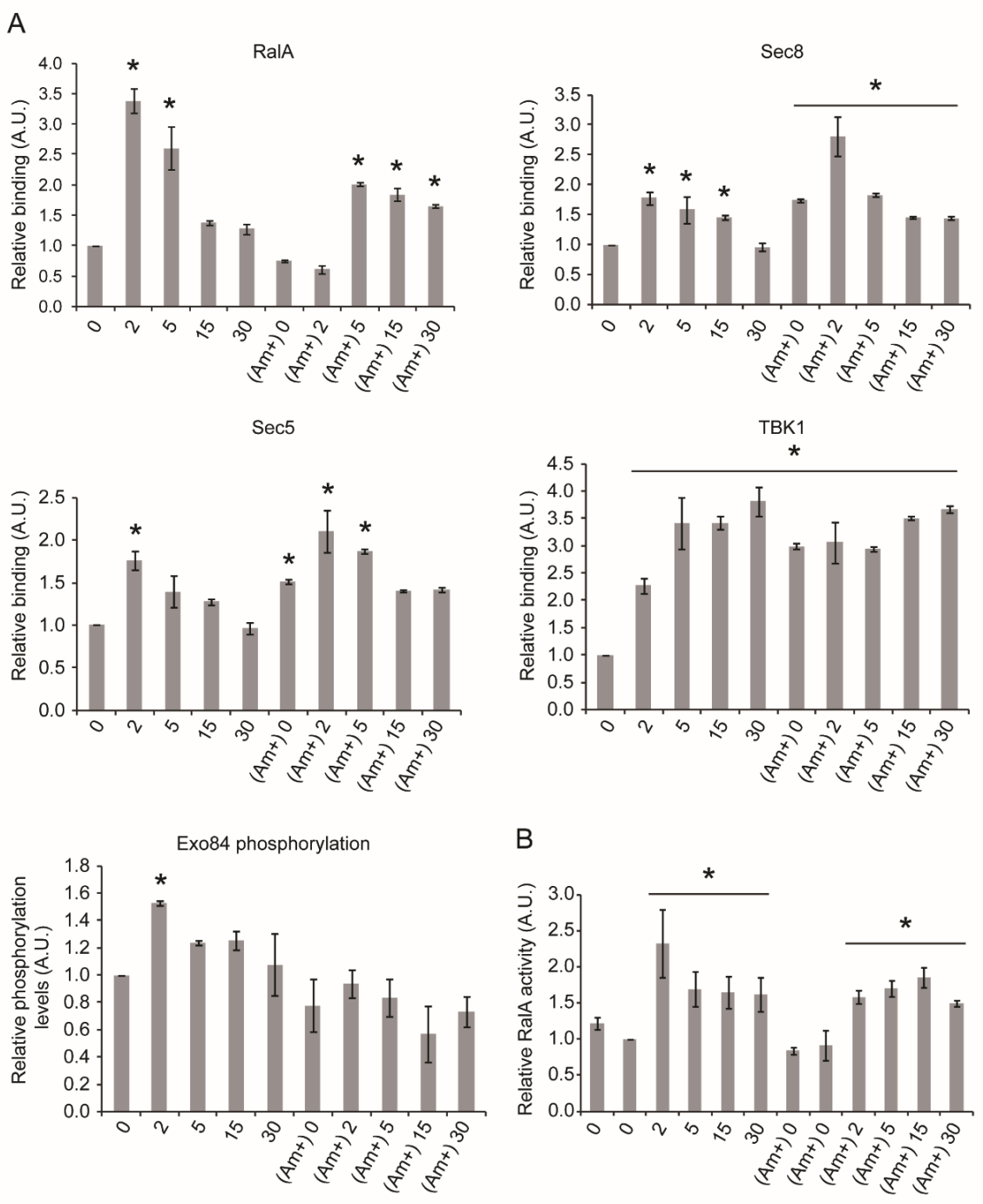

Figure 4.15 Quantification of disengagement of TBK1, Exo84, and RalA in insulin-stimulated GLUT4 trafficking.

(A) Quantification of the binding of RalA, Sec8, Sec5, and TBK1 with Exo84 as shown in Figure 4.14A. Quantification of levels of Exo84 phosphorylation is also shown. The levels were all normalized to the basal level at 0 minute. *$p < 0.05$ as compared to the basal level; $n = 3$. (B) Quantification of RalA activity as shown in Figure 4.14B. RalA activity (pull-down/total RalA) was normalized to the second lane. The normalized ratio is represented in arbitrary units. Data are shown as the mean ± SEM. *$p < 0.05$; $n = 3$.

stimulation, but returned to basal levels by 30 minutes. Interestingly, amlexanox pretreatment increased the binding of Exo84 to Sec5 and Sec8 even in the absence of insulin, while the disassociation of the complex was blocked; suggesting that phosphorylation of the exocyst by TBK1 reverses the assembly of the entire complex. TBK1 also associated with Exo84, reaching maximal levels 30 minutes after insulin stimulation. Amlexanox pretreatment enhanced the interaction between TBK1 and Exo84, and these effects were also seen with the structurally unrelated TBK1 inhibitor Cay (**Figure 4.16** and **Figure 4.17**).

To understand the dynamics of the protein interactions of TBK1, Exo84, and RalA in insulin-stimulated GLUT4 trafficking, we investigated whether these proteins reside in the same subcellular compartments. Previous studies have shown that RalA co-localizes with GLUT4 vesicles and translocates to the plasma membrane upon insulin stimulation (*4*). Insulin also stimulates the assembly of the exocyst complex at the plasma membrane (*2, 3*). We performed subcellular fractionation on 3T3-L1 adipocytes after treatment with or without insulin, followed by immunoblotting, as previously described (*4, 24*) (**Figure 4.18**). GLUT4, RalA, and the exocyst subunits Sec6, Sec8, Sec10, Sec5, and Exo84 were enriched in the plasma membrane fractions upon insulin stimulation, with a concurrent loss of these proteins in the low-density microsome (LDM) fractions. IRAP was also enriched in the plasma membrane fractions upon insulin stimulation, but transferrin receptor (TfR), Rab5, and caveolin showed no significant movement. In untreated cells, TBK1 protein was detected in most fractions. After treatment with insulin, TBK1 was enriched in the plasma membrane fractions, with a concurrent loss of this protein in the low-density microsome (LDM), mirroring GLUT4 trafficking. Interestingly,

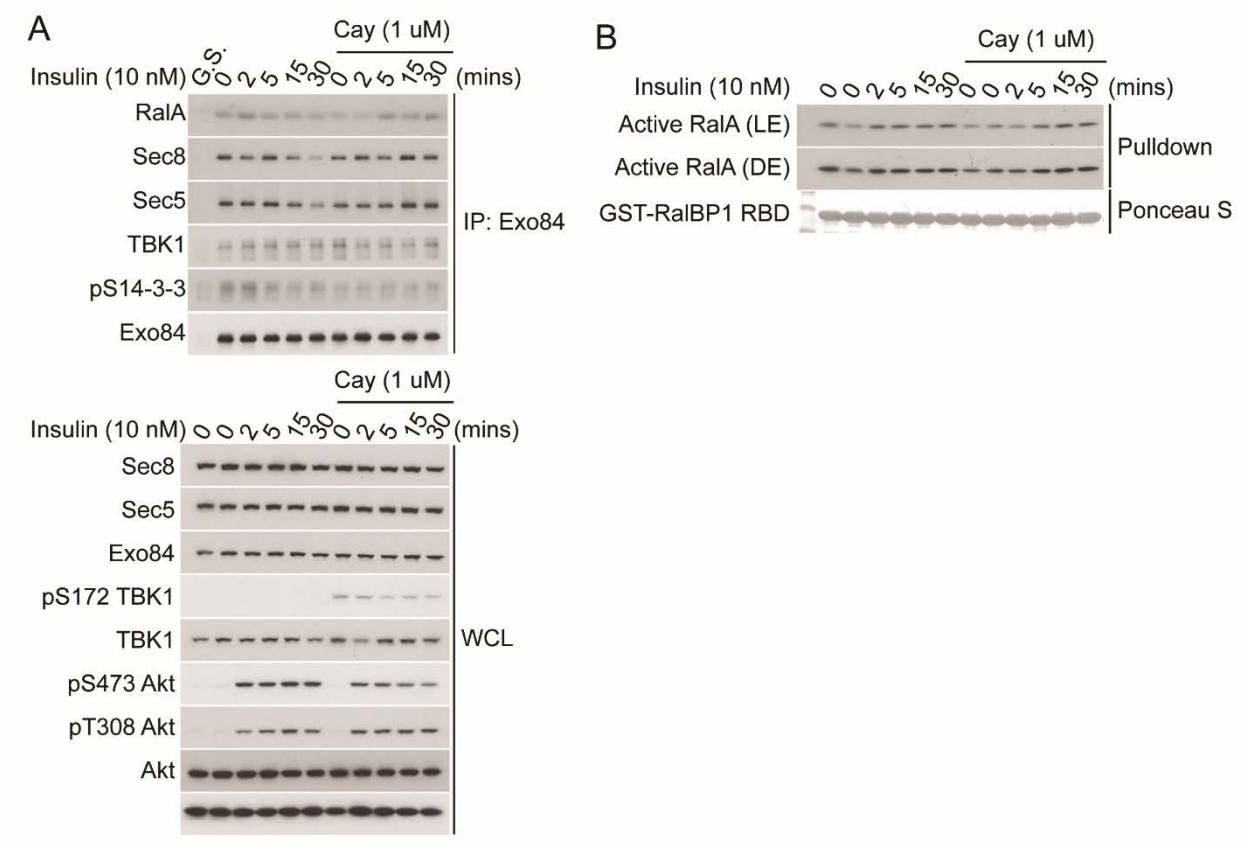

Figure 4.16 Disengagement of TBK1, Exo84, and RalA in insulin-stimulated GLUT4 trafficking.

(A) Disengagement of TBK1, Exo84, and RalA in insulin-stimulated GLUT4 trafficking is due to TBK1-mediated Exo84 phosphorylation. Exo84 was immunoprecipitated from 3T3-L1 adipocytes treated with or without insulin (10 nM) in the presence or absence of pretreatment with Cay (1 μM). As a control, goat serum (G.S) was used. Levels of indicated proteins in WCL and the immunoprecipitates are shown. (B) TBK1 does not directly affect RalA activity. Cell lysates from 3T3-L1 adipocytes treated with or without insulin (10 nM) in the presence or absence of pretreatment with Cay (1 μM) were incubated with GST-RalBP1 RBD beads. Pull downs were subjected to immunoblot analysis and probed using anti-RalA antibody. Amount of GST fusion proteins used in the pull down assay was visualized with Ponceau S. DE and LE stand for dark exposure and light exposure, respectively.

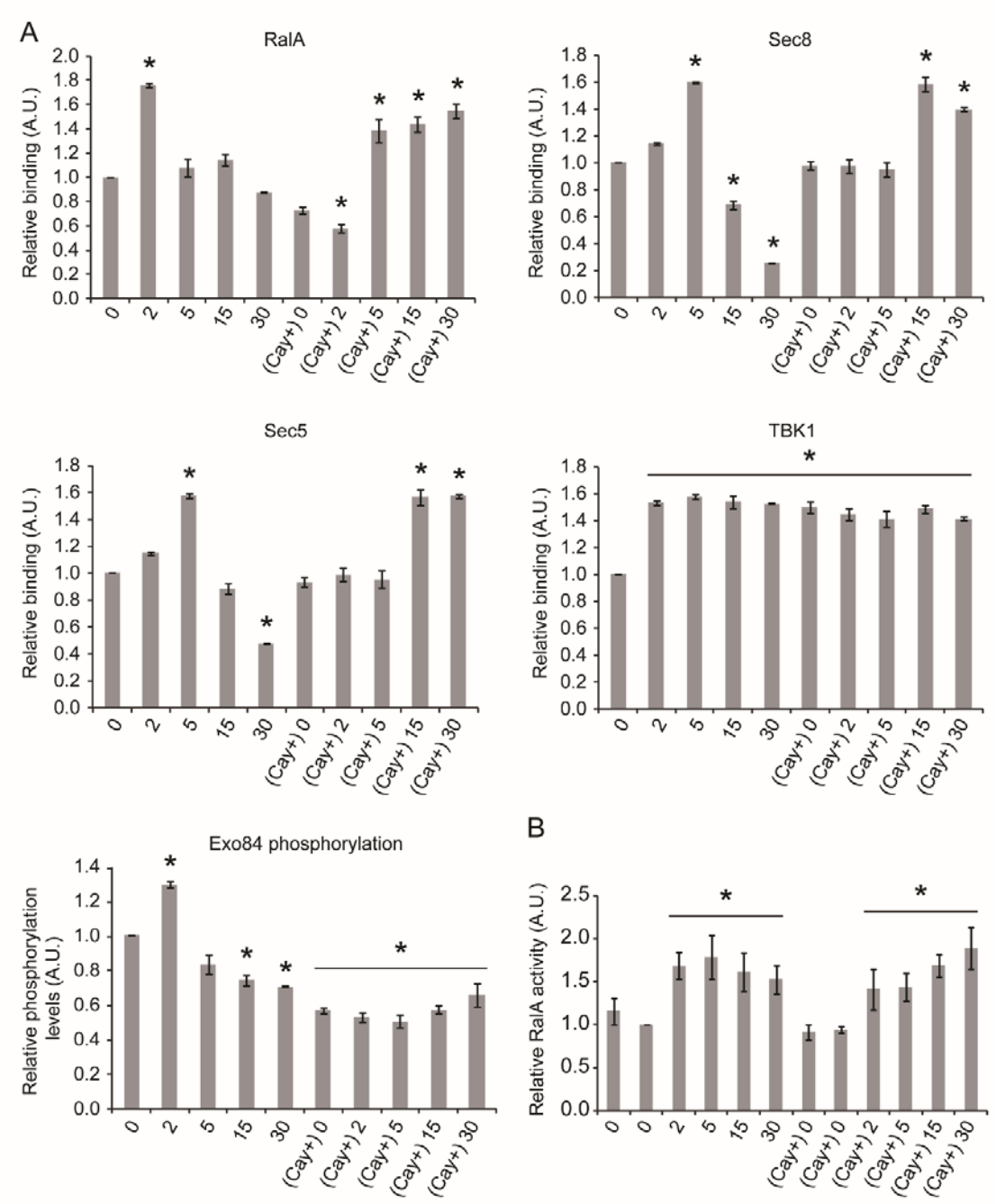

Figure 4.17 Quantification of disengagement of TBK1, Exo84, and RalA in insulin-stimulated GLUT4 trafficking.

(A) Quantification of the binding of RalA, Sec8, Sec5, and TBK1 with Exo84 as shown in Figure 4.16A. Quantification of levels of Exo84 phosphorylation is also shown. The levels were all normalized to the basal level at 0 minute. *$p < 0.05$ as compared to the basal level; $n = 3$. (B) Quantification of RalA activity as shown in Figure 4.16B. RalA activity (pull-down/total RalA) was normalized to the second lane. The normalized ratio is represented in arbitrary units. Data are shown as the mean ± SEM. *$p < 0.05$; $n = 3$.

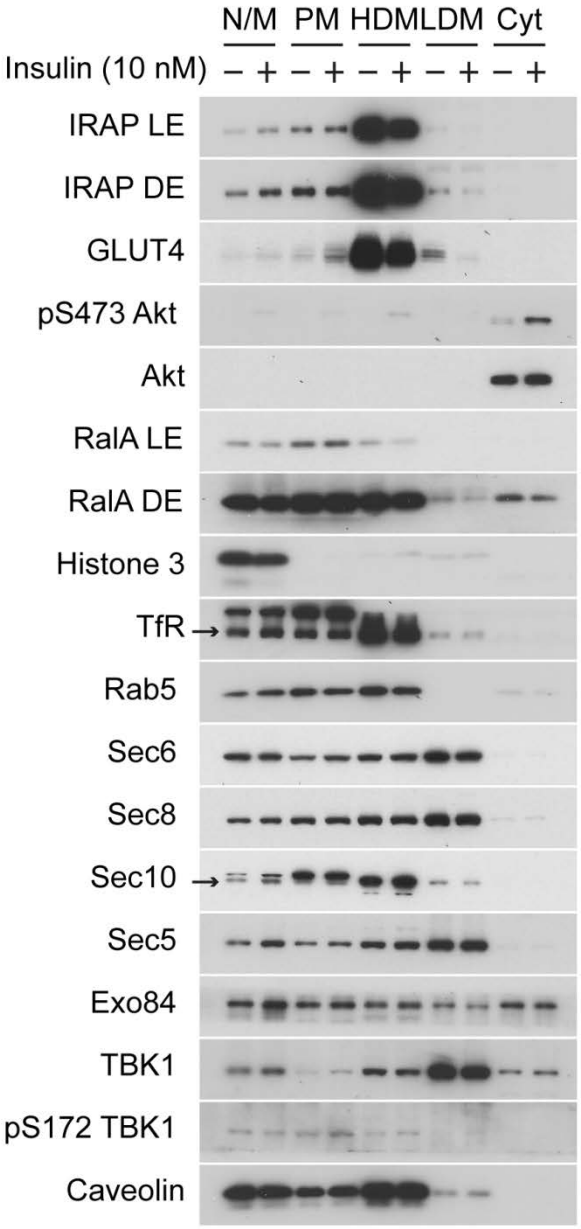

Figure 4.18 Endogenous TBK1, Exo84, and RalA translocate to the plasma membrane in response to insulin.
Subcellular fractionation was performed as described in materials and methods in 3T3-L1 adipocytes with or without insulin (10 nM) for 15 minutes. Indicated fractions were subjected to immunoblot analysis and probed using specific antibodies as indicated. N/M, nuclear and mitochondrial remnants; PM, plasma membrane; HDM, high-density microsomes; LDM, low-density microsomes; Cyt, cytosol. DE and LE stand for dark exposure and light exposure, respectively. Arrow indicates TfR and Sec10, respectively.

phosphorylation of TBK1 at its activating residue S172 was also increased in response to insulin in the plasma membrane fractions, although insulin does not produce an increase in kinase activity, as determined by an immune kinase assay (data not shown).

To further evaluate the kinetics of these insulin-induced changes in subcellular localization, we examined the time course (**Figure 4.19**). GLUT4, IRAP, TBK1, Sec8, Sec5, and RalA were rapidly translocated to the plasma membrane in response to insulin, detected within 5 minutes and reached maximal levels by 15 minutes after insulin stimulation following a decrease thereafter. Peak levels of IRAP and RalA translocation to the plasma membrane were detected at 30 min after insulin stimulation. Interestingly, amlexanox pretreatment increased the phosphorylation of TBK1 at S172 due to the relief of feedback inhibition, as previously reported (*25, 26*). In addition, amlexanox pretreatment significantly blocked translocation of GLUT4, IRAP, TBK1, Sec8, Sec5, and RalA in response to insulin, confirming that TBK1 activity is required for insulin-stimulated GLUT4 translocation.

Previous studies have shown that GLUT4 vesicles are targeted to discrete micro-domains on the plasma membrane, enriched in lipid rafts (*3*). To determine whether TBK1 is also enriched in lipid rafts in response to insulin, we performed sucrose density gradient fractionation of purified plasma membranes prepared from untreated and insulin-treated cells, followed by immunoblotting, as previously described (**Figure 4.20**) (*3*). Caveolin was exclusively detected in the lipid raft-enriched fraction 3 and 4 of the gradient and was unaffected by insulin treatment, as previously reported (*3*). In contrast, TfR was found exclusively at the bottom of the gradient in fractions 7-11, where it increased in response to insulin. GLUT4, IRAP, Sec5, Sec8, Exo84, and

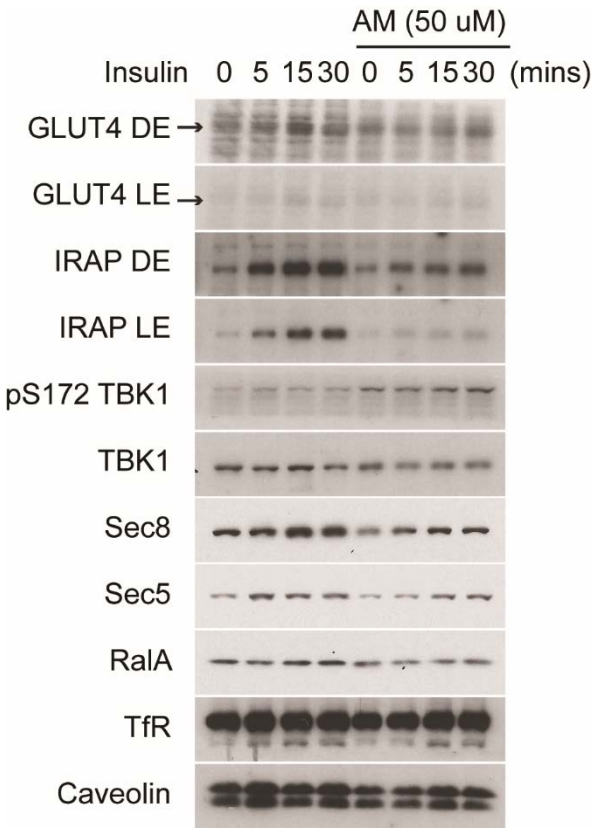

Figure 4.19 Inhibition of TBK1 blocks insulin-stimulated GLUT4 translocation.
After subcellular fractionation in 3T3-L1 adipocytes with or without insulin (10 nM) in the presence or absence of pretreatment with amlexanox (50 μM), only plasma membrane fractions were subjected to immunoblot analysis and probed using specific antibodies as indicated. DE and LE stand for dark exposure and light exposure, respectively. Arrow indicates GLUT4.

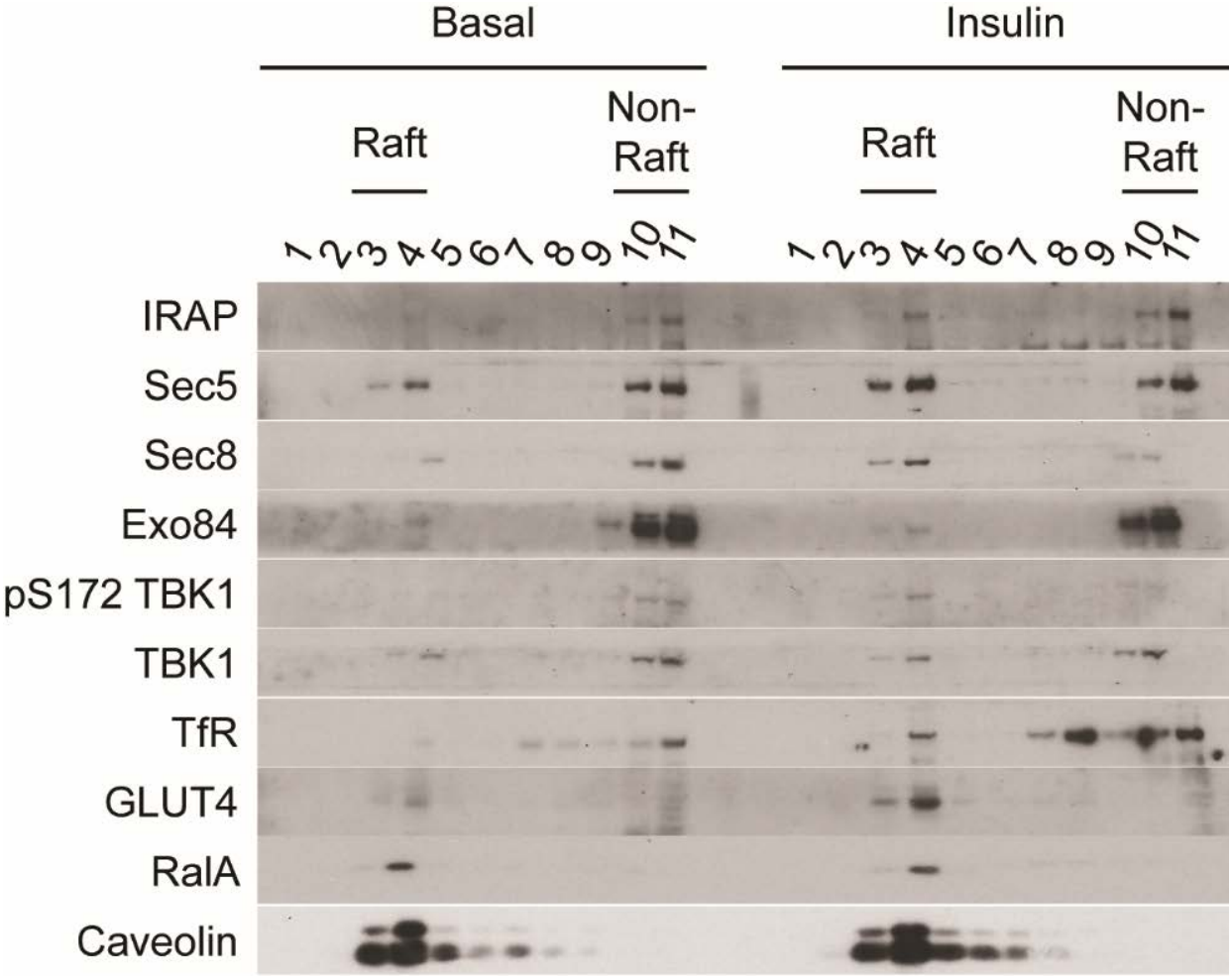

Figure 4.20 Insulin stimulates the translocation of TBK1, Exo84, and RalA to lipid rafts. After 15-minute insulin stimulation, 3T3-L1 adipocytes were harvested in a nondetergent buffer followed by sucrose density gradient fractionation as described in materials and methods. All fractions were subjected to immunoblot analysis with specific antibodies as indicated. Lipid raft (fractions 3 and 4) and nonraft fractions (fractions 10 and 11) are shown.

RalA were detected in both raft (fractions 3 and 4) and nonraft fractions (10 and 11) in untreated cells. However, these proteins were enriched only in the lipid raft fractions in cells treated with insulin. Interestingly, insulin-dependent changes in TBK1 localization were also observed, with a more pronounced effect on phosphorylation of TBK1 at S172.

To evaluate the importance of Exo84 phosphorylation in insulin-stimulated glucose transport, we examined the effects of HA-tagged Exo84 WT, 8A, or 8E mutant expression on the trafficking of GLUT4 in response to insulin by performing a GLUT4 translocation assay. 3T3-L1 adipocytes stably expressing a dual tagged-MYC-GLUT4-eGFP were treated with or without insulin (**Figure 4.21**). Overexpression of HA-tagged Exo84 WT, 8A, or 8E mutants was detected with anti-HA antibodies by immunohistochemistry (arrow head). In control cells and cells overexpressing WT Exo84, GLUT4 was detected in the intracellular compartment in the basal state, and translocated to the plasma membrane in response to insulin, along with the appearance of the exofacial MYC epitope signal. Expression of the phosphorylation-defective Exo84 8A mutant had no effect on the localization of GLUT4 in the basal state, but insulin-treated cells expressing the Exo84 8A mutant did not exhibit the exofacial MYC epitope signal. Expression of the phosphomimetic Exo84 8E mutant similarly blocked insulin-stimulated GLUT4 translocation. Quantitation of these data revealed that approximately 74% and 54% of the insulin-stimulated appearance of the MYC epitope signal on the plasma membrane was blocked by expression of phosphorylation-defective Exo84 8A and phosphomimetic Exo84 8E mutants, respectively (**Figure 4.22A**). In these experiments, the levels of overexpression of HA-tagged Exo84 WT, 8A, or 8E mutant were comparable to endogenous levels of Exo84, and did not affect Akt phosphorylation in the basal or insulin-stimulated states (**Figure 4.22B**). All together, these data

suggest that Exo84 phosphorylation by TBK1 terminates its interaction with RalA, and is thus important for insulin-stimulated glucose transport to control disengagement of RalA and disassociation of the exocyst.

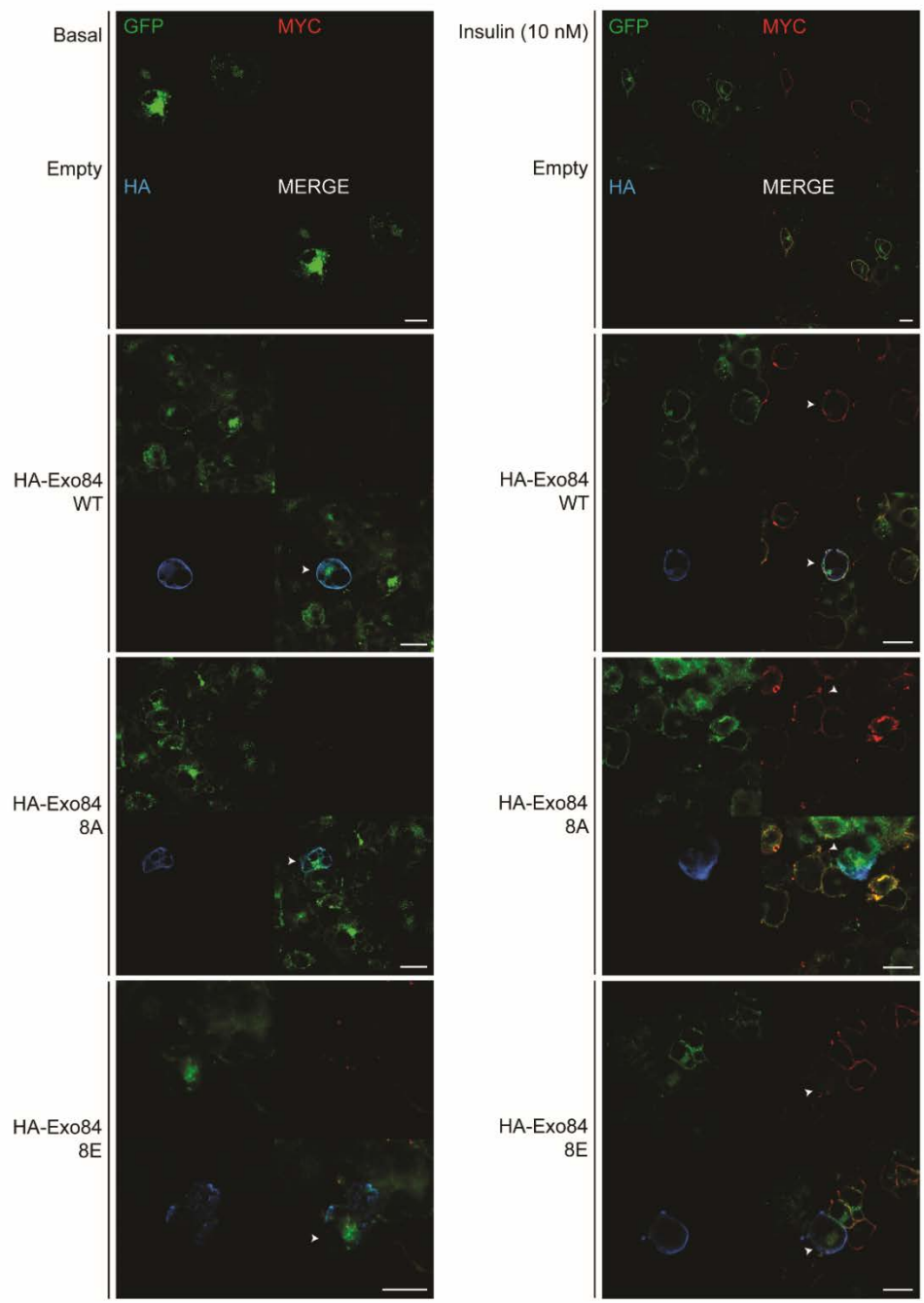

Figure 4.21 Engagement and disengagement of RalA and Exo84 mediated by TBK1 is required for insulin-stimulated GLUT4 translocation.
3T3-L1 adipocytes stably expressing MYC-GLUT4-eGFP were transfected with HA-tagged Exo84 WT, 8A, and 8E as indicated in the presence or absence of stimulation with 10 nM insulin for 15 minutes. Immunostaining for MYC (red) in nonpermeabilized cells indicates GLUT4 translocation to the plasma membrane. Immunostaining for HA (cyan) in permeablilized cells indicates Exo84 overexpression. GFP levels in cells indicate total GLUT4 expressed. A merge of GFP, HA, and MYC is shown. Arrow head indicates cells expressing Exo84. Bar, 20 μm.

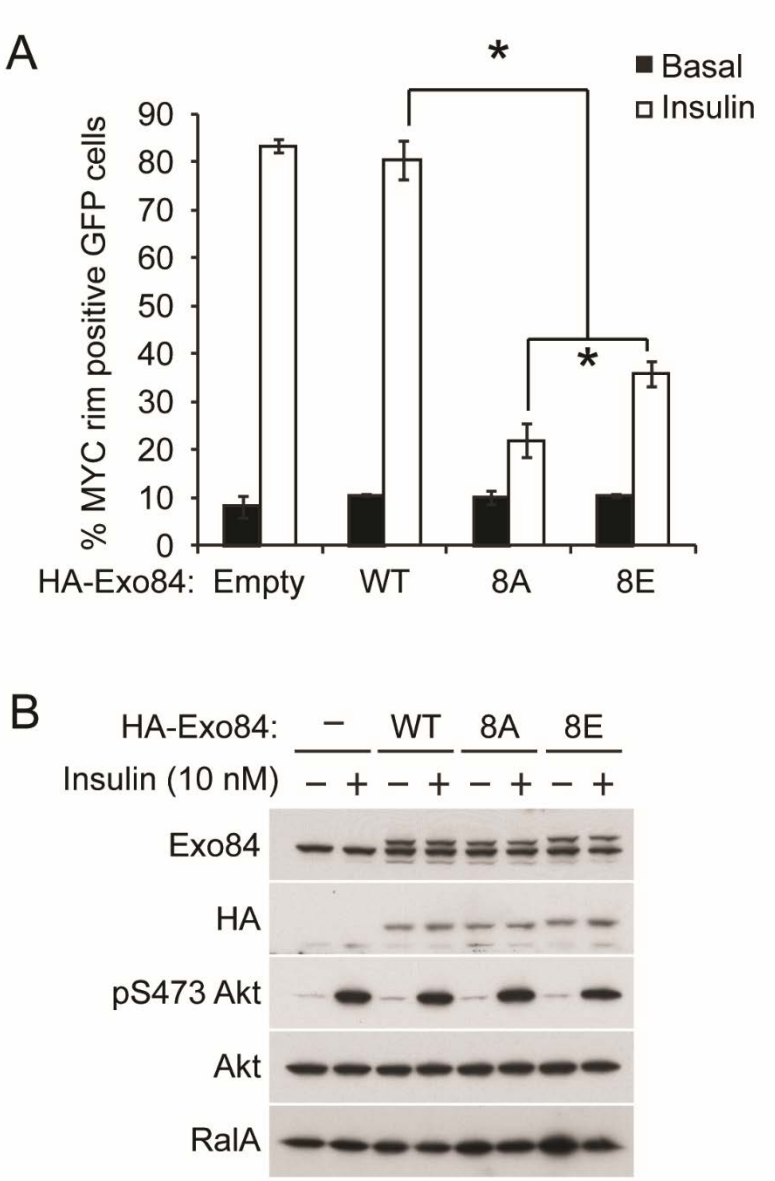

Figure 4.22 Exo84 phosphorylation mediated by TBK1 is required for insulin-stimulated GLUT4 translocation.

(A) Quantification of GLUT4 translocation as shown in Figure 4.21. Total number of cells that show MYC staining at the rim in GFP/HA-positive cells were counted in each condition. Percentage of cells that undergo GLUT4 translocation is graphed. Error bars are indicative of at least three independent experiments. Data are shown as the mean ± SEM. *$p < 0.05$; At least 100 cells per condition were counted for anti-MYC rim staining. (B) Ectopic overexpression of HA-tagged Exo84 WT, 8A, and 8E in 3T3-L1 adipocytes stably expressing MYC-GLUT4-eGFP as shown in Figure 4.21. Levels of indicated proteins in 3T3-L1 adipocytes were assessed by immunoblots.

Materials and Methods

Materials and reagents

Enhanced chemiluminescence (ECL) reagents were purchased from Thermo Scientific. EDTA-free protease inhibitor tablet was purchased from Roche Diagnostics. Amlexanox was purchased from Ontario Chemical Inc. The TBK1/IKKε inhibitor CAY10576 (Cay) was purchased from Cayman Chemical. BenchMark^{TM} Pre-stained protein ladder was purchased from Life Technologies. GST-tagged RalBP1 agarose beads were purchased from EMD Millipore.

Antibodies

Anti-Flag antibody was obtained from Sigma, and anti-HA, anti-MYC, anti-Exo84, and anti-Sec10 antibodies were obtained from Santa Cruz Biotechnology. Anti-TBK1, anti-phospho-TBK1 (Ser172), anti-AKT, anti-phospho-AKT (Ser473), anti-phospho-(Ser) 14-3-3 binding motif (R-X-Y/F-X-pS), anti-IRF3, anti-phospho-IRF (Ser396), anti-IRAP, anti-Histone 3, and Anti-Rab5 antibodies were purchased from Cell Signaling Technology. Anti-RalA, anti-Sec8, and anti-caveolin1 antibodies were purchased from BD Bioscience. Anti-GLUT4 was purchased from Alpha Diagnostics. Anti-Sec5 was purchased from Proteintech Group. Anti-TfR was purchased from Zymed Labs. Anti-Sec6 was purchased from Enzo Life Sciences.

Plasmids

The Flag-tagged human TBK1 WT and TBK1 K38A cDNAs were kindly provided by Dr. Tom Maniatis (Columbia University). The human TBK1 WT and K38A cDNAs were subcloned into pLVX-AcGFP1-N1 (Clontech) to generate stable cell lines. The rat Exo84 cDNA was kindly provided by Dr. Charles Yeaman (University of Iowa) and subcloned into pKH3 vector. Flag-tagged RalA constructs (WT, G23V, S28N, and F39L) have been previously described (*4*).

Cell culture and transfection

3T3-L1 fibroblasts (American Type Culture Collection) were cultured and differentiated as described previously (*27*). Cells were routinely used within 10 days after completion of the differentiation process; only cultures in which > 90% of cells displayed adipocyte morphology were used. 3T3-L1 adipocytes were routinely transfected with plasmids by electroporation as described previously (*7*). Electroporation into mature adipocytes was done within 1-4 days post-differentiation at 160 kV, 950 uF. 3T3-L1 preadipocytes stably expressing MYC-GLUT4-eGFP were maintained and differentiated as described previously (*4, 28*). COS-1 or HEK293T cells were cultured in DMEM containing 10% fetal bovine serum (FBS). These cells were cultured to 90% confluence and transfection was carried out using Opti-MEM media and Lipofectamine 2000 (Life Technologies) according to manufacturer's protocol. For overexpression experiments, cells were collected and lysed 18-36 hours after transfection. Lentiviral constructs expressing TBK1 WT or its K38A mutant in pLVX-AcGFP1-N1 were transfected in HEK293T cells with ViraPower^{TM} lentiviral packaging mix (Life Technologies) using Lipofectamine 2000. Conditioned media containing the viral particles were collected 24 and 48 hours post-transfection, filtered using a 0.45 um filter (Millipore) and concentrated by the University of Michigan Vector

Core. Infection was carried out by adding viral particles onto HEK293T cells in the presence of 8 ug/ml polybrene and spinning plates at 1,000 xg for 30 minutes at room temperature. The media was replaced with fresh media after 24 hours and incubated for 3 days, then stable cells were selected using 2 ug/ml puromycin. Before transfection, stable cells were maintained in DMEM supplemented with 10% FBS and 0.5 ug/ml puromycin. 3T3-L1 adipocytes were starved in reduced serum (0.5% FBS) medium for 12 hours. After serum starvation, cells were pretreated for 1 hour with amlexanox or Cay at the given concentrations and stimulated with 10 nM insulin for indicated time.

GLUT4 translocation assay

GLUT4 translocation was measured as described previously (*3*). Briefly, differentiated 3T3-L1 adipocytes stably expressing MYC-GLUT4-eGFP were used to overexpress HA-tagged Exo84 proteins. One day after electroporation, cells were stimulated with or without 10 nM insulin for 15 minutes and then washed once with ice-cold PBS. Cells were fixed for 10 minutes in 4% paraformaldehyde (PFA; Electron Microscopy Sciences), neutralized with 100 mM glycine-PBS, followed by blocking in 2% bovine serum albumin (BSA) in PBS for 1 hour at room temperature. Monoclonal anti-MYC and polyclonal anti-HA antibodies were used at 1:300 dilution. GLUT4 translocation to the plasma membrane was measured by staining with MYC antibodies in nonpermeabilized cells. Overexpressed proteins were measured by staining with HA antibodies in permeabilized cells with 0.5% Triton X-100 for 4 minutes. Percentage of cells with insulin-stimulated GLUT4 translocation was calculated as the percentage of cells with MYC staining in the GFP/HA-positive pool. Alexa-Fluor 568 conjugated goat anti-mouse and Alexa-Fluor 647

conjugated goat anti-rabbit secondary antibodies (Life Technologies) were used at 1:500 dilution. Confocal images were obtained using an inverted Olympus confocal microscope operated with the Fluoview300 program (Olympus America Inc.).

Immunoprecipitation and immunoblotting

For immunoprecipitation, cells were washed once with ice-cold PBS before lysis with IP buffer (100 mM Tris-HCL (pH 7.5), 130 mM NaCl, 1% Triton X-100, 1 mM EDTA, 1 mM Na_3VO_4, 10 mM NaF, 5 mM $MgCl_2$) supplemented with an EDTA-free protease inhibitor tablet (Roche). Lysates were cleared by centrifugation at 13,000 xg for 15 minutes and then incubated with 2 ug of antibody for 1 mg of protein for 4 hours to overnight at 4 °C. Immunoprecipitaes were adsorbed on Protein A/G plus agarose (Santa Cruz Biotechnology) for 1.5-2 hours, washed three times in lysis buffer, and eluted in 1.5X sodium dodecyl sulfate (SDS) sample buffer (240 mM Tris-HCL (pH6.8), 40% glycerol, 8% SDS, 0.04% bromophenol blue, and 5% beta-mercaptoethanol) by boiling the samples for 5 minutes at 95 °C. For regular cell lysis, cell were washed once with ice-cold PBS before lysis with SDS buffer (100 mM Tris-HCL (pH 8.0), 130 mM NaCl, 1% Nonidet P-40 (NP-40), 0.2% Sodium deoxycholate, 0.1% SDS, 10 mM Sodium Pyrophosphate, 1 mM Na_3VO_4, 10 mM NaF) supplemented with an EDTA-free protease inhibitor tablet (Roche), followed by sonication. The crude lysates were centrifuged at 13,000 xg for 15 minutes and protein concentration was determined using Protein Assay Reagent (Bio-Rad). Samples were diluted in 4X SDS sample buffer and boiled for 5 minutes at 95 °C. Proteins were resolved by SDS-polyacrylamide gel electrophoresis (PAGE; Life Technologies) and transferred to nitrocellulose membranes (Bio-Rad). Individual proteins were detected with specific

antibodies and visualized on X-ray film using horseradish peroxidase-conjugated secondary antibodies (Bio-Rad) and Western Lightning Enhanced Chemiluminescence (Perkin Elmer Life Sciences). Where necessary, blots were incubated in stripping buffer (50 mM Tris-HCL (pH 6.8), 150 mM NaCl, 110 mM beta-mercaptoethanol, and 2% SDS) and re-probed with the specific antibodies.

In vitro *kinase assay*

In vitro kinase assays were performed in kinase buffer containing 25 mM Tris (pH 7.5), 10 mM MgCl2, 1 mM dithiothreitol (DTT), and 50 μM ATP for 30 minutes at 30 °C in the presence of 0.5 μCi γ-[^{32}P]-ATP and 1 μg myelin basic protein (MBP) per sample as a substrate. The kinase reaction was stopped by adding 4X SDS sample buffer and boiling for 5 minutes at 95 °C. Supernatants were resolved by SDS-PAGE, transferred to nitrocellulose, and analyzed by autoradiography.

TBK1 immune complex kinase assay

Cells were washed once with ice-cold PBS and lysed with lysis buffer containing 50 mM Tris (pH 7.5), 150 mM NaCl, 2 mM EDTA, 5 mM NaF, 25 mM β-glycerophosphate, 1 mM sodium orthovanadate, 10% glycerol, 1% Triton X-100, 1 mM DTT and 1 mM PMSF supplemented with an EDTA-free protease inhibitor tablet (Roche). Lysates were cleared by centrifugation at 13,000 xg for 15 minutes. Each 1 mg of lysate was subjected to IP using 2 ug of monoclonal MYC, mouse IgG, rabbit IgG, or TBK1 rabbit polyclonal antibodies for 3 hours at 4 °C. The

immunocomplexes were harvested by incubation with Protein A/G plus agarose (Santa Cruz Biotechnology) for 1 hour at 4 °C. Immunoprecipitates were washed once with lysis buffer and three times with wash buffer containing 20 mM 4-(2-hydroxyethyl)-1-piperazineethanesulfonic acid (HEPES) (pH 7.4), 50 mM NaCl, 20 mM β-glycerophosphate, 1 mM Na_3VO_4, 5 mM NaF, 10 mM $MgCl_2$ and 1 mM DTT. I*n vitro* kinase assay was performed using the immunoprecipitated kinases as described above. Relative amounts of MBP phosphorylation were detected by autoradiography.

Protein purification and pull-down experiment

GST fusion proteins were expressed in Rosetta™ (DE3)pLysS competent cells (Novagen). GST proteins were induced 50-100 mM Isopropyl β-D-1-thiogalactopyranoside (IPTG) for 16 hours at 25 °C. Cells were pelleted by centrifugation at 4,000 xg for 10 minutes. Cells were lysed with lysis buffer containing 50 mM Tris (pH 7.5), 0.5 mM EDTA, and 0.3 M NaCl supplemented with an EDTA-free protease inhibitor tablet (Roche). Lysates were mixed with 1:10 dilution of 10 mg/ml lysozyme and 4 mM DTT and then incubated on ice for 15 minutes. 0.2% NP-40 were added to lysates and lysis was further performed by freeze-thaw cycle. To get soluble proteins, lysates were mixed with a buffer containing 1.5 M NaCl, 12 mM $MgCl_2$, and 1:1000 dilution of 10 mg/ml DNase I (Roche) supplemented with an EDTA-free protease inhibitor tablet (Roche). Lysates were passed through syringe with 18 gauge needle (BD Bioscience) every 10-15 minutes for 2 hours at 4 °C. Soluble proteins were collected by centrifugation at 15,000 xg for 20 minutes at 4 °C. Supernatants were incubated with glutathione sepharose beads (GE Healthcare Life Sciences) and washed four times with PBS (pH 8.0). Protein immobilized on beads were stored

at -80 °C in PBS containing 10% glycerol and 10 mM DTT. Sometimes, proteins were eluted from glutathione beads by washing the beads with 10 mM glutathione in PBS (pH 8.0). Purified GST-tagged Exo84 RBD proteins were cleaved with thrombin (GE Healthcare Life Sciences) according to manufacturer's protocol. For pull-down experiment, cells were washed once with ice-cold PBS and then lysed in pulldown buffer (100 mM Tris, pH 7.5, 130 mM NaCl, 1% NP-40, 10% glycerol, 1 mM Na_3VO_4, 10 mM NaF, 5 mM $MgCl_2$, 1 mM EDTA, 1 mM DTT) supplemented with a protease inhibitor tablet (Roche). Lysates were cleared by centrifuging at 13,000 xg for 15 minutes and then were incubated with GST fusion proteins bound to glutathione beads (GE Healthcare Life Sciences) for 40 minutes at 4 °C. Beads were washed three times with 1 mL of pull-down lysis buffer and then resuspended in 1.5X SDS sample buffer.

Nucleotide loading of GTPases

GST alone or GST-RalA fusion proteins bound to glutathione beads were incubated for 30 minutes at room temperature in loading buffer containing 20 mM Tris (pH 7.5), 1 mM DTT, and 50 mM NaCl, 5% glycerol, 0.1% NP-40 with 2 mM EDTA supplemented with a protease inhibitor tablet. GST fusion proteins were then loaded with nucleotide by incubating in loading buffer supplemented with 2 mM GDP or 1 mM GTPγS for 1 hour at room temperature. To stop loading, 10 mM $MgCl_2$ was added for 10 minutes at room temperature. Loaded GST or GST-RalA beads were then added to COS-1 cells that were lysed in buffer containing 25 mM Tris (pH 7.5), 137 mM NaCl, 10% glycerol, 1% NP-40, 5 mM $MgCl_2$, 10 mM NaF, and 1 mM DTT supplemented with EDTA-free protease inhibitor tablets. The reaction was incubated for 1 hour at 4°C, and then beads were washed three times in wash buffer containing 50 mM Tris (pH 7.5),

80 mM NaCl, 60 mM $MgCl_2$, 1% NP-40, and 1 mM DTT and once in rinse buffer containing 50 mM Tris (pH 7.5), 80 mM NaCl, 60 mM $MgCl_2$, 10 mM NaF, and 1 mM DTT supplemented with 10 μM GDP, 10 μM GTPγS, and complete EDTA-free protease inhibitor tablets. The pull downs were solubilized in 1.5X SDS sample buffer and subjected to SDS-PAGE, and immunoblotting was performed using the indicated antibodies.

Mass spectrometry

In-gel digestion followed by LC-MS/MS analysis was carried out by the mass spectrometry-based proteomics resource in the Department of Pathology, University of Michigan. Briefly, tryptic peptides were resolved on a nano-C18 reverse phase column and sprayed directly onto Orbitrap mass spectrometer (LTQ-Orbitrap XL, Thermofisher). Orbitrap was operated in a data-dependent mode to acquire one full MS spectrum (resolution of 30,000@400 m/z) followed by MS/MS spectra on 6 most intense ions (top 6). Proteins were identified by searching data against human and rat protein database (Uniprot, rel. 2010-9) using X!Tandem/TPP software suite. Oxidation of Met, carbamidomethylation of Cys and phosphorylation of Ser, Thr, and Tyr were considered as potential modifications (*29*).

Subcellular fractionation

3T3-L1 adipocytes that were 10 days postdifferentiation were stimulated as indicated, washed twice in ice-cold PBS (pH 7.5) and then were lysed in HES buffer (20mM HEPES (pH 7.5), 1 mM EDTA, and 250 mM sucrose supplemented with complete EDTA-free protease inhibitor

tablets) on ice by scraping with cell lifters (Corning Life Sciences). Samples were transferred and homogenized in a glass potter homogenizer (Wheaton) for 20 strokes on ice. Fractionation was performed in a NVT90 rotor (Beckman Coulter) by differential centrifugation using ultracentrifugation with established protocols as previously described (*4*, *24*). Equal amounts of proteins, as determined with Protein Assay Reagent (Bio-Rad), were subjected to SDS-PAGE, followed by immunoblotting analysis using various antibodies as indicated. Plasma membrane fractions were further fractionated by sucrose gradient centrifugation as described below.

Sucrose gradient centrifugation

3T3-L1 adipocytes were treated and homogenized same as where subcellular fractionation was performed. After homogenization, cells were centrifuged at 3,000 xg for 3 minutes to get the PNS and the supernatant was centrifuged at 15,700 rpm for 19 minutes to get a total plasma membrane fraction. This fraction was further fractionated in a sucrose gradient as previously described (*3*). Briefly, the total plasma membrane fraction was either directly subjected to immunoblotting analysis using various antibodies as indicated or solubilized by resuspending the pellet in MBS buffer (20 mM 2-(*N*-morpholino)ethanesulfonic acid (MES; pH 6.5) and 150 mM NaCl) with 0.2% Triton-X 100. Samples were homogenized in a glass potter homogenizer (Wheaton) for 10 strokes on ice. 0.4 ml of samples were mixed with 0.4 ml of 80% sucrose (wt/vol), and overlaid with 3.5 ml of 30%, 1 ml of 5% sucrose. The gradient was centrifuged at 35,000 rpm for 19 hours in a SW55 Ti rotor (Beckman Coulter), and 440 ul fractions were collected from the top of each gradient. Each fraction was run on SDS-PAGE, followed by immunoblotting analysis using various antibodies as indicated.

Statistical analyses

Averaged values are presented as the mean ± standard error of the mean (s.e.m). When comparing two groups, we performed Student's *t*-test to determine statistical significance. When more than two groups and two factors were investigated, we first performed a two-way analysis of variance (ANOVA) to establish that not all groups were equal. After a statistically significant ANOVA result, we performed between-group comparisons using the Tukey *post hoc* analysis for comparisons of all means and Sidak for comparisons of within factor main effect means. ANOVA and Tukey/Sidak tests were performed using GraphPad Prism version 6.

References

1. S. H. Chiang *et al.*, Insulin-stimulated GLUT4 translocation requires the CAP-dependent activation of TC10. *Nature* **410**, 944 (Apr 19, 2001).
2. M. Inoue, L. Chang, J. Hwang, S. H. Chiang, A. R. Saltiel, The exocyst complex is required for targeting of Glut4 to the plasma membrane by insulin. *Nature* **422**, 629 (Apr 10, 2003).
3. M. Inoue, S. H. Chiang, L. Chang, X. W. Chen, A. R. Saltiel, Compartmentalization of the exocyst complex in lipid rafts controls Glut4 vesicle tethering. *Mol Biol Cell* **17**, 2303 (May, 2006).
4. X. W. Chen, D. Leto, S. H. Chiang, Q. Wang, A. R. Saltiel, Activation of RalA is required for insulin-stimulated Glut4 trafficking to the plasma membrane via the exocyst and the motor protein Myo1c. *Dev Cell* **13**, 391 (Sep, 2007).
5. X. W. Chen *et al.*, A Ral GAP complex links PI 3-kinase/Akt signaling to RalA activation in insulin action. *Molecular biology of the cell* **22**, 141 (Jan 1, 2011).
6. C. P. Miinea *et al.*, AS160, the Akt substrate regulating GLUT4 translocation, has a functional Rab GTPase-activating protein domain. *Biochem J* **391**, 87 (Oct 1, 2005).
7. S. Karunanithi *et al.*, A Rab10:RalA G protein cascade regulates insulin-stimulated glucose uptake in adipocytes. *Molecular biology of the cell* **25**, 3059 (Oct 1, 2014).
8. H. Sano *et al.*, Rab10, a target of the AS160 Rab GAP, is required for insulin-stimulated translocation of GLUT4 to the adipocyte plasma membrane. *Cell Metab* **5**, 293 (Apr, 2007).
9. H. Sano, W. G. Roach, G. R. Peck, M. Fukuda, G. E. Lienhard, Rab10 in insulin-stimulated GLUT4 translocation. *Biochem J* **411**, 89 (Apr 1, 2008).
10. X. W. Chen *et al.*, Exocyst function is regulated by effector phosphorylation. *Nature cell biology* **13**, 580 (May, 2011).
11. K. Matsubara, T. Hinoi, S. Koyama, A. Kikuchi, The post-translational modifications of Ral and Rac1 are important for the action of Ral-binding protein 1, a putative effector protein of Ral. *FEBS letters* **410**, 169 (Jun 30, 1997).
12. Y. Chien *et al.*, RalB GTPase-mediated activation of the IkappaB family kinase TBK1 couples innate immune signaling to tumor cell survival. *Cell* **127**, 157 (Oct 6, 2006).
13. J. Reinstein, I. Schlichting, M. Frech, R. S. Goody, A. Wittinghofer, p21 with a phenylalanine 28----leucine mutation reacts normally with the GTPase activating protein GAP but nevertheless has transforming properties. *The Journal of biological chemistry* **266**, 17700 (Sep 15, 1991).
14. K. H. Lim *et al.*, Activation of RalA is critical for Ras-induced tumorigenesis of human cells. *Cancer cell* **7**, 533 (Jun, 2005).
15. K. Clark, L. Plater, M. Peggie, P. Cohen, Use of the pharmacological inhibitor BX795 to study the regulation and physiological roles of TBK1 and IkappaB kinase epsilon: a distinct upstream kinase mediates Ser-172 phosphorylation and activation. *The Journal of biological chemistry* **284**, 14136 (May 22, 2009).
16. K. A. Fitzgerald *et al.*, IKKepsilon and TBK1 are essential components of the IRF3 signaling pathway. *Nature immunology* **4**, 491 (May, 2003).
17. S. Sharma *et al.*, Triggering the interferon antiviral response through an IKK-related pathway. *Science* **300**, 1148 (May 16, 2003).

18. H. Hemmi *et al.*, The roles of two IkappaB kinase-related kinases in lipopolysaccharide and double stranded RNA signaling and viral infection. *The Journal of experimental medicine* **199**, 1641 (Jun 21, 2004).
19. A. K. Miyahira, A. Shahangian, S. Hwang, R. Sun, G. Cheng, TANK-binding kinase-1 plays an important role during in vitro and in vivo type I IFN responses to DNA virus infections. *Journal of immunology* **182**, 2248 (Feb 15, 2009).
20. S. M. McWhirter *et al.*, IFN-regulatory factor 3-dependent gene expression is defective in Tbk1-deficient mouse embryonic fibroblasts. *Proceedings of the National Academy of Sciences of the United States of America* **101**, 233 (Jan 6, 2004).
21. D. Soulat *et al.*, The DEAD-box helicase DDX3X is a critical component of the TANK-binding kinase 1-dependent innate immune response. *The EMBO journal* **27**, 2135 (Aug 6, 2008).
22. J. E. Hutti *et al.*, Development of a high-throughput assay for identifying inhibitors of TBK1 and IKKepsilon. *PloS one* **7**, e41494 (2012).
23. J. Liu, W. Guo, The exocyst complex in exocytosis and cell migration. *Protoplasma* **249**, 587 (Jul, 2012).
24. M. Hashiramoto, D. E. James, Characterization of insulin-responsive GLUT4 storage vesicles isolated from 3T3-L1 adipocytes. *Molecular and cellular biology* **20**, 416 (Jan, 2000).
25. S. M. Reilly *et al.*, An inhibitor of the protein kinases TBK1 and IKK-varepsilon improves obesity-related metabolic dysfunctions in mice. *Nature medicine* **19**, 313 (Mar, 2013).
26. J. Mowers *et al.*, Inflammation produces catecholamine resistance in obesity via activation of PDE3B by the protein kinases IKKepsilon and TBK1. *eLife* **2**, e01119 (2013).
27. J. Liu, S. M. DeYoung, M. Zhang, A. Cheng, A. R. Saltiel, Changes in integrin expression during adipocyte differentiation. *Cell metabolism* **2**, 165 (Sep, 2005).
28. I. J. Lodhi *et al.*, Gapex-5, a Rab31 guanine nucleotide exchange factor that regulates Glut4 trafficking in adipocytes. *Cell Metab* **5**, 59 (Jan, 2007).
29. G. N. Maine *et al.*, A bimolecular affinity purification method under denaturing conditions for rapid isolation of a ubiquitinated protein for mass spectrometry analysis. *Nature protocols* **5**, 1447 (Aug, 2010).

Chapter 5

Conclusions and future directions

Although there has been significant progress in the identification of insulin signaling pathways leading to GLUT4 translocation and glucose uptake (*1*), our understanding of the mechanisms by which these upstream signaling pathways converge on intracellular GLUT4-storage vesicles for translocation to the plasma membrane remains incomplete. Insulin increases the activity of numerous protein kinases in adipocytes, and some of these are required for the actions of insulin on glucose transport (*2, 3*). We report here another protein kinase that appears to play a critical role in this process, TBK1, which is required for insulin-stimulated glucose transport and GLUT4 translocation to and insertion in the plasma membrane.

As a non-canonical member of the IKK family of kinases, TBK1 was initially identified through its sequence homology with IKKα and IKKβ, key regulators of the NFκB transcription pathway (*4, 5*). However, numerous studies have shown that NFκB is not activated in mouse embryonic fibroblasts from IKKα and IKKβ double knockout mice, while TBK1 is dispensable, suggesting that TBK1 does not play an important role in the activation of the NFκB pathway (*6-13*). TBK1 has also been implicated in regulation of the expression of type I IFNs through phosphorylation of IRFs (*7-10, 12*). Furthermore, recent reports have highlighted counter-inflammatory roles for TBK1, based on its effects as a negative regulator of the canonical IKKs, in the process

preventing the overproduction of inflammatory mediators (*14, 15*). In this regard, both IKKε and TBK1 are induced as a consequence of chronic, low-grade inflammation that is associated with obesity (*16, 17*). Because both kinases contain NFκB regulatory sites in their promoter regions, it is thought that they are induced upon NFκB activation, and in turn play a part in a counter-inflammatory program that attenuates the extent to which inflammatory signals are effective (*17, 18*). At the same time, TBK1 can promote energy storage by co-opting insulin targets to repress lipolysis and thermogenesis while increasing lipogenesis (*15, 19-21*). Other alternative roles for TBK1 have been described outside inflammatory signaling pathways, including interaction with Rab8b to direct maturation of autophagosomes into lytic bactericidal organelles (*22*); phosphorylation of the autophagic adaptor protein, optineurin, allowing specific recruitment of cargo molecules for the autophagic clearance of pathogens (*23*); and regulation of recycling endosome distribution via phosphorylation of Rab11 effector proteins (*24, 25*).

Data presented here suggest a new, specific substrate for TBK1 that also indicates a novel anabolic role for the kinase in insulin-stimulated glucose transport and GLUT4 translocation. Experiments with inhibitors or siRNA knockdown indicate that although TBK1 is a known upstream kinase for Akt (*19, 20*), its effect on glucose uptake is not regulated solely through Akt. Here we present evidence that direct phosphorylation of the exocyst subunit Exo84 by TBK1 disassociates the effector protein from RalA and the rest of the exocyst subunits, in the process ensuring that GLUT4 trafficking is not arrested at the plasma membrane.

The regulation of GLUT4 by insulin involves a complicated process of regulated recycling by coordinating the sorting, trafficking, tethering, docking and fusion of exocytotic vesicles (*1*). In

untreated cells, GLUT4 resides in specialized storage vesicles in intracellular compartments, which are transported along cytoskeletal tracks to the plasma membrane. While GLUT4 vesicle fusion is catalyzed by SNARE proteins present on the vesicle and target membranes, efficient control of the process requires that the vesicle is first targeted to discrete microdomains in the plasma membrane that are enriched in SNARE proteins (*26*). This targeting step is carried out by tethering to the exocyst complex (*27, 28*). Both the assembly and recognition of the exocyst are required for efficient GLUT4 vesicle delivery to the plasma membrane preceding SNARE-mediated vesicle fusion. However, the size and architecture of the exocyst also indicate that once bound to the vesicle, it may serve as a barrier for fusion, and thus a disengagement step is needed (*29, 30*). While little is known about the mechanisms controlling the disengagement of the exocyst from the vesicle, previous studies indicate that effector phosphorylation may represent a critical step (*30*).

Data presented here lead us to propose that after activation of RalA by insulin, the G protein binds to both Sec5 and Exo84, thus directing GLUT4 vesicles to regions on the plasma membrane where fusion machineries are enriched. Although the requirement for two RalA effector proteins remains unexplained, we speculate that RalA undergoes sequential interactions with these proteins during vesicle trafficking, in which Exo84 first escorts the vesicle to the plasma membrane, where the remainder of the exocyst, including Sec5, is partially assembled (*31*). Because the Ral GAP is reserved for activation of the G protein, as it is persistently inhibited by insulin-dependent phosphorylation via Akt (*32*), we further propose that effector switching from Exo84 to Sec5 requires a specific release of RalA from Exo84, accomplished by phosphorylation of Exo84 by TBK1, which may be relocalized to the plasma membrane with the

exocyst complex in response to insulin. Upon phosphorylation, Exo84 is further disrupted from the rest of the exocyst subunits, enabling active recycling of the complex to continuously provide tethering machineries for next round of exocytosis. While there is no evidence that insulin acutely increases the intrinsic kinase activity of TBK1, we speculate that the unification of the exocyst complex brings it into proximity with its substrate to control GLUT4 vesicle disengagement from the exocyst (**Figure 5.1**). Thus, these data suggest that the exocyst is more than just a tethering complex for the GLUT4 vesicle, but also a gatekeeper controlling access of the vesicle to control fusion at the plasma membrane.

While it is somewhat unexpected that a protein kinase generally associated with an inflammatory response is utilized for an anabolic program such as insulin-stimulated glucose uptake, the idea is not unprecedented. Previous studies indicate that TBK1 induction in obesity is associated with continuous energy storage (*16, 21*). Along with IKKε, the kinase has been shown to phosphorylate and activate PDE3B, leading to decreased lipolysis and thermogenesis (*15*). Moreover, cells in which TBK1 has been inhibited or knocked out are hypersensitive to inflammatory signals (*14, 21, 33*), suggesting that the kinase may also play a feedback role in countering catabolic stimuli. Future studies will explore the physiological role of the kinase in the regulation of energy homeostasis.

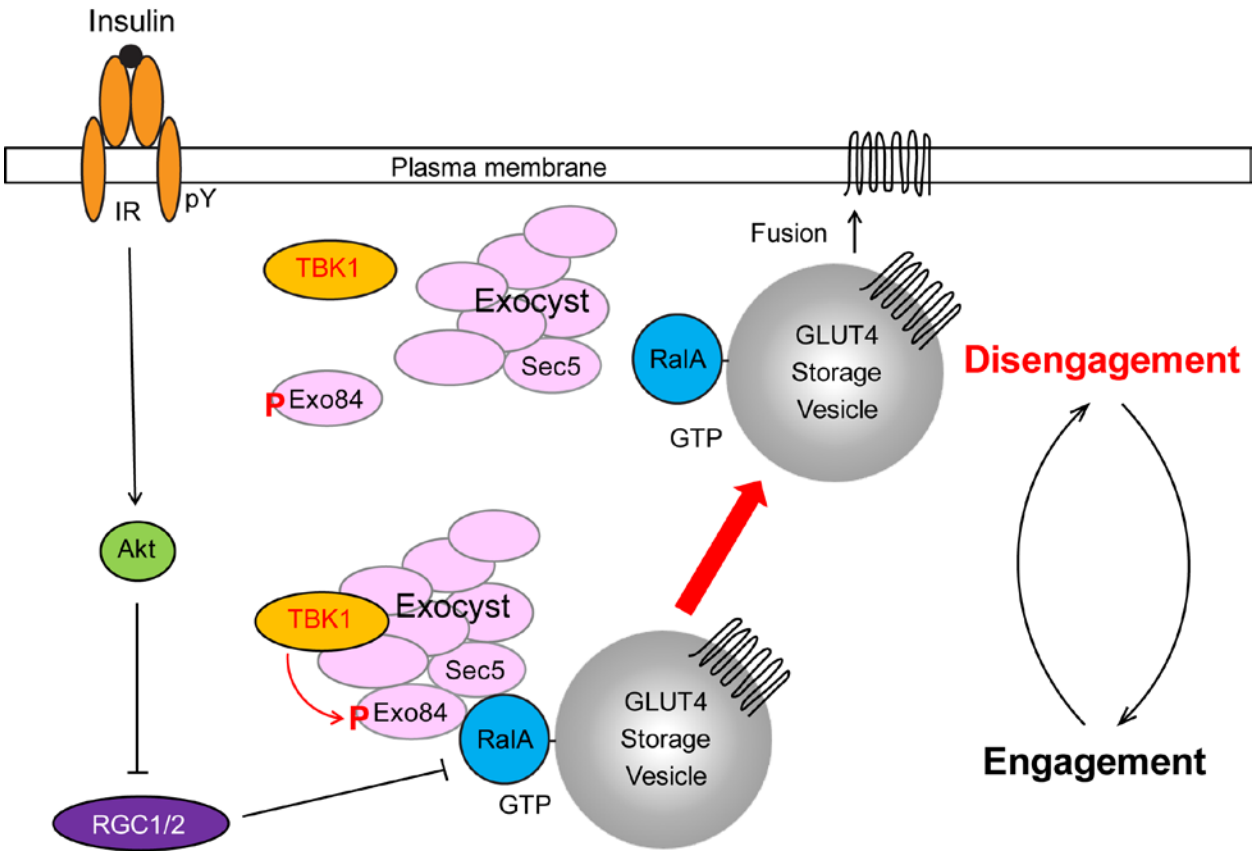

Figure 5.1 Proposed model for the role of TBK1-mediated Exo84 phosphorylation in insulin-stimulated GLUT4 translocation.
Insulin activates RalA as the RalGAP complex RGC1/2 is persistently turned off by insulin-dependent phosphorylation via Akt (*32*). After activation of RalA by insulin, the G protein binds to both Sec5 and Exo84, thus engaging and directing Glut4 vesicles to sites on the plasma membrane where fusion machineries are enriched (*34*). In addition, direct phosphorylation of the exocyst subunit Exo84 by TBK1 disengages the effector protein from RalA and the rest of the exocyst subunits, in the process ensuring that Glut4 trafficking is not arrested at the plasma membrane.

References

1. D. Leto, A. R. Saltiel, Regulation of glucose transport by insulin: traffic control of GLUT4. *Nature reviews. Molecular cell biology* **13**, 383 (Jun, 2012).
2. R. T. Watson, M. Kanzaki, J. E. Pessin, Regulated membrane trafficking of the insulin-responsive glucose transporter 4 in adipocytes. *Endocrine reviews* **25**, 177 (Apr, 2004).
3. L. Chang, S. H. Chiang, A. R. Saltiel, Insulin signaling and the regulation of glucose transport. *Mol Med* **10**, 65 (Jul-Dec, 2004).
4. J. L. Pomerantz, D. Baltimore, NF-kappaB activation by a signaling complex containing TRAF2, TANK and TBK1, a novel IKK-related kinase. *The EMBO journal* **18**, 6694 (Dec 1, 1999).
5. Y. Tojima *et al.*, NAK is an IkappaB kinase-activating kinase. *Nature* **404**, 778 (Apr 13, 2000).
6. Q. Li, G. Estepa, S. Memet, A. Israel, I. M. Verma, Complete lack of NF-kappaB activity in IKK1 and IKK2 double-deficient mice: additional defect in neurulation. *Genes & development* **14**, 1729 (Jul 15, 2000).
7. S. Sharma *et al.*, Triggering the interferon antiviral response through an IKK-related pathway. *Science* **300**, 1148 (May 16, 2003).
8. K. A. Fitzgerald *et al.*, IKKepsilon and TBK1 are essential components of the IRF3 signaling pathway. *Nature immunology* **4**, 491 (May, 2003).
9. H. Hemmi *et al.*, The roles of two IkappaB kinase-related kinases in lipopolysaccharide and double stranded RNA signaling and viral infection. *The Journal of experimental medicine* **199**, 1641 (Jun 21, 2004).
10. S. M. McWhirter *et al.*, IFN-regulatory factor 3-dependent gene expression is defective in Tbk1-deficient mouse embryonic fibroblasts. *Proceedings of the National Academy of Sciences of the United States of America* **101**, 233 (Jan 6, 2004).
11. A. K. Perry, E. K. Chow, J. B. Goodnough, W. C. Yeh, G. Cheng, Differential requirement for TANK-binding kinase-1 in type I interferon responses to toll-like receptor activation and viral infection. *The Journal of experimental medicine* **199**, 1651 (Jun 21, 2004).
12. A. K. Miyahira, A. Shahangian, S. Hwang, R. Sun, G. Cheng, TANK-binding kinase-1 plays an important role during in vitro and in vivo type I IFN responses to DNA virus infections. *Journal of immunology* **182**, 2248 (Feb 15, 2009).
13. H. Chen *et al.*, Activation of STAT6 by STING is critical for antiviral innate immunity. *Cell* **147**, 436 (Oct 14, 2011).
14. K. Clark *et al.*, Novel cross-talk within the IKK family controls innate immunity. *The Biochemical journal* **434**, 93 (Feb 15, 2011).
15. J. Mowers *et al.*, Inflammation produces catecholamine resistance in obesity via activation of PDE3B by the protein kinases IKKepsilon and TBK1. *eLife* **2**, e01119 (2013).
16. S. H. Chiang *et al.*, The protein kinase IKKepsilon regulates energy balance in obese mice. *Cell* **138**, 961 (Sep 4, 2009).
17. A. R. Saltiel, Insulin resistance in the defense against obesity. *Cell metabolism* **15**, 798 (Jun 6, 2012).

18. V. V. Kravchenko, J. C. Mathison, K. Schwamborn, F. Mercurio, R. J. Ulevitch, IKKi/IKKepsilon plays a key role in integrating signals induced by pro-inflammatory stimuli. *The Journal of biological chemistry* **278**, 26612 (Jul 18, 2003).
19. Y. H. Ou *et al.*, TBK1 directly engages Akt/PKB survival signaling to support oncogenic transformation. *Molecular cell* **41**, 458 (Feb 18, 2011).
20. X. Xie *et al.*, IkappaB kinase epsilon and TANK-binding kinase 1 activate AKT by direct phosphorylation. *Proceedings of the National Academy of Sciences of the United States of America* **108**, 6474 (Apr 19, 2011).
21. S. M. Reilly *et al.*, An inhibitor of the protein kinases TBK1 and IKK-varepsilon improves obesity-related metabolic dysfunctions in mice. *Nature medicine* **19**, 313 (Mar, 2013).
22. M. Pilli *et al.*, TBK-1 promotes autophagy-mediated antimicrobial defense by controlling autophagosome maturation. *Immunity* **37**, 223 (Aug 24, 2012).
23. P. Wild *et al.*, Phosphorylation of the autophagy receptor optineurin restricts Salmonella growth. *Science* **333**, 228 (Jul 8, 2011).
24. E. K. Jo, J. M. Yuk, D. M. Shin, C. Sasakawa, Roles of autophagy in elimination of intracellular bacterial pathogens. *Frontiers in immunology* **4**, 97 (2013).
25. T. Otani *et al.*, IKKepsilon regulates cell elongation through recycling endosome shuttling. *Developmental cell* **20**, 219 (Feb 15, 2011).
26. J. Stockli, D. J. Fazakerley, D. E. James, GLUT4 exocytosis. *Journal of cell science* **124**, 4147 (Dec 15, 2011).
27. M. Inoue, L. Chang, J. Hwang, S. H. Chiang, A. R. Saltiel, The exocyst complex is required for targeting of Glut4 to the plasma membrane by insulin. *Nature* **422**, 629 (Apr 10, 2003).
28. M. Inoue, S. H. Chiang, L. Chang, X. W. Chen, A. R. Saltiel, Compartmentalization of the exocyst complex in lipid rafts controls Glut4 vesicle tethering. *Mol Biol Cell* **17**, 2303 (May, 2006).
29. M. R. Heider, M. Munson, Exorcising the exocyst complex. *Traffic* **13**, 898 (Jul, 2012).
30. X. W. Chen *et al.*, Exocyst function is regulated by effector phosphorylation. *Nature cell biology* **13**, 580 (May, 2011).
31. S. Moskalenko *et al.*, Ral GTPases regulate exocyst assembly through dual subunit interactions. *The Journal of biological chemistry* **278**, 51743 (Dec 19, 2003).
32. X. W. Chen *et al.*, A Ral GAP complex links PI 3-kinase/Akt signaling to RalA activation in insulin action. *Molecular biology of the cell* **22**, 141 (Jan 1, 2011).
33. M. Bonnard *et al.*, Deficiency of T2K leads to apoptotic liver degeneration and impaired NF-kappaB-dependent gene transcription. *The EMBO journal* **19**, 4976 (Sep 15, 2000).
34. X. W. Chen, D. Leto, S. H. Chiang, Q. Wang, A. R. Saltiel, Activation of RalA is required for insulin-stimulated Glut4 trafficking to the plasma membrane via the exocyst and the motor protein Myo1c. *Dev Cell* **13**, 391 (Sep, 2007).